

A Survey on Deep Learning based Brain Computer Interface: Recent Advances and New Frontiers

XIANG ZHANG, University of New South Wales
LINA YAO, University of New South Wales
XIANZHI WANG, University of Technology Sydney
JESSICA MONAGHAN, Macquarie University
DAVID MCALPINE, Macquarie University

Brain-Computer Interface (BCI) bridges human's neural world and the outer physical world by decoding individuals' brain signals into commands recognizable by computer devices. Deep learning has lifted the performance of brain-computer interface systems significantly in recent years. In this article, we systematically investigate brain signal types for BCI and related deep learning concepts for brain signal analysis. We then present a comprehensive survey of deep learning techniques used for BCI, by summarizing over 230 contributions most published in the past five years. Finally, we discuss the applied areas, opening challenges, and future directions for deep learning-based BCI.

Additional Key Words and Phrases: Brain-Computer Interface, deep learning, survey

ACM Reference format:

Xiang Zhang, Lina Yao, Xianzhi Wang, Jessica Monaghan, and David McAlpine. 2018. A Survey on Deep Learning based Brain Computer Interface: Recent Advances and New Frontiers. 1, 1, Article 1 (January 2018), 66 pages.

DOI: 10.1145/1122445.1122456

1 INTRODUCTION

Brain-Computer Interface (BCI)¹ is a system that translates activity patterns of the human brain into messages or commands to communicate with the outer world [119]. BCI underpins many novel applications that are important to people's daily life, especially to people with psychological/physical deceases or disabilities. For example, ordinary individuals can enjoy enhanced entertainment and security when brain waves-based techniques are applied for high fake-resistant user identification [249]. Another example is that BCI can assist the disabled, elders and people with limited motion ability (e.g., people with muscle diseases) in controlling wheelchairs, home appliances, and robots. The key challenge of BCI is to recognize human intents accurately given the meager Signal-to-Noise Ratio (SNR) of brain signals. Both low classification accuracy and poor generalization ability limit the real-world application of BCI.

To overcome the above challenges, deep learning techniques, i.e., deep neural networks, have been investigated to deal with the brain information in the past few years. Deep Learning is a sub-field of machine learning inspired by the structure and function of the brain. It has shown excellent representation learning ability since 2006 [42] and therefore been impacting a wide range of information-processing domains such as computer version, natural language processing, activity recognition, and logic reasoning [217]. Differing from traditional machine learning algorithms,

¹There are several terms similar to BCI, e.g., Brain Machine Interface (BMI), Brain Interface (BI), Direct Brain Interface (DBI), and Adaptive Brain Interface (ABI). They all describe machines that are directly controlled by human brain signals.

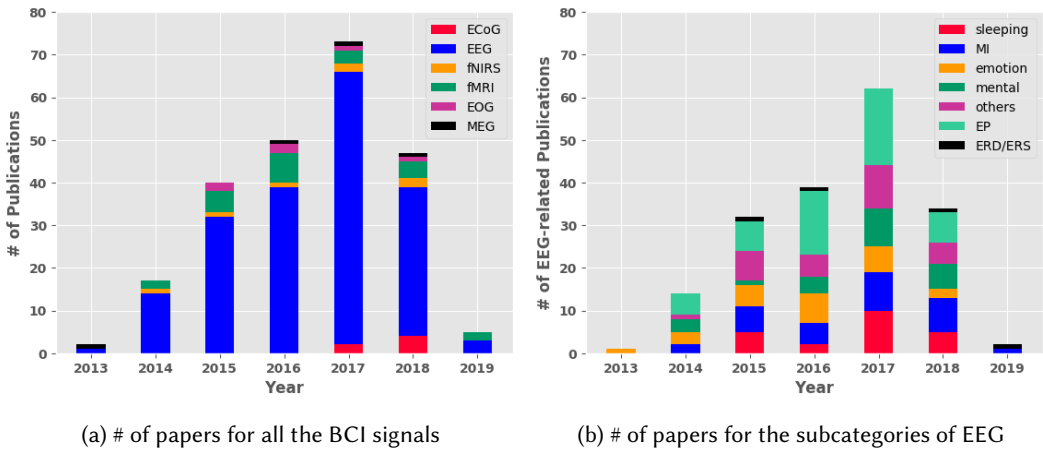


Fig. 1. Breakdown of the papers included in this survey in year of publication and BCI signals. Not all papers are counted for the years 2018 and 2019 due to limited availability of the related data.

deep learning can learn distinct high-level features from raw brain signals without manual feature selection, and its accuracy scales well with the size of the training set.

1.1 Why Deep Learning?

Although traditional BCI systems have made tremendous progress [2, 20] in the past decades, the research in BCI still faces significant challenges. First, brain signals are easily corrupted by various biological (e.g., the eye blink, the muscle artifacts, the fatigue and concentration level) and environmental artifacts (e.g., environmental noise) [2]. Therefore, it is crucial to distill informative data from corrupted brain signals and build a robust BCI system that work under different situations.

Second, BCI has a low SNR due to the non-stationary electrophysiological brain signals [168]. Although several preprocessing and feature engineering methods have been developed to decrease the noise level, such methods (e.g., feature selection and extraction both in the time domain and frequency domain) are time-consuming and may cause information loss in the extracted features [250].

Third, feature engineering highly depends on human expertise in the specific domain. For example, it requires the basic knowledge of a biologist to investigate the sleep state through EEG signals. The human experience may help capture features on some particular aspects but fall insufficient in more general conditions. Therefore, an algorithm is required to extract representative features automatically.

Moreover, most existing machine learning research focuses on the static data and therefore cannot classify the rapidly changing brain signals accurately. For example, the state-of-the-art classification accuracy for motor imagery EEG is merely 60% to 80% [120], which is unfeasible for practical uses. It generally requires novel learning methods to deal with dynamical data streams in BCI systems.

Until now, deep learning has been applied extensively in BCI applications and shown success in addressing the above challenges [30, 124]. Deep learning possess two advantages. First, it avoids the time-consuming preprocessing and feature engineering steps by working directly on raw brain signals to learn distinguishable information through back-propagation. Second, deep neural networks can capture both representative high-level features and latent dependencies through

Table 1. The existing survey on BCI in the last decade. The column ‘comprehensive on signals’ indicates whether the survey has summarized all the BCI signals or not.

No.	Reference	Comprehensive on Signals?	Signal	Deep Learning	Publication Time	Area
1	[48]	No	EMG, EOG	No	2007	
2	[222]	No	fMRI	Yes	2018	Mental Disease Diagnosis
3	[120]	Partial	EEG (mainly MI EEG and P300)	No	2007	Classification
4	[119]	Partial	EEG (Mainly MI EEG, P300)	Partial	2018	Classification
5	[133]	Partial	EEG (ERD, P300, SSVEP, VEP, AEP)	No	2007	
6	[113]	No	MRI, CT	Partial	2017	Medical Image Analysis
7	[233]	No	EEG	Yes (but without any model introduction)	2019	
8	[20]	No	EEG	No	2007	Signal Processing
9	[220]	Partial	EEG	No	2016	BCI Applications
10	[2]	Yes		No	2015	
11	[140]	No	EEG	Partial (only DBN)	2018	
12	[184]	No	EEG, fMRI	No	2015	Neurorehabilitation of Stroke
13	[5]	No	MI EEG	No	2015	
14	[165]	No	fMRI	No	2014	
15	[63]	No	ERP (P300)	No	2017	Applications of ERP
16	[114]	No	fMRI	Yes	2018	Applications of fMRI
17	[206]	No	ERP	No	2017	Classification
18	[61]	Partial	EEG	No	2019	Brain Biometrics
19	Ours	yes	Invasive, EEG and the subcategories, fNIRS, fMRI, EOG, MEG	Yes		

deep structures. Our investigation (Figure 1) shows a surge of publications in deep learning based BCI since 2014.

1.2 Why this Survey is Necessary?

We conduct this survey for three reasons. First, there lacks systematic and comprehensive introduction of BCI signals. Table 1 shows a summary of the existing survey on BCI. To the best of our knowledge, the limited existing surveys [2, 20, 48, 114, 119, 120, 133, 222] only focus on partial EEG signals. For example, Lotte et al. [120] and Wang et al. [220] focus on EEG without analyzing EEG signal types; Cecotti et al. [32] focus on Event-Related Potentials (ERP); Haseer et al. [142] focus on functional near-infrared spectroscopy (fNIRS); Fatourehchi et al. [48] only focus on EMG and EOG; Wen et al. [222] and Liu et al. [114] only focus on Functional magnetic resonance imaging (fMRI); Mason et al. [133] brief the neurological phenomenons like event-related desynchronization (ERD), P300, SSVEP, Visual Evoked Potentials (VEP), Auditory Evoked Potentials (AEP) but have not organized them systematically; Abdulkader et al. [2] present a topology of brain signals but have not mentioned spontaneous EEG and Rapid Serial Visual Presentation (RSVP).; Lotte et al. [119] have not considered ERD and RSVP; Roy et al. [233] list some deep learning based EEG studies but provide little analysis.

Second, although some overviews have conducted in deep learning ([42, 43, 174]) and BCI ([2, 20, 48, 119, 120, 133]), few focus on their combination. To the best of our knowledge, this paper is the *first comprehensive summary* of the recent advances on deep learning-based BCI. This work also presents the current frontiers and potential directions in research.

Lastly, unlike this survey, all previous BCI surveys focus on specific areas or applications without given an overview of the broad scenarios. For example, Litjens et al. [113] review some leading deep learning concepts pertinent to medical image analysis without covering many other deep

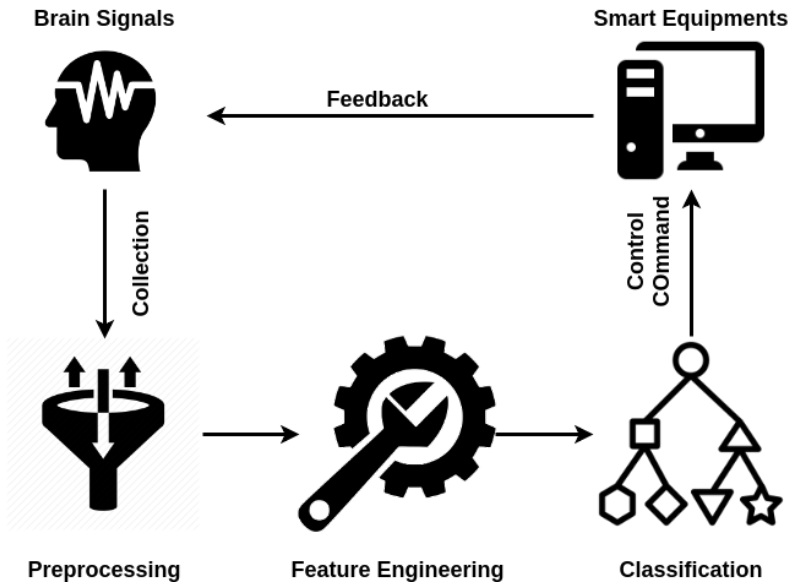


Fig. 2. Generally workflow of BCI system.

learning models; Soekadar et al. [184] review the BCI systems and machine learning methods that help overcome stroke-related motor paralysis and focus on Sensori-Motor Rhythms (SMR); Vieira et al. [213] investigate the application of BCI systems on the neurological disorder and psychiatric.

1.3 Our Contributions

This survey aims to present a comprehensive and systematic introduction of the recent advances and new frontiers of deep learning based brain-computer interface techniques. We summarize over 240 contributions in this field, most of which were published in the last five years (after 2014). We make several key contributions in this survey:

- We first comprehensively summarized the brain signals used for BCI. Also, this is the first investigation of the biometric signals in deep learning based BCI.
- We summarize deep learning techniques for BCI applications. To our best knowledge, *we are the very first to systemically review the Deep learning models for BCI.*
- We provide guidelines for choosing the suitable deep learning model for a specific BCI system and a specific brain signal type.
- We discuss the challenges of deep learning based BCI and highlight the promising topics for the future research.

The rest of this survey is structured as followed. Section 2 briefly introduces the paradigm of BCI systems. Section 3 gives a comprehensively introduction of biometric signals used in BCI. Section 4 overviews the commonly used deep learning models. Section 5 presents the state-of-the-art deep learning techniques for BCI. Section 6 discusses the applications related to brain signals. Section 7 points out the opening challenges and future directions. Finally, Section 8 gives the concluding remarks.

2 GENERAL BCI SYSTEM

Figure 2 shows the general paradigm of a BCI system, which receives brain signals and converts them into control commands for computers. The system includes several key components: brain signal collection, signal preprocessing, feature engineering, classification, and smart equipment. The brain signals are collected from humans and sent to the preprocessing component for denoising and enhancement. Then, the discriminating features are extracted from the processed signals and sent to the classifier, which recognizes the signals and convert then into external device commands.

The collection methods differ from signal to signal. For example, EEG signals measure the voltage fluctuation resulting from ionic current within the neurons of brain. Collecting EEG signals requires placing a series of electrodes on the scalp of the human head to record the electrical activity of the brain. Since the ionic current is erupted within the brain but measured at the scalp, the obstacles (e.g., skull) heavily decrease the signal quality—the fidelity of the collected EEG signals, measured as Signal-to-Noise Ratio (SNR), is approximately 5% of that of original brain signals [17]. Therefore, brain signals are usually preprocessed before feature engineering to increase the SNR. The preprocessing component contains multiple steps such as signal cleaning (smoothing the noisy signals or resolving the inconsistencies), signal normalization (normalizing each channel of the signals along time-axis), signal enhancement (removing direct current), and signal reduction (presenting a reduced representation of the signal).

Feature engineering refers to the process of extracting discriminating features from the input signals through domain knowledge. Traditional features are extracted from time-domain (e.g., variance, mean value, kurtosis), frequency-domain (e.g., fast Fourier transform), and time-frequency domains (e.g., discrete wavelet transform). They will enrich distinguishable information regarding user intention. Feature engineering is highly dependent on the domain knowledge. For example, biomedical knowledge is required to extract features from brain signals of epileptic seizure. The manual feature extraction is also time-consuming and difficult. Recently, deep learning provides a better option to automatically extract the distinguishable features.

The classification component refers to the machine learning algorithms that classify the extracted features into logical control signals recognizable by external devices. Deep learning algorithms are shown to be more powerful than traditional classifiers such as Support Vector Machine (SVM) and Linear discriminant analysis (LDA).

In this survey, we summarize the state-of-the-art studies which adopt deep learning models (will be detailed in Section 5): 1) for feature engineering only; 2) for classification only; 3) for both feature engineering and classification. BCI has vast potential applications for both the disabled and ordinary individuals. For instance, a BCI system can control household appliances through patients' brain signals. Such a system can also serve for entertainment and security purposes. More BCI applications based on deep learning are introduced in Section 6.

3 BCI SIGNAL RECORDING

In this section, we present a comprehensive and systematic introduction of brain signals used in BCI systems. Figure 3 shows a taxonomy of brain signals including invasive and non-invasive signals based on the signal collection method (Section 3.1). Invasive signals are collected from the surface of the cortex or under the cortex surface (Section 3.2); Non-invasive signals are collected by the external sensors. EEG signal plays a dominant role among non-invasive signals. Therefore, we introduce EEG signal and its subordinate categories in particular in Section 3.3. The basic characteristics of various brain signals are summarized in Table 2.

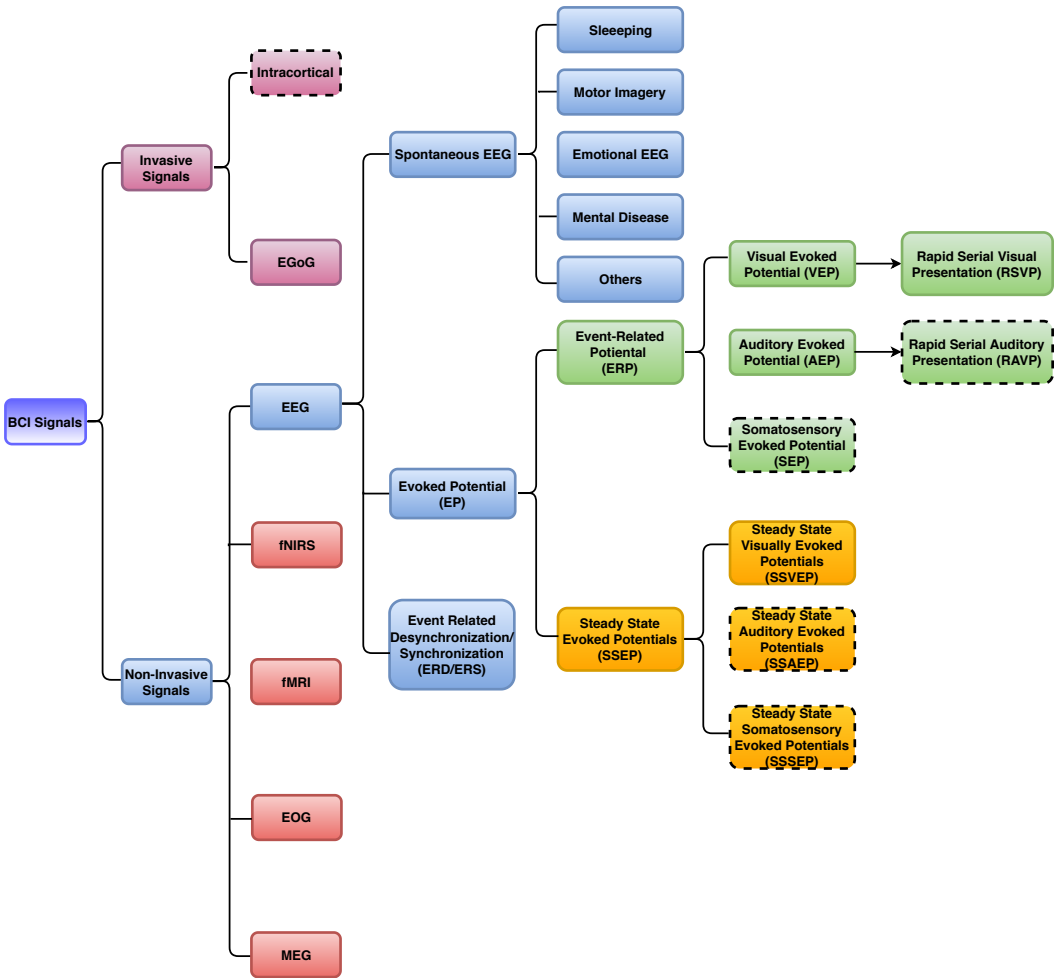


Fig. 3. The biometric signals generally used in BCI system. The dash quadrilaterals (Intracortical, RAVP, SEP, SSAEP, and SSSEP) are not included in this survey for the reason that there's no existing work focus on them by deep learning algorithms. P300, which is a positive potential recorded approximately 300 ms after the onset of presented stimuli, is not listed in this signal tree because it's included by ERP (which refers to all the potentials after the presented stimuli).

3.1 Invasive Recording

Invasive recordings are realized by electrodes deployed under the scalp. Figure 4 [102] shows both 'intraparencham signals' gathered from the cortex and 'Electrocorticography (ECoG)'² gathered from the surface of cortex (dura and arachnoid).

The invasive techniques can provide high-quality brain signals as electrodes collect signals directly from locations near the brain neurons. The collected signals have high temporal and spatial resolution³ and high SNR. Nevertheless, invasive methods suffer from two challenges. First, the

²Some studies name the Intracortical as 'invasive' while name the ECoG as 'semi-invasive'. In this survey, we combine the so-called 'invasive' and 'semi-invasive' into 'invasive' since they both require surgery.

³Spatial resolution refers to how well the signal discriminates between nearby locations.

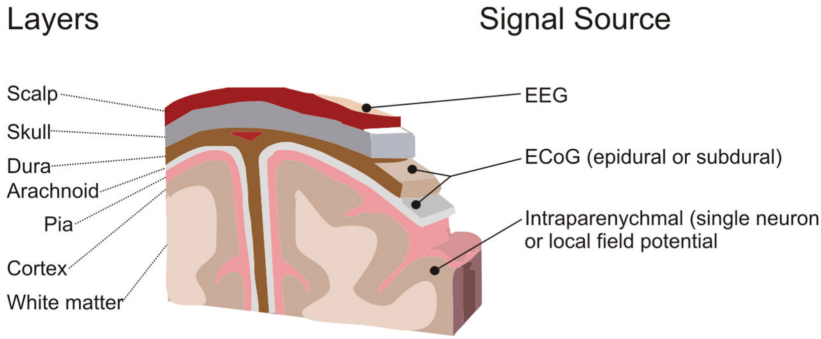


Fig. 4. Signal source locations in the brain

Table 2. Summary of various brain signals’ characteristics.

Signals	Invasive		Non-invasive				
	Intracortical	EcoG	EEG	fNIRS	fMRI	EOG	MEG
Risk	High	High	Low	Low	Low	Low	Low
Spatial resolution	Very High	High	Low	Mediate	High	Low	Mediate
Temporal resolution	High	High	Mediate	Low	Low	Mediate	High
Signal-to-Noise Ratio	High	High	Low	Low	Mediate	Mediate	Low
Portability	Mediate	Mediate	High	High	Low	High	Low
Cost	High	High	Low	Low	High	Low	High
Characteristic	Electrical	Electrical	Electrical	Optical	Metabolic	Electrical	Magnetic

implantation of electrodes requires a surgical procedure, which is expensive and risky due to the potential medical complications such as transplant rejection. Second, implanted electrodes are fixed and therefore can only measure the brain signals from the same locations. For the above reasons, invasive BCI techniques mainly used for animals (e.g., money and rat) and people with severe disabilities (e.g., ALS patients) [2] in practice.

3.1.1 Intracortical. Intracortical collection technique inserts electrodes into the cortex of the object brain (Figure 4). The planted microelectrode can be a single electrode or an array of electrodes. Generally, the intracortical electrodes provide high-resolution motor control brain signals as movement is the most observable phenomenon compared to other phenomena such as hearing. Under the cortex, the electrodes are sensitive enough to pick up the discrete all-or-none output of single neurons, the action potential, commonly referred to as a “spike”, as well as the summed voltage fluctuations from small to large numbers of neurons, called field potentials. Each electrode provides spiking from up to a few neurons, yielding the population’s time evolving output pattern. These represent but a small sample of the entire set of neurons in this limited region, as spiking can only be detected by microelectrodes closely approximated to a neuron [76]. [151] developed a high-performance BCI system for communication of ALS patients. This work implanted a 96-channel silicon microelectrode array in the motor cortex corresponding to hand area and record user’s motor intention by the microelectrode array. The array was then decoded into point-and-click commands to control a cursor.

3.1.2 Electrocorticography (ECoG). Electrocorticography (ECoG) is an extracortical invasive electrophysiological monitoring method to record brain activity. The electrodes collecting ECoG

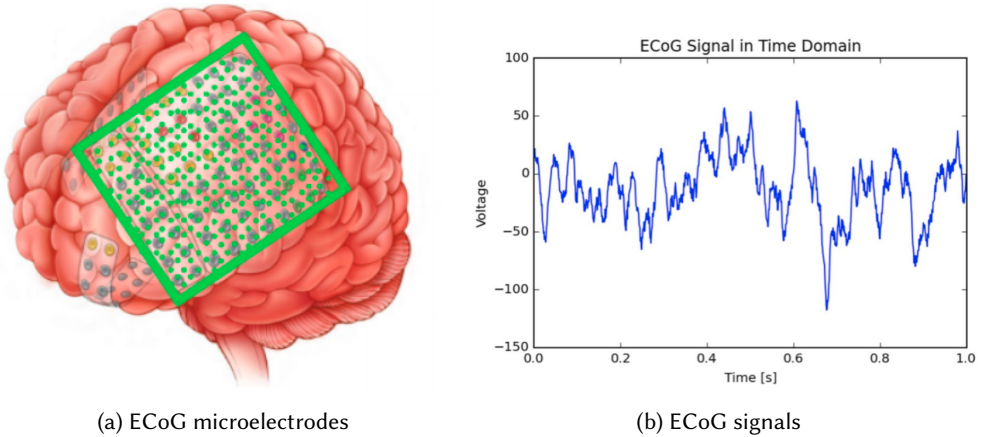


Fig. 5. ECoG grid on cortical surface and ECoG signals.

are attached under the skull, above (epidural) or below (subdural) the dura mater, but not within the brain parenchyma itself (Figure 4) [102]. ECoG locates at the trade-off point between higher SNR and less risky. It provides a higher spatial resolution and a rather high SNR with a lower surgical risk. Therefore, ECoG has a better prospect in the medical area than intracortical signals.

The ECoG collection scenario and the signals are shown in Figure 5 [19]. The ECoG signals have a higher amplitude compared to non-invasive brain wave signals. For instance, ECoG has higher than $50 \mu V$ maximum amplitude while the EEG amplitude is generally lower than $20 \mu V$. The higher amplitude empowers ECoG less vulnerability to artifacts such as eye blink activity. Moreover, ECoG has a bandwidth of 0-500 Hz which is much wider than EEG (0-40Hz). The wider frequency bands take substantial information from functional areas of a brain (e.g., motor and language) and thus can be used to train a higher-performance BCI system. However, the disadvantages of an invasive method (like the risky surgery and inconvenient permanent attached devices) of ECoG naturally limit the wide deployment in real-world scenarios.

3.2 Noninvasive Recording

Noninvasive recordings can gather user's brain information without electrodes inserting. The signals can be collected in the electrical, magnetic or metabolic method. Noninvasive signals mainly include Electroencephalogram (EEG), Functional near-infrared spectroscopy (fNIRS), Functional magnetic resonance imaging (fMRI), Electrooculography (EOG), and Magnetoencephalography (MEG). EEG related studies take a considerable part of noninvasive signals and have a lot of sub-classes. We will introduce more details and sub-classes of EEG in Section 3.3.

3.2.1 Electroencephalography (EEG). Electroencephalography (EEG) is the most commonly used noninvasive technique for measuring brain activities. EEG monitors the voltage fluctuations generated by an electrical current within the human neurons. Electrodes placed on the scalp measure the amplitude of EEG signals. EEG signals have a low spatial resolution because the amount of electrodes is limited. EEG electrodes location generally follows the international 10-20 system or the intermediate 10% electrode positions [125]. The international 10-20 system divides the scalp in 10% and 20% intervals and totally contains 21 electrode locations (Figure 6). The intermediate 10% electrodeposition is standardized by the American Electroencephalographic Society and split the scalp with 10% intervals, which contains 75 electrodes. The existing EEG

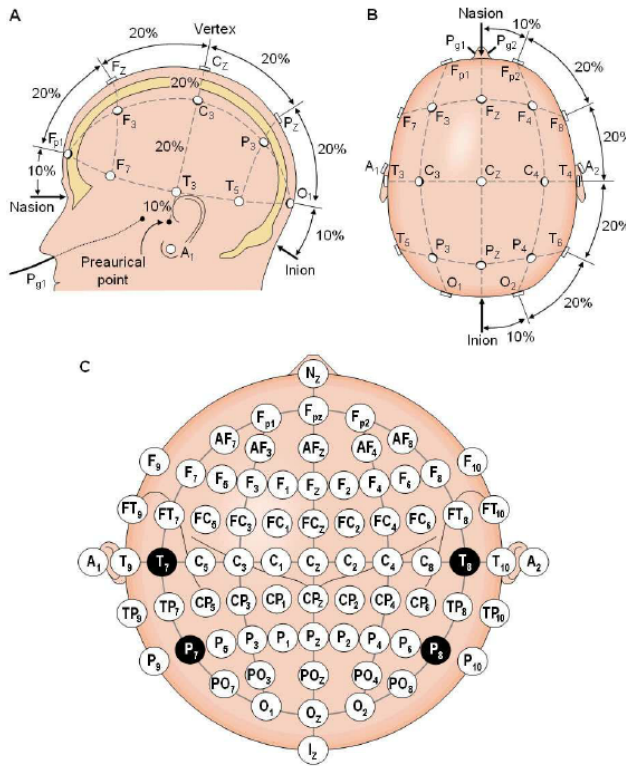


Fig. 6. (A) and (B) are the left and above view of the international 10-20 system. (C) presents the intermediate 10% electrodes positions.

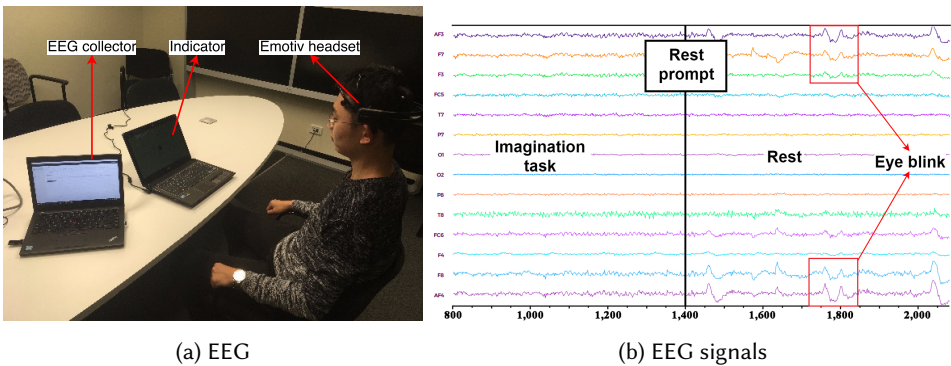


Fig. 7. EEG collection scenario and the gathered signals. The subject is undertaking imagination task.

collection system is generally less than 75 electrodes, in specific, 64 electrodes (BCI 2000 system), 32 electrodes (openBCI headset), 14 electrodes (Emotiv EPOC+ headset), five electrodes (Emotiv insight headset), and one electrode (Mindware headset).

Table 3. EEG patterns and corresponding characters. Awareness Degree denotes the awareness the degree of being aware of an external world.

Patterns	Frequency (Hz)	Amplitude	Brain State	Awareness Degree	Produced Location
Delta	0.5-4	Higher	Deep sleep pattern	Lower	Frontally and posteriorly
Theta	4-8	High	Light sleep pattern	Low	Entorhinal cortex, hippocampus
Alpha	8-12	Medium	Closing the eyes, relax state	Medium	Posterior regions of head
Beta	12-30	Low	Active thinking, focus, high alert, anxious	High	Most evident frontally
Gamma	30-100	Lower	During cross-modal sensory processing	Higher	Somatosensory cortex

The temporal resolution of EEG signals is much better than the spatial resolution. The ionic current changes rapidly, which offers a temporal resolution highest at 1000 Hz. The SNR of EEG is generally very poor due to both objective and subjective factors. Objective factors include environmental noises, the obstruction of the skull and other tissues between cortex and scalp, and different stimulations. Subjective factors contain the subject's mental stage, fatigue status, and the variance among different subjects.

The EEG collection equipment can be installed in a cap-like headset. As shown in Figure 7 [250], the EEG headset can be mounted on the user's head to gather signals. Compared to other brain signals collect equipment, EEG headsets are portable and more accessible for various occasions.

The EEG signals collected from any typical EEG hardware have several non-overlapping frequency bands (Delta, Theta, Alpha, Beta, and Gamma) based on the strong intra-band correlation with a distinct behavioral state [250]. Each EEG pattern contains signals associated with particular brain information. Table 3 shows EEG frequency patterns and the corresponding characteristics. The awareness degree in this paper denotes the perception of individuals while facing outside stimuli. Each frequency band represents a brain state and a qualitative assessment of awareness:

- Delta pattern (0.5 – 4 Hz) corresponds to deep sleep when the subject has lower awareness.
- Theta pattern (4 – 8 Hz) corresponds to light sleep in the realm of low awareness.
- Alpha pattern (8 – 12 Hz) mainly occurs during eyes closed and deeply relaxed state and corresponds to the medium awareness.
- Beta pattern (12 – 30 Hz) is the dominant rhythm while the subject's eyes are open and is associated with high awareness. Beta patterns capture most of our daily activities (such as eating, walking, and talking).
- Gamma pattern (30 – 100 Hz) represents the co-interaction of several brain areas to carry out a specific motor and cognitive function. This pattern is associated with the highest awareness.

3.2.2 Functional Near-infrared Spectroscopy (fNIRS). Functional near-infrared spectroscopy (fNIRS) is a noninvasive functional neuro-imaging technology using near-infrared (NIR) light [143]. In specific, fNIRS employs NIR light to measure the aggregation degree of oxygenated hemoglobin (Hb) and deoxygenated-hemoglobin (deoxy-Hb) because Hb and deoxy-Hb have higher absorbers of light than other head components such as skull and scalp. fNIRS relies on blood-oxygen-level-dependent (BOLD) response or hemodynamic response to form a functional neuro-image. The BOLD response can detect the oxygenated or deoxygenated blood level in the brain blood. Finally, the relative levels can reflect the blood flow and neural activation, where the increased blood flow infers a higher metabolic demand caused by active neurons. For example, when the user is concentrating on a mental task, the prefrontal cortex neurons will be activated, and the BOLD response in the prefrontal cortex area will be stronger [72].

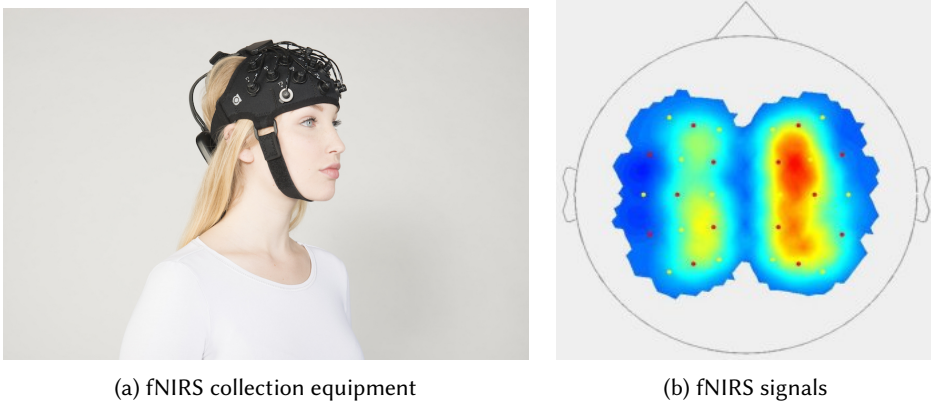


Fig. 8. fNIRS collection equipment and the gathered signals

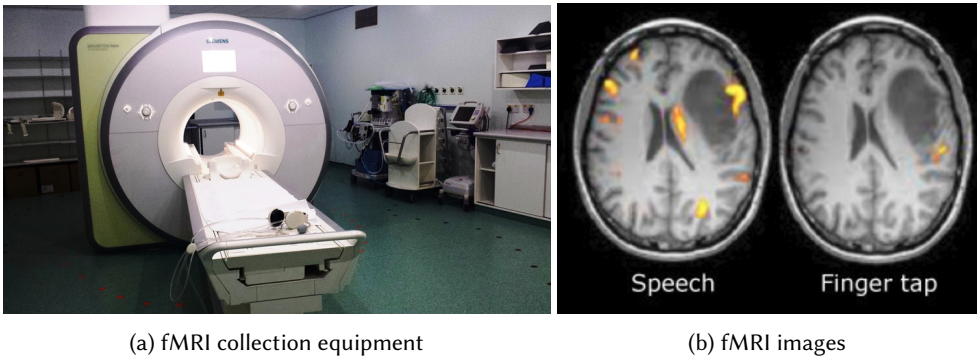


Fig. 9. fMRI collection equipment and the gathered fMRI signals while the subject is speaking and finger tapping

Figure 8⁴ shows the fNIRS collection hardware and the collected signals. Single or multiple emitter-detector pairs measure the Hb and deoxy-Hb: the emitter transmits NIR light through the blood vessel to the detector. Most existing studies use fNIRS technologies to measure the status of prefrontal and motor cortex. The former responds to mental tasks and music/image imagery while the latter is a response to motor-related tasks (e.g., motor imagery). The monitored Hb and deoxy-Hb change slowly since the blood speed varies in a relatively slow ratio compared to electrical signals. Therefore, fNIRS signals have lower temporal resolution⁵ compared with electrical or magnetic signals. The spatial resolution depends on the amount of emitter-detector pairs. In current studies, three emitters and eight detectors would suffice for adequately acquiring the prefrontal cortex signals; and six emitters and six detectors would suffice for covering the motor cortex area [142]. fNIRS has one drawback in that it cannot be used to measure cortical activity occurred under 4cm in the brain due to the limitations in light emitter power and spatial resolution.

3.2.3 Functional Magnetic Resonance Imaging (fMRI). Functional magnetic resonance imaging (fMRI) monitors brain activities by detecting changes associated with blood flow in brain areas

⁴<https://www.artinis.com/fnirs>

⁵Temporal resolution refers to the smallest time of neural activity reliably separated by the signal.

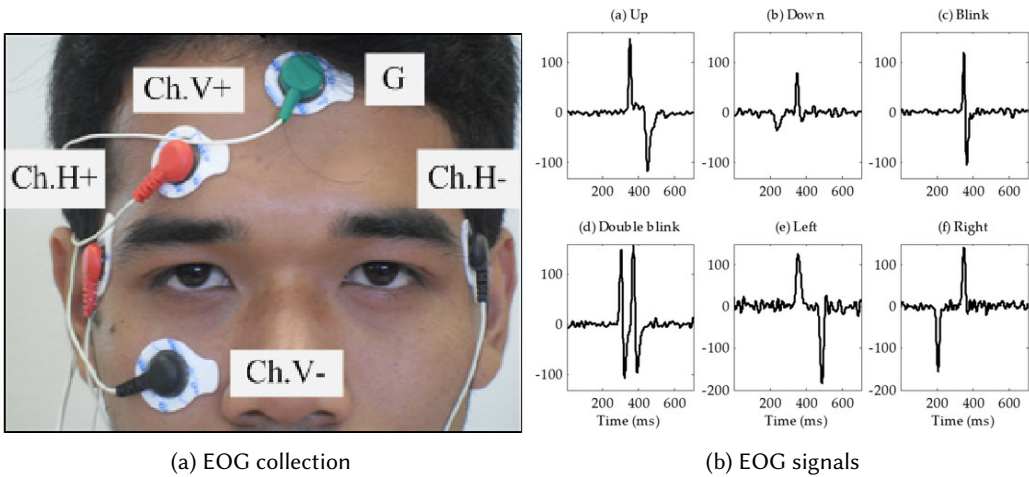


Fig. 10. EOG collection equipment and the gathered vertical signals while the subject is looking in different directions and blinking

[222]. Similar to fNIRS, fMRI relies on the BOLD response. The main differences between fNIRS and fMRI are as follows [114]. First, as the name, fMRI measures BOLD response through magnetic instead of optical methods. Hemoglobin differs in how it responds to magnetic fields, depending on whether it has a bound oxygen molecule. The magnetic fields are more sensitive to and are easier to be distorted by deoxy-Hb than Hb molecule. Second, the magnetic fields have higher penetration than NIR light, which empowers fMRI stronger ability to capture information from deep parts of the brain than fNIRS. Third, fMRI has a higher spatial resolution than fNIRS since the latter's spatial resolution is limited by the emitter-detector pairs. However, the temporal resolutions of fMRI and fNIRS are at an equal level because they both constrained by the blood flow speed.

fMRI has several flaws compared to fNIRS: 1) fMRI requires an expensive scanner to generate magnetic fields; 2) the scanner is heavy and has poor portability. Figure 9⁶ shows the fMRI acquisition machine, and the gathered brain images. fMRI images of speaking and finger tapping have a significant difference, which indicates that it has high SNR.

3.2.4 Electrooculography (EOG). Electrooculography (EOG) is a technique for measuring the corneo-retinal standing potential that exists between the front and the back of the human eyes. Most patients who lost volunteer motor movements (e.g., LIS patients) remain part of the control of eyes [231]. The eye movements can be detected by EOG signals to interact with the external devices. Therefore, we regard EOG signals as one class of BCI signals in this survey. EOG can be used to communicate the user and the outer world because different eye movements will cause different electrical potentials. Pairs of electrodes are typically placed above/below the eye or to the left/right of the eye to measure EOG signals. The EOG collection equipment [15] and the collected signals [166] can be found in Figure 10. In Figure 10a, EOG electrode placements where electrodes Ch.V+ and Ch.V- measure the vertical movements, and Ch.H+ and Ch.H- measure the horizontal movements. G electrode representing the ground line works as a reference point. Figure 10b shows the vertical EOG in time domain under six scenarios (looking upward, looking downward, single blink, double blink, looking leftward, and looking rightward). We can observe EOG signals have

⁶<https://www.jameco.com/Jameco/workshop/HowItWorks/what-is-an-fmri-scan-and-how-does-it-work.html>

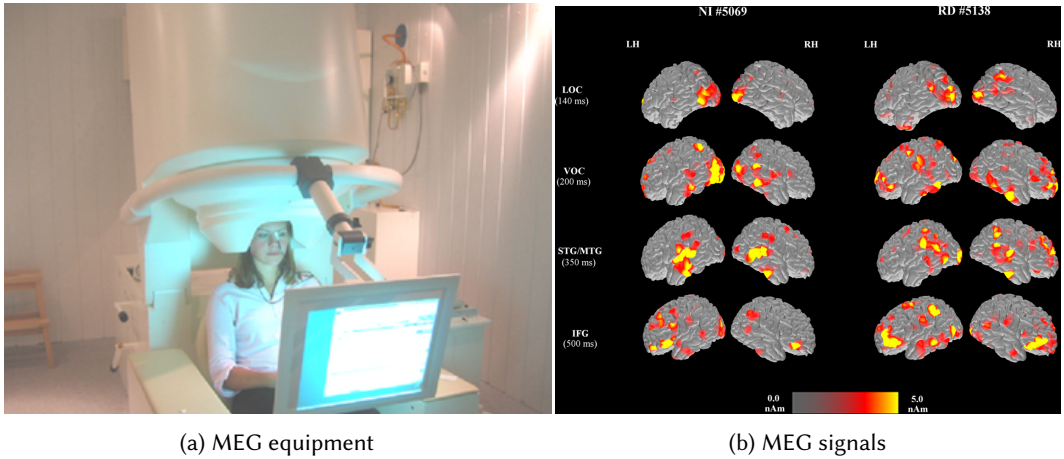


Fig. 11. MEG collection equipment and the gathered signals

large variances among different scenarios, indicating they have a relatively high SNR and are easier recognizable by machine learning algorithms. EOG has low spatial resolution compared to other brain signals since we can only detect the vertical and horizontal potentials. The temporal resolution of EOG is higher than neuroimaging techniques because the electrical potentials vary faster than metabolic features (e.g., blood flow).

3.2.5 Magnetoencephalography (MEG). Magnetoencephalography (MEG) is a functional neuroimaging technique for mapping brain activity by recording magnetic fields produced by electrical currents occurring naturally in the brain, using very sensitive magnetometers [39]. The ionic currents of active neurons will create weak magnetic fields. The generated magnetic fields can be measured by magnetometer like SQUIDs (superconducting quantum interference devices). However, 50,000 active neurons with similar orientation are required to produce a detectable magnetic field. The source of MEG is the pyramidal cells which are perpendicular to the cortex surface. Besides, motor intentions are difficult to be detected by MEG because the electrical currents generated by the motor neurons have opposite directions and the magnetic fields cancel out. Therefore, motor imagery and other motor-related tasks are not suited to be monitored by MEG.

MEG has a relatively low spatial resolution since the signal quality highly depends on the measuring factors (e.g., brain area, neuron orientations, neuron depth). However, MEG can provide very high temporal resolution ($\geq 1000\text{Hz}$) since MEG directly monitor the brain activity from the neuron level, which is in the same level of intracortical signals. The MEG equipment⁷ and the gathered signals [163] are shown in Figure 11. The MEG equipment is expensive and not portable which limits the real-world deployment. The brain map snapshots of MEG signals are collected at different times (140, 200, 350, and 500 ms) from two subjects under different mental tasks.

3.3 EEG Paradigms

Compared to other noninvasive signals (e.g., fMRI, fNIRS, EOG, MEG), EEG has several important advantages: 1) the hardware has higher portability with much lower price; 2) the temporal resolution is very high (milliseconds level)⁸; 3) EEG is relatively tolerant of subject movement and artifacts

⁷<https://www.biomagcentral.org/biomagnetism/meg>

⁸Among other noninvasive techniques, only MEG has the same level temporal resolution.

which can be minimized by existing signal processing methods; 4) the subject doesn't need to exposure to high-intensity (>1 Tesla) magnetic fields. Thus, EEG can serve subjects that have metal implants in their body (such as metal-containing pacemakers).

As the most commonly used signals, there are a huge number of sub-classes of EEG signals. In this section, we present a systematic introduction of EEG sub-class signals. As shown in Figure 3, we divided EEG signals into spontaneous EEG, evoked potentials, and event-related desynchronization/synchronization. Where the evoked potentials can be spat into event-related potentials and steady-state evoked potentials based on the frequency of the external stimuli. Each potential contains visual-, auditory-, and somatosensory- potentials based on the external stimuli types. The dash quadrilaterals in Figure 3, such as Intracortical, SEP, SSAEP, SSSEP, and RSAP, are not included in this survey because there are very few existing studies work on them by deep learning algorithms. We list these signals for systematic completeness.

3.3.1 Spontaneous EEG. Generally, when we talk about the term 'EEG,' we refer to *spontaneous* spontaneous EEG which measures the brain signals under a specific state without external stimulation. For example, spontaneous EEG includes the EEG signals while the user is sleeping, undertaking a mental task (e.g., counting), under fatigue stage, suffering brain disorders, undertaking motor imagery tasks, etc.

The EEG signals while the user staring at the color/shape/image belong to this category. While the subject is gazing at a specific image, the visual stimuli are steady without any twinkle. This scenario differs with the visual stimuli in evoked potential, where the visual stimuli are twinkling in a specific frequency. Thus, we regard the image stimulation as a particular state and sort it as spontaneous EEG. BCI systems based on spontaneous EEG are challenging to train, due to the lower SNR and the larger variation across subjects [155].

3.3.2 Evoked Potential (EP). Evoked Potential (EP) or evoked response refers to the EEG signals which are evoked by event stimulus instead of spontaneous. EP is time-locked to the external stimulus while the aforementioned spontaneous EEG is non-time-locked. In contrast to spontaneous EEG, EP generally has higher amplitude and lower frequency. As a result, the EP signals are more robust across subjects. According to the stimulation method, there exist two categories of EP: the Event-Related Potential (ERP) and the Steady State Evoked Potential (SSEP). ERP records the EEG signals in response to an isolated discrete stimulus event. To achieve this isolation, stimuli in an ERP experiment are typically separated from each other by a long inter-stimulus interval, allowing for the estimation of a stimulus-independent baseline reference [144]. The stimuli frequency of ERP is generally lower than 2 Hz. In contrast, SSEP is generated in response to a periodic stimulus at a fixed rate. The stimuli frequency of SSET generally ranges within 3.5-75 Hz.

Event-related potential (ERP). There are three kinds of evoked potentials in extensive research and clinical use: Visual Evoked Potentials (VEP); Auditory Evoked Potentials (AEP); and Somatosensory Evoked Potentials (SEP) [32]. The VEP signals are mainly on the occipital lobe, and the highest signal amplitudes are collected at the Calcarine sulcus.

1) Visual Evoked Potentials (VEP). Visual Evoked Potentials are a specific category of ERP which is caused by visual stimulus (e.g., an alternating checkerboard pattern on a computer screen). VEP signals are hidden within the normal spontaneous EEG. To separate VEP signals from the background EEG readings, the repetitive stimulation and time-locked signal-averaging techniques are generally employed.

Rapid Serial Visual Presentation (RSVP) [101] can be regarded as one kind of VEP. RSVP diagram is commonly used to examine the temporal characteristics of attention. The subject is required to stare at a screen where a series of items (e.g., images) are presented one-by-one. There is a specific

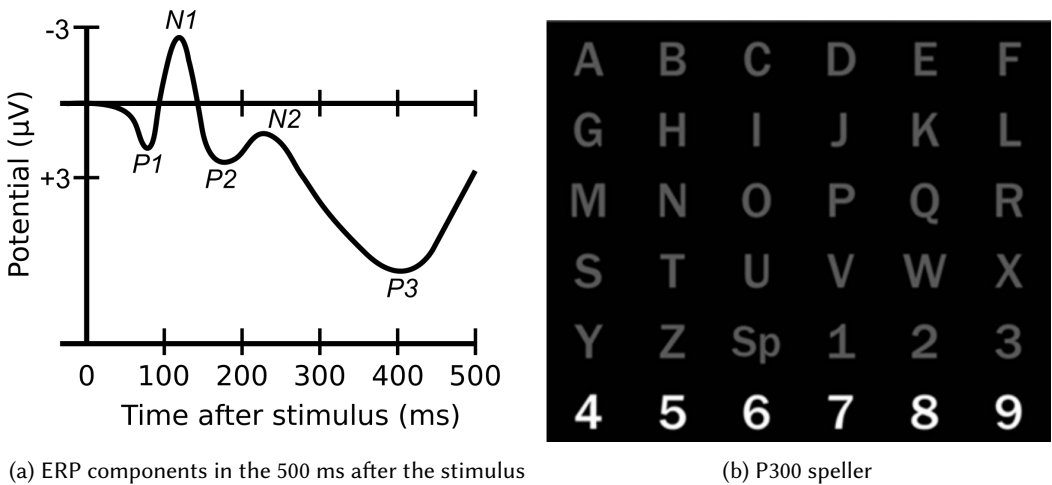


Fig. 12. P300 waves and visual-based P300 speller

item (called target) separates from the rest of the other items (called distracter). The subject knows which is the target before the RSVP experiment. Generally, the distracters can either be a color change or letters among numbers. RSVP contains a static mode (the items appear to the screen and then disappear without moving) and a moving mode (the items appear on the screen, move to another place, and finally disappear). Nowadays, BCI research mainly focuses on the static mode RSVP. Usually, the frequency of RSVP is 10Hz which refers that each item will stay on the screen for 0.1 seconds.

2) Auditory Evoked Potentials (AEP). Auditory Evoked Potentials are a specific subclass of ERP which responds to the audio (sound) stimuli. AEP is mainly recorded from the scalp but originating at the brainstem. The most common AEP experiment is auditory brainstem response (ABR) which is generally employed to inspect newborns and infants. In the BCI area, AEP is mainly used in clinical tests for its accuracy and reliability in detecting unilateral loss [36]. Similar to RSVP, Rapid Serial Auditory Presentation (RSAP) refers to the experiment with the rapid serial presentation of audios. The subject is supposed to recognize the target audio among the distracters.

3) Somatosensory Evoked Potentials (SEP).⁹ Somatosensory Evoked Potentials are another commonly used subcategory of ERP which is elicited by electrical stimulation of the peripheral nerve. SEP signals conclude a series of amplitude deflection that can be elicited by virtually any sensory stimuli.

P300. P300 (also called P3) is an important component in ERP [60]. Here we introduce P300 signal separately for the widely-used. Figure 12a shows the ERP signal fluctuation in 500 ms after the stimuli onset¹⁰. The waveform mainly concludes five components, P1, N1, P2, N2, and P3. The capital character P/N represents positive/negative electrical potentials. The following number refers to the occurrence time of the specific potential. Thus, P300 denotes the positive potential of ERP waveform at approximately 300 ms after the presented stimuli. Compared to other components, P300 has the highest amplitude and easier to be detected. Thus, a large number of BCI studies pay attention to P300 analysis. P300 is more like a kind of informative feature instead of brain signals

⁹Generally, Somatosensory Evoked Potentials is abbreviated as SSEP or SEP. In this paper, we choose SEP as the abbreviation in case of the conflict with Steady-State Evoked Potentials (SSEP).

¹⁰Note that the negative voltage of ERP is plotted upward, which is common in ERP research.

(e.g., VEP). Therefore, we do not list P300 in Figure 3. P300 can analyze most of the ERP signals such as VEP, AEP, SEP.

In practice, P300 can be elicited by rare, task-relevant events in an ‘oddball’ paradigm (e.g., P300 speaker). In the oddball paradigm, the subject receives a series of stimuli where low-probability target items are mixed with high-probability non-target items. The visual and audio stimulus is most commonly used in the oddball paradigm. Figure 12b shows an example of visual-based P300 speller which enables the subject to spell letters/numbers directly through brain signals [47]. The 26 letters of the alphabet and the Arabic numbers are displayed on a computer screen which serves as the keyboard. The subject focuses attention successively on the characters he wishes to spell. The computer detects the chosen character online at real time. This detection is achieved by repeatedly flashing rows and columns of the matrix. When the elements containing the selected characters are flashing, a P300 fluctuation is elicited. In the 6×6 matrix screen, the rows and columns flash in mixed random order. The flash and interval among adjacent flash are generally set as 100 ms [25]. The columns and rows are flashing separately. First, the columns flash for six times with each column one time. Second, the rows will flash for six times. After that, this paradigm repeats for several times (e.g., N times). The P300 signals of the total $12N$ flash will be analyzed to output a single outcome (i.e., one letter/number).

Steady State Evoked Potentials (SSEP). Steady State Evoked Potentials is another subcategory of evoked potentials, which are periodic cortical responses evoked by certain repetitive stimuli with a constant frequency. It is demonstrated that the brain oscillation generally keeps at a steady level over time while the potentials are evoked by the steady state stimuli (e.g., the flickering light with fixed frequency). Technically, SSEP is defined as a form of response to repetitive sensory stimulation in which the constituent frequency components of the response remain constant with time in both amplitude and phase [161]. Based on the type of stimuli, SSEP can be divided into three subcategories: Steady-State Visually Evoked Potentials (SSVEP), Steady-State Auditory Evoked Potentials (SSAEP), and Steady-State Somatosensory Evoked Potentials (SSSEP). In the BCI area, most studies are focused on visual evoked steady potentials, and rarely paper pays attention to auditory and somatosensory stimuli. Therefore, in this survey, we mainly introduce SSVEP rather than SSAEP and SSSEP.

Difference Among various visual evoked potentials diagrams. Visual evoked potentials are the most common used potentials. Therefore, it is essential to distinguish the three different visual evoked potential diagrams: VEP, RSVP, SSVEP. Here, we theoretically introduce the characteristics of each diagram and then give three demonstration videos to provide a better understanding. First, the frequencies are different: the frequency of VEP is less than 2Hz while the frequency of RSVP is around 10Hz, and the frequency of SSVEP ranges from 3.5 to 75Hz. Second, they have various presentation protocols. In the VEP diagram, different visual patterns will be presented on the screen to check the user’s brain signals changes. For instance, in this video¹¹, the image pattern is full of the screen and changes dramatically. In RSVP diagram, several items will be presented on a screen one-by-one. All the items are shown in the same place and share the same frequency. For example, the video¹² shows an RSVP scenario which is called speed reading. In SSVEP diagram, several items will be presented on a screen at the same time while the items are shown at *variant positions* with different frequencies. For example, in this demonstration video¹³, there are four circles distributed on the up, down, left, and right sides of a screen and the frequency of each item differs from each other.

¹¹https://www.youtube.com/watch?v=iUW_L5YAEEM

¹²<https://www.youtube.com/watch?v=5yddRrd0hA&t=36s>

¹³<https://www.youtube.com/watch?v=t96rl1SFHII>

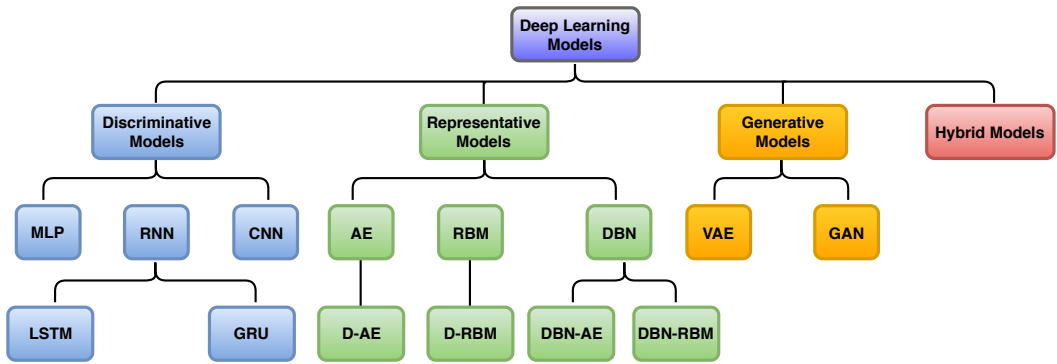


Fig. 13. Deep learning models. They can be divided into discriminative, representative, generative and hybrid models based on the algorithm function. D-AE denotes Stacked-Autoencoder which refers to the autoencoder with multiple hidden layers. Deep Belief Network can be composed of AE or RBM, therefore, we divided DBN into DBN-AE (stacked AE) and DBN-RBM (stacked RBM).

3.3.3 Event-related Desynchronization/Synchronization (ERD/ERS). Event-related desynchronization/synchronization (ERD/ERS) refers to the phenomena that the change of EEG signal power during a specific brain state [81]. In particular, ERD denotes the power decreasing of EEG ongoing signals while ERS represents the power increasing of EEG signals. This characteristic of ERD/ERS of brain signals can be used to detect the event which causing the EEG fluctuation. For example, [154] presents the ERD/ERS phenomena in motor cortex recorded during a motor-imagery task. The task causes an ERD in the mu band (8-13 Hz) of EEG and an ERS in the beta band (13-30 Hz).

Compared to spontaneous EEG singles, ERD/ERS is not only a kind of spontaneous brain signal but also a decreasing/increasing phenomena. Differ from other spontaneous EEG, ERD/ERS analysis supposed to exploit the power fluctuation. Compare to evoked potentials, ERD/ERS does not require external stimuli. ERD/ERS can be collected by performing mental tasks, such as motor imagery, mental arithmetic, or mental rotation. However, to collect the high-quality ERD/ERS signals, the subjects are required to take extensive training which may take several weeks. Moreover, the performance of ERD/ERS among users is quite variable, and the accuracy is not very high [2]. Thus, this paradigm is not one of the BCI dominate signals.

4 DEEP LEARNING MODELS

In this section, we formally introduce the deep learning models including concept, architectures, and techniques commonly used in BCI area. Deep learning is a class of machine learning techniques that umany layers of information-processing stages in hierarchical architectures for pattern classification and feature/representation learning [42]. The standard neural network (Figure 14a) contains three neuron layers including an input layer, a hidden layer, and an output layer. Any neural network with more than four layers (one input layer, ≥ 2 hidden layers, and one output layer) can be called deep neural network for the reason that it's 'deeper' than the standard/shallow neural networks (3 layers).

In this survey, we will give relative detail introduction of various deep learning models for the reason that a part of the potential readers who are from non-computer area (e.g., biomedical) are not familiar to deep learning.

Deep learning algorithms divide into several subcategories based on the aim of the techniques (as shown in Figure 13):

Table 4. Summary of deep learning model types

Deep Learning	Input	Output	Function	Training method
Discriminative	Input data	Label	Feature extraction, Classification	Supervised
Representative	Input data	Representation	Feature extraction	Unsupervised
Generative	Input data	New Sample	Generation, Reconstruction	Unsupervised
Hybrid	Input data	–	–	–

- Discriminative deep learning models, which classify the input data into a pre-known label based on the adaptively learned discriminative features. Discriminative algorithms are empowered to learn distinctive features through the non-linear transformation and classification through probabilistic prediction¹⁴. Thus these algorithms can play the role of both feature engineering and classification (corresponding to Figure 2). Discriminative architectures mainly include Multi-Layer Perceptron (MLP), Recurrent Neural Networks (RNN), Convolutional Neural Networks (CNN), along with their variations.
- Representative deep learning models, which learn the pure and representative features from the input data. These algorithms only have the function of feature engineering (corresponding to Figure 2) but fail to classification. Common used deep learning algorithms for representation are Autoencoder (AE), Restricted Boltzmann Machine (RBM), Deep Belief networks (DBN), along with the variations.
- Generative deep learning models, which learn the joint probability distribution of the input data and the target label. In BCI scope, generative algorithms are mostly used in reconstruction or generate a batch of brain signals samples to enhance the training set. Generative models commonly used in BCI include variational Autoencoder (VAE)¹⁵, Generative Adversarial Networks (GANs), etc.
- Hybrid deep learning models, which combine more than two deep learning models. For example, the typical hybrid deep learning model employs a representation algorithm for feature extraction and discriminative algorithms for classification.

The summary of the characteristics of each deep learning subcategories are listed in Table 4. Almost all the classification function in neural networks are implemented by softmax layer, which will not be regarded as an algorithmic component in this survey. For instance, a model combined a DBN, and a softmax layer will still be regarded as a representative model instead of a hybrid model.

4.1 Discriminative Deep Learning Models

Since the main task of BCI is brain signal recognition, the discriminative deep learning models are the most popular and powerful algorithms. Suppose we have a dataset of brain signal samples $\{\mathbb{X}, \mathbb{Y}\}$ where \mathbb{X} denotes the set of brain signal observations and \mathbb{Y} denotes the set of sample ground truth (i.e., labels). Suppose an specific sample-label pair $\{\mathbf{x} \in \mathbb{R}^N, \mathbf{y} \in \mathbb{R}^M\}$ where N and M denote the dimension of observations and the number of sample categories, respectively. The aim of discriminative deep learning models is to learn a function with the mapping: $\mathbf{x} \rightarrow \mathbf{y}$. In short, the discriminative models receive the input data and output the corresponding category or label. All the discriminative models introduced in this section are supervised learning techniques which require the information of both the observations and the ground truth.

¹⁴The classification function is achieved by the combination of softmax layer and one-hot label encoding. The one-hot label encoding refers to encode the label by the one-hot method which is a group of bits among which the legal combinations of values are only those with a single high (1) bit and all the others low (0) bits. For instance, a set of label 0, 1, 2, 3 can be encoded as (1, 0, 0, 0), (0, 1, 0, 0), (0, 0, 1, 0), (0, 0, 0, 1).

¹⁵VAE is a variation of AE. However, they are working on different aspects. Therefore, we separately introduce AE and VAE.

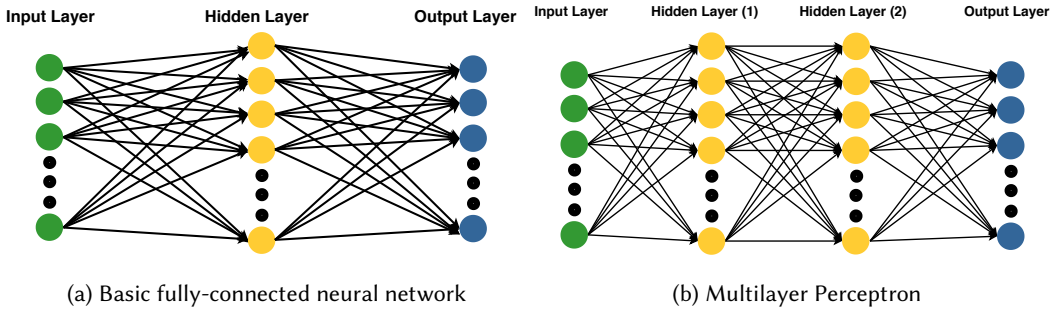


Fig. 14. Illustration of standard neural network and multilayer perceptron. (a) The basic structure of the fully-connected neural network. The input layer receives the raw data or extracted features of brain signals while the output layer shows the classification results. The term ‘fully-connected’ denotes each node in a specific layer is connected with all the nodes in the previous and next layer. (b) MLP could have as much as hidden layers, the more, the deeper. This is an example of MLP with two hidden layers, which is the simplest MLP model.

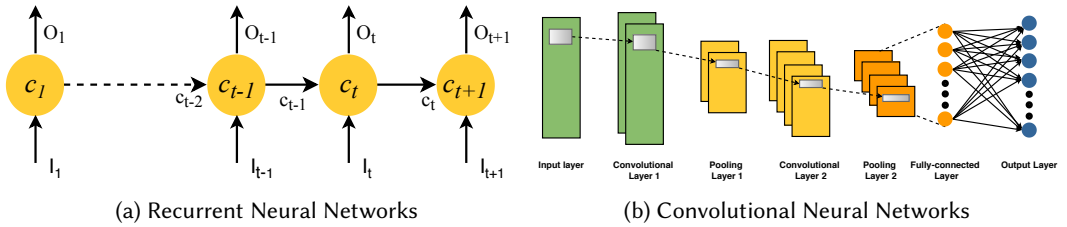


Fig. 15. Illustration of RNN and CNN models. (a) The recurrent procedure of RNN model. This procedure describes the recurrent procedure of a specific node in time range $[1, t + 1]$. The node at time t receives two inputs variables (I_t denotes the input at time t and c_{t-1} denotes the hidden state at time $t - 1$) and exports two variables (the output O_t and the hidden state c_t at time t). (b) The paradigm of CNN model which includes two convolutional layers, two pooling layers, and one fully-connected layer.

4.1.1 *Multi-Layer Perceptron (MLP)*. Multilayer Perceptron is the simplest and the most basic deep learning model. The key difference between MLP and the shallow neural network is that MLP has more than one hidden layers. All the nodes are fully-connected with the nodes of the adjacent layers but without connection with the other nodes of the same layer. MLP includes multiple hidden layers. As shown in Figure 14b, we take a structure with two hidden layers as an example to describe the data flow in MLP. First, we define an operation $\mathcal{T}(\cdot)$ as

$$\mathcal{T}(\mathbf{x}) = \mathbf{w} * \mathbf{x} + \mathbf{b}$$

$$\mathcal{T}(\mathbf{x}, \mathbf{x}') = \mathbf{w} * \mathbf{x} + \mathbf{b} + \mathbf{w}' * \mathbf{x}' + \mathbf{b}'$$

where \mathbf{x} and \mathbf{x}' denote two variables while \mathbf{w} , \mathbf{w}' , \mathbf{b} , and \mathbf{b}' denote the corresponding weights and basis.

The input layer receives the observation \mathbf{x} and feed forward to the first hidden layer,

$$\mathbf{x}^{h1} = \sigma(\mathcal{T}(\mathbf{x}))$$

where \mathbf{x}^{h1} denotes the data flow in the first hidden layer and σ represents the non-linear activation function. There several commonly used activation function such as sigmoid/Logistic, Tanh, ReLU,

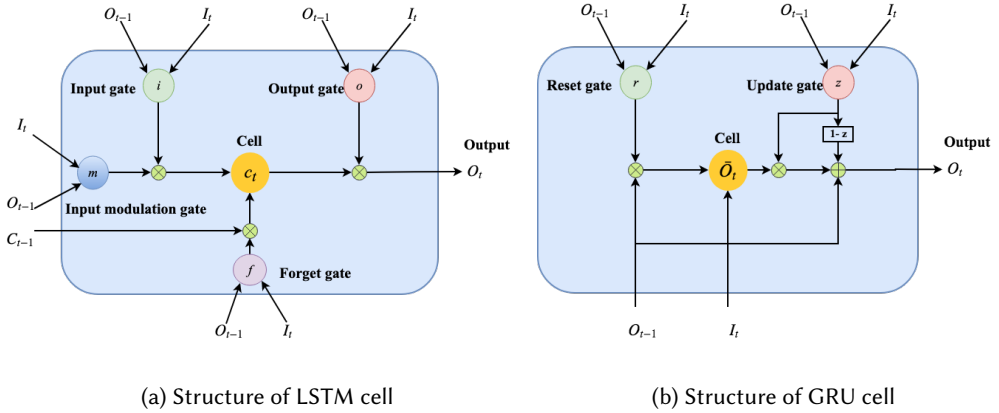


Fig. 16. Illustration of detailed LSTM and GRU cell structures. (a) LSTM cell receives three inputs (I_t denotes the input at time t , O_{t-1} denotes the output of previous time, and c_{t-1} denotes the hidden state of the previous time) and exports two outputs (the output of this time O_t and the hidden state of this time c_t). LSTM cell contains four gates in order to control the data flow, which are the input gate, output gate, forget gate, and input modulation gate. (b) GRU cell receives two inputs (the input of this time I_t and the output of the previous time O_{t-1}) and exports its output O_t . GRU cell only contains two gates which are the reset gate and the update gate. Unlike the hidden state c_t in LSTM cell, there's no transmittable hidden state in GRU cell except one intermediate variable \bar{O}_t .

we choose sigmoid activation function as an example in this section. Then, the data flow the second hidden layer and the output layer,

$$\mathbf{x}^{h2} = \sigma(\mathcal{T}(\mathbf{x}^{h1}))$$

$$\mathbf{y}' = \sigma(\mathcal{T}(\mathbf{x}^{h2}))$$

where \mathbf{y}' denotes the predict results in one-hot format. The error (i.e., loss) could be calculated based on the differentiation between \mathbf{y}' and the ground truth \mathbf{y} . For instance, the Euclidean distance based error can be calculated by

$$error = \|\mathbf{y}' - \mathbf{y}\|_2 \quad (1)$$

where $\|\cdot\|_2$ denotes the Euclidean norm. Afterward, the error will be back-propagated and optimized by a suitable optimizer. The optimizer will adjust all the weights and basis in the model until the error converges. The widely used loss function includes cross-entropy, negative log likelihood, mean square estimation, etc. The widely used optimizer includes Adaptive moment estimation (Adam), Stochastic Gradient Descent (SGD), Adagrad (Adaptive subgradient method), etc.

Several terms may be easily confused with each other: Artificial Neural Network (ANN), Deep Neural Network (DNN), and MLP. These terms have no strict difference and often mixed in literature. Generally, ANN represents the neural networks with less hidden layers (shallow) while DNN with more (in this case, DNN equals to MLP). Besides, DNN can describe the overall deep learning models includes not only fully-connected networks but also other networks (e.g., recurrent, convolutional networks).

4.1.2 Recurrent Neural Networks (RNN). Recurrent Neural Network is a specific subclass of discriminative deep learning model which are designed to capture the temporal dependencies among input data. Figure 15a describes the activity of a specific RNN node in the time domain.

At each time ranges from $[1, t + 1]$, the node receives an input I ¹⁶ and a hidden state c from the previous time (except the first time). For instance, at time t it receives not only the input I_t but also the hidden state of the previous node c_{t-1} . The hidden state can be regarded as the ‘memory’ of the nodes which can help the RNN ‘remember’ the historical input.

Next, we will report two typical RNN architectures which have attracted much attention and achieved great success: long short-term memory and gated recurrent units. They both follow the basic principles of RNN, and we will pay our attention to the complicated internal structures in each node. Since the structure is much more complicated than general neural nodes, we call it ‘cell’. Cell for RNN equals to the node to MLP.

Long Short-Term Memory (LSTM). Figure 16a shows the structure of a single LSTM cell at time t . The LSTM cell has three inputs (I_t , O_{t-1} , and c_{t-1}) and two outputs (c_t and O_t). The operation is as follows:

$$I_t, O_{t-1}, c_{t-1} \rightarrow c_t, O_t$$

I_t denotes the input value at time t , O_{t-1} denotes the output at the previous time (i.e., time $t - 1$), and c_{t-1} denotes the hidden state at the previous time. c_t and O_t separately denote the hidden state and the output at time t . Therefore, we can observe that the output O_t at time t not only related to the input I_t but also related to the information at the previous time. In this way, LSTM is empowered to remember the important information in the time domain. Moreover, the essential idea of LSTM is to control the memory of specific information. For this aim, LSTM cell adopts four gates: the input gate, forget gate, output gate, and input modulation gate. Each gate is a weight to control how much information can flow through this gate. For example, if the weight of the forget gate is zero, the LSTM cell would remember all the information passed from the previous time $t - 1$; if the weight is one, the LSTM cell would remember nothing. The corresponding activation function determines the weight. The detailed data flow as follows:

$$\begin{aligned} f &= \sigma(\mathcal{T}(I_t, O_{t-1})) \\ i &= \sigma(\mathcal{T}(I_t, O_{t-1})) \\ o &= \sigma(\mathcal{T}(I_t, O_{t-1})) \\ m &= \tanh(\mathcal{T}(I_t, O_{t-1})) \\ c_t &= f * c_{t-1} + i * m \\ h_t &= o * \tanh(c_t) \end{aligned}$$

where i , f , o and m represent the input gate, forget gate, output gate and input modulation gate, respectively.

Gated Recurrent Units (GRU). Another widely used RNN architecture is GRU. Similar to LSTM, GRU attempts to exploit the information from the previous time. GRU doesn’t require the hidden state, however, explore the temporal information only from the output of time $t - 1$. Thus, as shown in Figure 16b, GRU has two inputs (I_t and O_{t-1}) and one output (O_t). The mapping can be described as:

$$I_t, O_{t-1} \rightarrow O_t$$

GRU contains two gates: reset gate r and update gate z . The former decides how to combine the input with previous memory. The latter decides how much of previous memory to keep around, which is similar to the forget gate of LSTM. The data flow as follows:

$$\begin{aligned} z &= \sigma(\mathcal{T}(I_t, O_{t-1})) \\ r &= \sigma(\mathcal{T}(I_t, O_{t-1})) \end{aligned}$$

¹⁶The subscript represents the specific time.

$$\begin{aligned}\bar{O}_t &= \tanh(\mathcal{T}(I_t, r * O_{t-1})) \\ O_t &= (1 - z) * O_{t-1} + z * \bar{O}_t\end{aligned}$$

It can be observed that there's a intermediate variable \bar{O}_t which is similar to the hidden state of LSTM. However, \bar{O}_t only works on this time point and unable to pass to the next time point.

We here give a brief comparison between LSTM and GRU since they are very similar. First, LSTM and GRU have comparable performance as studied by literature. In the specific task, it's recommended to try both of them to find better performance. Second, GRU is lightweight since it only has two gates and without the hidden state. Therefore, GRU is faster to train and requires few data for generalization. Third, in contrast, LSTM generally works better if the training dataset is big enough.

4.1.3 Convolutional Neural Networks (CNN). Convolutional Neural Networks is one of the most popular deep learning models specialized in spatial information exploration. This section will briefly introduce the working mechanism of CNN. CNN is widely used to discover the latent spatial information in applications such as image recognition, ubiquitous, and object searching due to their salient features such as regularized structure, good spatial locality, and translation invariance. In BCI, specifically, CNN is supposed to capture the distinctive dependencies among the patterns associated with different brain signals.

We present a standard CNN architecture as shown in Figure 15b. The CNN contains one input layer, two convolutional layers with each followed by a pooling layer, one fully-connected layer, and one output layer. The square patch in each layer shows the processing progress of a specific batch of input values. The key of CNN is to reduce the input data into a form which is easier to recognize, without as few as information loss. CNN has three stacked layers: the convolutional Layer, pooling Layer, and fully-connected Layer.

The convolutional layer is the core block of CNN, which contains a set of filters to convolve the input data followed by the nonlinear transformation to extract the geographical features. In deep learning implementation, there are several key hyper-parameters should be set in the convolutional layer, like the number of filters, the size of each filter, etc. The pooling layer generally follows the convolutional layer. Pooling layer aims to reduce the spatial size of the features progressively. In this way, it can help to decrease the number of parameters (e.g., weights and basis) and computing burden. There are three kinds of pooling operation: max, min, average. Take max pooling for example. The pooling operation outputs the maximum value of the pooling area as a result. The hyper-parameters in pooling layer includes the pooling operation, the size of the pooling area, the strides, etc. In the fully-connected layer, as the basic neural network, the nodes have full connections to all activations in the previous layer.

The CNN is the most popular deep learning model in BCI research, which can be used to exploit the latent spatial dependencies among the input brain signals like fMRI image, spontaneous EEG, and so on. More details will be reported in Section 5.

4.2 Representative Deep Learning Models

The essential blocks of representative deep learning models are autoencoder, and restricted Boltzmann machine¹⁷. Deep Belief Networks are composed of AE or RBM. The representative models including AE, RBM¹⁸, and DBN, are unsupervised learning methods. Thus, they can learn the representative features from only the input observations \mathbf{x} without the ground truth \mathbf{y} . In short, representative models receive the input data and output a dense representation of the data. There

¹⁷AE and RBM are generally regarded as kind of deep learning although they only have three and two layers, respectively.

¹⁸We regard AE, and RBM as representative methods as most researches in BCI adopt them for feature representation.

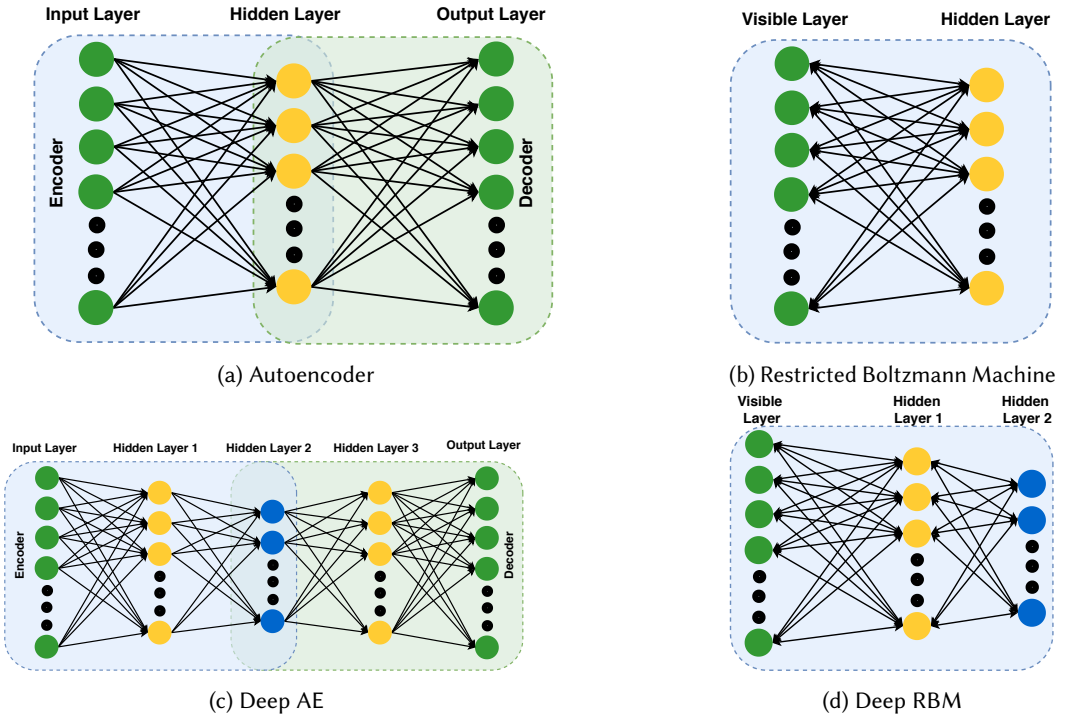


Fig. 17. Illustration of several standard representative deep learning models. (a) Basic autoencoder contains three layers where the input layer and the output layer are supposed to have the same values. The process from the input layer to the hidden layer is an encoder while the process from the hidden layer to the output layer is a decoder. (b) In the Restricted Boltzmann Machine, the encoder and the decoder share the same transformation weights. The input layer and the output layer are merged into the visible layer. (c) The stacked autoencoder has more than one hidden layers. Generally, the number of hidden layers is odd, and the middle layer is the learned representative features. (d) The deep RBM has one visible layer and multiple hidden layers, the last layer is the encoded representation.

are various definitions in different studies for several models (such as DBN, Deep RBM, and Deep AE), in this survey, we choose the most understandable definitions and will present them in detail in this section.

4.2.1 *Autoencoder (AE)*. As shown in Figure 17a, A autoencoder is a neural network that has three layers: the input layer, the hidden layer, and the output layer. Differ from the regular neural network, AE is trained to reconstruct its inputs, which forces the hidden layer to try to learn good representations of the inputs.

The structure of AE contains two blocks. The first block is named encoder, which embeds the observation to a latent representation (also called ‘code’),

$$\mathbf{x}^h = \sigma(\mathcal{T}(\mathbf{x}))$$

where \mathbf{x}^h represents the hidden layer. The second block is named decoder, which decode the representation into the original space,

$$\mathbf{y}' = \sigma(\mathcal{T}(\mathbf{x}^h))$$

where \mathbf{y}' represents the output.

AE forces \mathbf{y}' to equal to the input \mathbf{x} and calculates the error based on the distance between them. Thus, AE can computer the loss function only by \mathbf{x} without the ground truth \mathbf{y}

$$error = \|\mathbf{y}' - \mathbf{x}\|_2 \quad (2)$$

Compared to Equation 1, this equation is not involved to the variable \mathbf{y} because it regards the input \mathbf{x} as the ground truth. This is the reason why AE ables to perform unsupervised learning.

Naturally, one variant of AE is Deep-AE (D-AE) which has more than one hidden layers. We present the structure of D-AE with three hidden layers in Figure 17c. From the figure, we can observe that there is one more hidden layer in both the encoder and the decoder. The symmetrical structure ensures the smooth of encoding and decoding procedure. Thus, D-AE generally has an odd number of hidden layers (e.g., $2n + 1$) where the first n layers belong to the encoder, the $(n + 1)$ -th layer works as the code which belongs to both encoder and decoder, and the last n layers belong to the decoder. The data flow of D-AE (Figure 17c) can be represented as

$$\mathbf{x}^{h1} = \sigma(\mathcal{T}(\mathbf{x}))$$

$$\mathbf{x}^{h2} = \sigma(\mathcal{T}(\mathbf{x}^{h2}))$$

where \mathbf{x}^{h2} denotes the median hidden layer (the code). Then decode the hidden layer, we can get

$$\mathbf{x}^{h3} = \sigma(\mathcal{T}(\mathbf{x}^{h2}))$$

$$\mathbf{y}' = \sigma(\mathcal{T}(\mathbf{x}^{h3}))$$

It's almost the same with AE except that D-AE has more hidden layers. Apart from D-AE, AE has many other variants like denoising autoencoder, sparse autoencoder, contractive AE, etc. Here we only introduce the D-AE because it's easy to be confused with the AE based deep belief network. The key difference between them will be provided in Section 4.2.3.

The core idea of AE and its variants is simple, which is that condensing the input data \mathbf{x} into a code \mathbf{x}^h (generally the code layer has lower dimension) and then reconstruct the data based on the code. If the reconstructed \mathbf{y}' can approximate to the input data \mathbf{x} , it can be demonstrated that the condensed code \mathbf{x}^h carries enough information of \mathbf{x} , thus, we can regard \mathbf{x}^h as a representation of the input data for future operation (e.g., classification).

4.2.2 Restricted Boltzmann Machine (RBM). Restricted Boltzmann Machine is a stochastic artificial neural network that can learn a probability distribution over its set of inputs. It contains two layers including one visible layer (input layer) and one hidden layer, as shown in Figure 17b. From the figure, we can see that the connection lines between the two layers are bidirectional. RBM is a variant of Boltzmann Machine with stronger restriction without intra-layer connection¹⁹. Similar to AE, the procedure of RBM also includes two steps. The first step condenses the input data from the original space to the hidden layer in a latent space. After that, the hidden layer is used to reconstruct the input data through the identical way. Compared to AE, RBM has a stronger constraint which is that the encoder weights and the decoder weights should be equal. We have

$$\mathbf{x}^h = \sigma(\mathcal{T}(\mathbf{x}))$$

$$\mathbf{x}' = \sigma(\mathcal{T}(\mathbf{x}^h))$$

In the above two equations, the weights of $\mathcal{T}(\cdot)$ are the same. Then, the error for training can be calculated by

$$error = \|\mathbf{x}' - \mathbf{x}\|_2$$

¹⁹In a general Boltzmann machine, the nodes in the same hidden layer will connect.

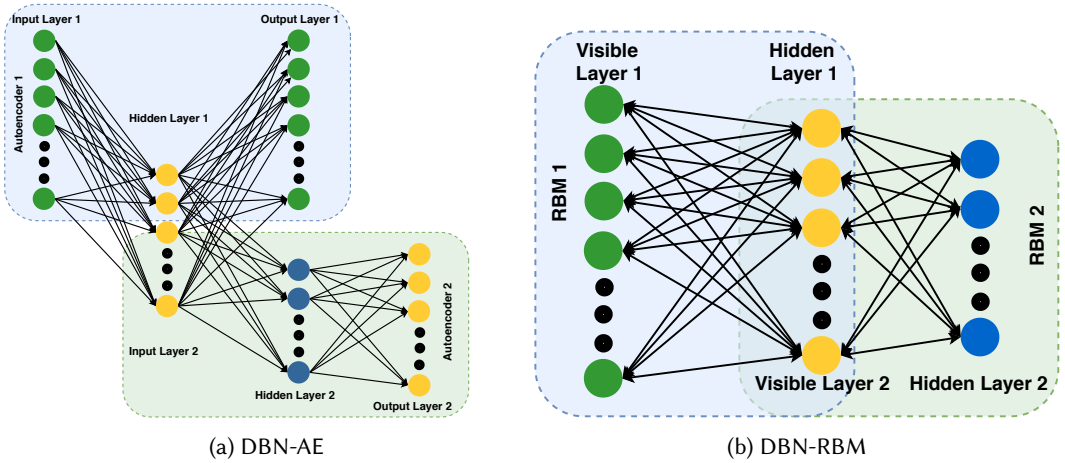


Fig. 18. Illustration of deep belief networks. (a) DBN composed of autoencoders. DBN-AE contains multiple AE components (in this case, two AE), the hidden layer of the previous AE working as the input layer of the next AE. The hidden layer of the last AE is the learned representation. (b) DBN composed of RBM. In this illustration, there are two RBM components where the hidden layer of the first RBM working as the visible layer of the second RBM. The last hidden layer is the encoded representation. While DBN-RBM and D-RBM (Figure 17d) have similar architecture, the former is trained greedily while the latter is trained jointly .

We can observe from the Figure 17d that the Deep-RBM (D-RBM) is an RBM with multiple hidden layers. The input data from the visible layer firstly flow to the first hidden layer and then the second hidden layer. Then, the code will flow backward until the visible layer for reconstruction.

4.2.3 *Deep Belief Networks (DBN)*. A Deep Belief Network (DBN) is a stack of simple networks, such as AEs or RBMs [55]. Thus, we divided DBN into DBN-AE (also called stacked AE) which is composed of AE and DBN-RBM (also called stacked RBM) which is composed of RBM.

As shown in Figure 18a, the DBN-AE contains two AE structures while the hidden layer of the first AE works as the input layer of the second AE. This diagram has two stages. In the first stage, the input data feed into the first AE follows the rules introduced in Section 4.2.1. The reconstruction error is calculated and back propagated to adjust the corresponding weights and basis. This iteration continues until the AE converges. We get the mapping,

$$\mathbf{x}^1 \rightarrow \mathbf{x}^{h1}$$

Then, we move on to the second stage that the learned representative code in the hidden layer \mathbf{x}^{h1} will be used as the input layer of the second AE, which is

$$\mathbf{x}^2 = \mathbf{x}^{h1}$$

and then, after the second AE converges, we have

$$\mathbf{x}^2 \rightarrow \mathbf{x}^{h2}$$

where \mathbf{x}^{h2} denotes the hidden layer of the second AE, meanwhile, it is the finally outcome of the DBN-AE.

Since the core idea of AE is that learning a representative code with lower dimension but contains most information of the input data. The idea behind DBN-AE is to learn a more representative and purer code.

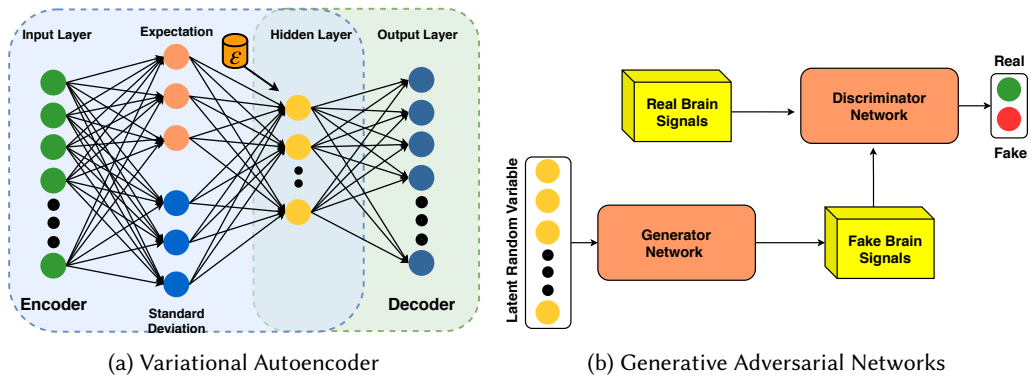


Fig. 19. Illustration of generative deep learning models. (a) VAE contains two hidden layers. The first hidden layer is composed of two components: the expectation and the standard deviation, which are learned separately from the input layer. The second hidden layer represents the encoded information. ϵ denotes the standard normal distribution. (b) GAN mainly contains two crucial components: the generator and the discriminator network. The former receives a latent random variable to generate a fake brain signal while the latter receives both the real and the generated brain signals and attempt to distinct it's generated or not. In BCI, GAN reconstructs or arguments data instead of classification.

Similarly, the DBN-RBM is composed of several single RBM structures. Figure 18b shows a DBN with two RBMs where the hidden layer of the first RBM is used as the visible layer of the second RBM.

Compare the DBN-RBM (Figure 18b) and D-RBM (Figure 17d). They almost have the same architecture. Moreover, DBN-AE (Figure 18a) and D-AE (Figure 17c) have similar architecture. The most important difference between the DBN and the deep AE/RBM is that the former is trained greedily while the latter is trained jointly. In particular, for the DBN, the first AE/RBM is trained first, after the converge, then train the second AE/RBM [74]. For the deep AE/RBM, jointly training means that the whole structure is trained together no matter how layers it has.

4.3 Generative Deep Learning Models

Generative deep learning models are mainly used to generate training samples or data augmentation. In other words, generative deep learning models play a supporting role in BCI area to enhance the training data quality and quantity. After the data augmentation, the discriminative models will be employed for the classification. This procedure is created to improve the robustness and effectiveness of the trained deep learning networks, especially when the training data is limited. In short, the generative models receive the input data and output a batch of similar data. In this section, we will introduce two typical generative deep learning models: variational Autoencoder (VAE) and Generative Adversarial Networks (GAN).

4.3.1 Variational Autoencoder (VAE). Variational Autoencoder, proposed in 2013 [92], is an important variant of AE, which is one of the most powerful generative algorithms. The standard AE and its other variants can be used for representation but fail in generation for the reason that the learned code (or representation) may not be continuous. Therefore, we cannot generate a random sample which is similar to the input sample. In other words, the standard AE not allows interpolation. Thus, we can replicate the input sample but cannot generate a similar one. VAE has one fundamentally unique property that separates it from other AEs, and it is this property that

makes VAE so useful for generative modeling: the latent spaces are designed continuous which allows easy random sampling and interpolation. Next, we will introduce how VAE works.

Similar to the standard AE, VAE can be divided into an encoder and a decoder while the former embeds the input data to a latent space and the latter transfers the data from the latent space to the original space. However, the learned representation in the latent space is forced to approximate a prior distribution $p(\mathbf{z})$ which is generally set as Standard Gaussian distribution. Based on the reparameterization trick [92], the first hidden layer of VAE is designed to have two parts where one denotes the expectation $\boldsymbol{\mu}$ and another denotes the standard deviation $\boldsymbol{\sigma}$, thus we have

$$\begin{aligned}\boldsymbol{\mu} &= \sigma(\mathcal{T}(\mathbf{x})) \\ \boldsymbol{\sigma} &= \sigma(\mathcal{T}(\mathbf{x}))\end{aligned}$$

Then, the latent code in the hidden layer is not directly calculated but sampled from a Gaussian distribution $\mathcal{N}(\boldsymbol{\mu}, \boldsymbol{\sigma}^2)$. The statistic code

$$\mathbf{z} = \boldsymbol{\mu} + \boldsymbol{\sigma} * \boldsymbol{\varepsilon} \quad (3)$$

where $\boldsymbol{\varepsilon} \sim \mathcal{N}(\mathbf{0}, \mathbf{I})$. The representation \mathbf{z} is forced to a prior distribution, and the distance $error_{KL}$ is measured by Kullback-Leibler divergence,

$$error_{KL} = D_{KL}(z, p(\mathbf{z}))$$

where $p(\mathbf{z})$ denotes the prior distribution. In the decoder, \mathbf{z} is decoded into the output \mathbf{y}' ,

$$\mathbf{y}' = \sigma(\mathcal{T}(\mathbf{z}))$$

and the reconstruction error is

$$error_{recon} = \|\mathbf{y}' - \mathbf{x}\|_2$$

The overall error for VAE is combined by the DL divergence and the reconstruction error,

$$error = error_{KL} + error_{recon}$$

The key point of VAE is that all the latent representations \mathbf{z} are forced to obey the normal distribution. Thus, we can randomly sample a representation $\mathbf{z}' \in p(\mathbf{z})$ from the prior distribution and then reconstruct a sample based on \mathbf{z}' . This is why VAE is so powerful in generation.

4.3.2 Generative Adversarial Networks (GAN). Generative Adversarial Networks [57] is proposed in 2014 and achieved great success in a wide range of research areas (e.g., computer vision and natural language processing). GAN is composed of two simultaneously trained neural networks with a generator and a discriminator. The generator captures the distribution of the input data, and the discriminator is used to estimate the probability that a sample came from the training data. The generator aims at generating fake samples while the discriminator aims at distinguishing whether the sample is true. The functions of the generator and the discriminator are opposite; that's why GAN is called 'adversarial.' After the convergence of both the generator and the discriminator, the discriminator is supposed unable to recognize the generated samples. Thus, the pre-trained generator can be used to create a batch of samples and use them for further operations such as classification.

Figure 19b shows the procedure of a standard GAN. The generator receives a noise signal \mathbf{s} which is randomly sampled from a multimodal Gaussian distribution and output the fake brain signals \mathbf{x}_F . The discriminator receives the real brain signals \mathbf{x}_R and the generated fake sample \mathbf{x}_F , and then it predicts whether the received sample is real or fake. The internal architecture of the generator and discriminator are designed depending on the data types and scenarios. For instance, we can build the GAN by convolutional layers on fMRI images since CNN has an excellent ability to extract spatial features. The discriminator and the generator are trained jointly. After the convergence,

several brain signals \mathbf{x}_G can be created by the generator. Thus, the training set is enlarged from \mathbf{x}_R to $\{\mathbf{x}_R, \mathbf{x}_G\}$ to train a more effective and robust classifier.

4.4 Hybrid Model

The hybrid deep learning models refer to the models which are composed of at least two deep basic learning models while the basic model belongs to a discriminative, representative, or generative deep learning model. The hybrid models cover two subcategories based on their targets: classification-aimed (CA) hybrid models and the non-classification-aimed (NCA) hybrid models.

Most of the deep learning related studies in BCI are working on the first category. Based on the existing literature, the representative and generative models are employed to enhance the discriminative models. The representative models can provide more informative and low dimensional features for the discrimination while the generative models can help to augment the training data quality and quantity which supply more information for the classification. The CA hybrid models can be further subdivided into²⁰: 1) several discriminative models combined to extract more distinctive and robust features (e.g., CNN+RNN); 2) representative model followed by a discriminative model (e.g., DBN+MLP); 3) generative + representative model followed by a discriminative model; 4) generative + representative model followed by a non-deep learning classifier.

A few NCA hybrid models aim for brain signal reconstruction. For example, St-yves et al. [188] adopted GAN to reconstruct the visual stimuli based on the fMRI images.

5 STATE-OF-THE-ART DL TECHNIQUES FOR BCI

In this section, we will systematically summarize the existing state-of-the-art studies for BCI based on deep learning. Some literature combined deep learning and traditional machine learning methods are also listed.

5.1 Intracortical and ECoG

As a highly invasive method, intracortical brain signals are mainly investigated by researchers in medical or biology area who may not pay much attention to deep learning techniques. Thus, few publications work on intracortical brain signal and ECoG through deep learning algorithms.

Antoniades et al. [12] employed CNN to automatic extract features from epileptic intracortical data in the field of interictal epileptic discharge (IED) detection. IEDs are transients of electrical activities that appear in brainwaves of patients with epilepsy. Their accurate detection and localization are vital to the diagnosis and treatment of epilepsy. This paper designed a CNN model with two convolutional layers to automatically explore the latent features from the raw input signals. The input data are sliced into many 80 ms segments with 40 ms overlapping, and the designed model achieved an epilepsy state recognition accuracy of 87.51%. To solve the problem that the intracortical signals are expensive to collect, the authors also proposed a deep neural architecture to aiming at mapping the scalp signals to pseudo-intracranial brain signals [11].

Most of the ECoG related studies focused on medical healthcare, especially epileptic seizure diagnosis. For example, Hosseini et al. [77] worked on seizure prediction and localization based on scalp EEG and ECoG. The ECoG signals are filtered by a fourth-order Butterworth Bandpass filter (0.5 ~ 150 Hz). After that, the authors manually extracted features through Principal Component Analysis (PCA), ICA, and Differential Search Algorithm (DSA). Then they compared two deep learning structures. The first structure is composed of three convolutional layers followed by a softmax layer, which achieved the binary recognition accuracy of 96%. The second structure

²⁰The representative model followed by a non-deep learning classifier is regarded as a representative deep learning model.

adopted a DBN-AE model with two AE components, and the learned representations were feed into a softmax layer for classification, which obtained the accuracy of around 93%. This work demonstrated that CNN is more powerful than DBN in feature engineering of seizure signals. Kiral-Kornek et al. [93] attempted to develop an epileptic seizure prediction system operatable on a wearable device for the ultra-low power requirement. They proposed an MLP algorithm for the prediction and achieved a mean sensitivity of 69% and a mean time in warning of 27%. Apart from the seizure diagnosis, Xie et al. [225, 226] focused on the finger trajectory from ECoG signals. They developed a hybrid deep learning model based on convolutional layer and LSTM cells. However, the contribution of this paper is that they employed CNN for not only spatial convolution but also temporal convolution. The motivation of temporal convolutional layer was to make the model learn the optimal band partition in a data-driven way. The convolution operation produced fixed-length vector representations to send to the LSTM cell for trajectory tracking. Each ECoG segment lasts for 1 second with 40 ms overlapping. Thus, the model was enabled to receive a stream of ECoG and form a complete finger trajectory.

5.2 EEG

More than half of the recent publications are related to EEG signals for the non-invasive, high-portable and low-price. In this section, we will summarize the state-of-the-art researches based on three aspects which include EEG oscillatory, evoked potentials, and ERD/ERS.

5.2.1 EEG Oscillatory. The spontaneous EEG has a vast range of applications since it has various implications in different scenarios. In particular, the spontaneous EEG contains sleeping EEG, motor imagery EEG, emotional EEG, mental disease EEG, and others. Next, we will present the studies in each scenario and the deep learning models they used.

(1) **Sleeping EEG.** The sleep quality is significant for diagnosing sleep disorders and cultivating the healthy habit. Sleep EEG are mainly used to recognize the sleep stage (or sleep score/state) [35]. In Rechtschaffen and Kales (R&K) rules, the sleep stage includes wakefulness, non-REM (rapid eye movement) 1, non-REM 2, non-REM 3, non-REM 4, and REM. However, there is no clear distinction between non-REM 3 and non-REM 4. Therefore, they are combined into slow wave sleep (SWS) [241]. The American Academy of Sleep Medicine (AASM) recommends segmentation of sleep in five stages: wakefulness, non-REM (rapid eye movement) 1, non-REM 2, SWS, and REM. Generally, in the sleep stage analysis, the EEG signals are preprocessed by a filter which has various passband in different papers, but all notched at 50 Hz. The EEG signals are usually segmented into 30s windows.

(i) *Discriminative models.* Many publications have adopted CNN for sleep stage classification on single-channel EEG [186, 206]. Viamala et al. [214] manually extracted the time-frequency features from the sleeping EEG signals and adopted a CNN algorithm to analyze them. The EEG signals stream, collected from $Fpz - Cz$ and $Pz - Oz$ channels, was sliced into 30 s segments. The employed CNN achieved an accuracy of 86% in five-class classification. Shahin et al. [177] manually extract 57 features in the frequency domain and fed into an MLP for classification, which obtained the accuracy of 90% in insomnia detection. Fernande et al. [49] adopted CNN to analyze the physiological signals including EEG, EOG, and EMG. The model was evaluated over the Sleep Heart Health Scoring dataset and achieved the precision of 91%, recall of 90%, and F-1 score of 90%.

RNN is also often used in sleep disorder detection. Biswal et al. [27] demonstrated that RNN performed better than MLP, CNN on the sleep stage prediction. Tsiouris et al. [207] extracted many features from the time domain, frequency domain, correlation, and graph theoretical features. An LSTM was employed to discover the latent dependencies of the features for seizure detection.

(ii) *Representative models.* Zhang et al. [241] combined a DBN-RBM with three RBMs for sleep feature extraction and traditional machine learning classifiers (e.g., SVM) for classification. Tan et al. [201] adopted a DBN-RBM algorithm to detect sleep spindle from the extracted PSD features of the sleeping EEG signals. They finally reached an F-1 measure of 92.78% in a local dataset.

(iii) *Hybrid models.* Manzano et al. [128, 129] proposed a multi-view model to predict sleep stage by combining CNN and MLP. The CNN was employed to receive the raw EEG data in the time domain while the MLP received the spectrum obtained by Short-Time Fourier Transform (STFT) among 0.5-32 Hz. Supratak et al. [197] proposed a model by combining a multi-view CNN and LSTM for automatic sleep stage scoring based on raw single-channel EEG. The proposed method utilizes convolutional neural networks to extract time-invariant features, and bidirectional-long short-term memory to learn transition rules among sleep stages. Dong et al. [44] proposed a hybrid deep learning model aiming at temporal sleep stage classification. They have taken advantage of MLP for detecting hierarchical features and LSTM for sequential data learning to optimize classification performance with single-channel recordings.

(2) **MI EEG.** Extreme Learning Machine (ELM) [46] Deep learning models have shown the superior on the classification of MI EEG and real-motor EEG [69, 145].

(i) *Discriminative models.* CNN is widely used for the recognition of MI EEG [245]. On the one hand, some studies CNN is only used as a classifier to recognize the manually extracted features [86, 232]. Uktveris et al. [210] extracted a large number of EEG features including Mean channel energy (MCE), Mean window energy (MWE), Channel variance (CV), Mean band power (BP), etc. All the extracted features were sent into a 2-D CNN for classification. Lee et al. [100] first processed the MI EEG signals through wavelet transformation and then manually extracted PSD from mu and beta bands. At last, they employed a CNN model for recognition and achieved an accuracy of 78.93%. Apart from CNN, Zhang et al. [247] used a modified LSTM structure to learn affective information from EEG signals to control smart home appliances.

On the other hand, CNN deals with the raw EEG data based on feature engineering and classification results [202]. Wang et al. [219] designed a fast convolutional feature extraction approach based on CNN to learn the latent features from MI-EEG signals. Several weak classifiers are applied to choose important features for the final classification. Hartmann et al. [69] worked on the EEG signals aroused by real motor action. They investigated how CNN represent spectral features through the sequence of intermediate stages of the network, which showed higher sensitivity to EEG phase features at earlier stages and higher sensitivity to EEG amplitude features at later stages. Moreover, MLP is also applied for MI EEG recognition [193].

(ii) *Representative models.* DBN is widely employed for MI EEG classification for the high representative ability [97, 121]. Ren et al. [162] applied a convolutional DBN based on RBM components. They claimed that the DBN worked better in feature representation than the traditional hand-crafted features (e.g., CSP, band powers). Li et al. [103] processed the EEG signals with discrete wavelet transformation and then applied a DBN-AE based on denoising AE. They achieved the accuracy of 73.86% over a local MI EEG dataset. The authors also use denoising AE to generate the lost values in incomplete EEG signals such as an EEG segment with a portion of data removed (unevenly spaced). Rekar et al. [160] employed an AE model for feature extraction followed by a KNN classifier, which achieved the accuracy of 72.38% in binary classification over a local dataset.

Nurse et al. [146] proposed a model combined MLP with Genetic Algorithm (GA) while the GA was used for optimal hyper-parameter selection (e.g., the number of hidden layers in MLP) and the MLP worked as the classifier. Zhang et al. [252] combined AE with an XGBoost classifier to recognize the EEG signals in a multi-person scenario. The authors also proposed a complex

framework by combing LSTM with reinforcement learning to classify multi-modality signals [248, 253].

(iii) *Hybrid models*. Several studies proposed hybrid models for the recognition of MI EEG [41]. Fraiwan et al. [50] combined DBN with MLP for neonatal sleep state identification. There are twelve features are extracted from the time and frequency domain of the sleeping EEG signals, which will be refined by a designed DBN-AE. After that, the MLP classifier gave an accuracy of 80.4% on a public dataset. Tabar et al. [198] combined the time, frequency and location information of the EEG signals as the input data which would be fed into a CNN for high-level feature extraction. The features are classified through a DBN-AE with seven AEs while the hidden layer of AE only has two nodes which responding to the probability of the two labels. Tan et al. [200] proposed a complicated system to achieve the multimodal EEG classification. A denoising AE is employed for dimensional reduction. A multi-view CNN combined with RNN was proposed to discover the latent temporal and spatial information from the low-dimension representations. They obtained an average accuracy of 72.22% over the Ila dataset from BCI competition IV.

(3) **Emotional EEG**. The emotion of an individual can be evaluated by three aspects: the valence, arousal, and dominance. Each aspect can be rated by an integer between 1 to 9 or can be divided into positive and negative. The combination of the three aspects formed the emotions which are familiar to us like fear, sadness, anger. The subject's EEG signals could predict the affective state.

(i) *Discriminative models*. In the beginning, the basic MLP is adopted to classify the manually extracted features when deep learning first arose [234]. Frydenlund et al. [51] extracted the average and standard deviation of each EEG band and then fed them into an MLP for emotional affect estimation.

However, CNN is the most popular in the area of EEG based emotion prediction [105, 117]. Li et al. [105] proposed a hierarchical CNN to implement the EEG-based emotion classifier (positive, negative and neutral) in a movie-watching task. Differential Entropy (DE) is calculated as the main feature. This paper first proposes that converting multi-channel EEG signals into a 2-D matrix, which take advantage of the spatial dependencies among EEG channels. For the emotion recognition task, this paper compared the proposed CNN with a DBN-AE and demonstrated that CNN has better performance than DBN, which is similar to [77]. Wang et al. [216] employed a CNN algorithm to classification the emotional EEG singles. The interesting part is that they augmented the training set by generating new EEG samples by adding Gaussian noise on the original samples. Li et al. [106] proposed a novel hierarchical convolutional neural network (HCNN) to recognize the subject's emotion (positive, neutral, and negative) and obtained the accuracy of 88.2%. In the HCNN structure, each convolutional kernel only has localized receptive field, so the kernels can capture the correlations among adjacent electrodes, which might be of great value for the recognition task.

RNN and the variations are another widely used discriminative models. Talathi [199] utilized a discriminative deep learning model composed of GRU cells to detect early seizure disease and achieved competitive performance. Zhang et al. [244] proposed a spatial-temporal recurrent neural network (STRNN) to integrate the feature learning from both spatial and temporal information. To capture those spatially co-occurrent variations of human emotions, a multidirectional RNN layer can capture long-range contextual cues by traversing the spatial regions of each temporal slice along with different directions. Then, a bi-directional temporal RNN layer is further used to learn the discriminative features characterizing the temporal dependencies of the sequences produced by the spatial RNN layer.

(ii) *Representative models*. DBN, especially DBN-RBM, is widely used for the unsupervised representation ability in emotion recognition [53, 107, 110]. For instance, Xu et al. [227] claimed that they proposed a DBN-RBM algorithm with three RBMs and an RBM-AE to predict the subject's

affective state. Nevertheless, it is not a strictly semi-supervised method that the model claimed by [227] is composed of unsupervised feature representation and a supervised softmax layer. The authors also tried to manually extract the PSD features from 14 narrow-down bands of the EEG signals and then fed into DBN-RBM for classification [228]. In Alzheimer's Disease diagnosis, Zhao et al. [254] adopted DBN-RBM with three RBMs to extract informative representations after the filtering (0.5 ~ 30 Hz). The proposed representative model is combined with a traditional classifier (SVM) and achieved the accuracy of 92%. Another work combined DBN-RBM with Hidden Markov Model (HMM) and achieved an accuracy of 87.62% in a local dataset [258].

Compared to other repetitive models, D-RBM only appears in a few studies. Zheng et al. [255, 256] introduced a D-RBM with five hidden RBM layers to investigate the critical frequency bands and channels in emotion recognition. The authors claimed that they hired a DBN-RBM; however, the RBMs are trained jointly. Thus it is regarded as D-RBM in this survey. Jia et al. [85] proposed an interesting algorithm which is composed of RBMs. The algorithm contains a channel selection section and an RBM classifier. The data from each EEG channels are reconstructed through RBM; then, the channels with high error would be eliminated. Then the representative features of the residual channels are sent to D-RBM for affective state recognition.

The emotion is affected by many subjective and environmental factors, such as gender, fatigue, etc. Yan et al. [118, 230] investigated the differences between males and females in emotion recognition using EEG and eye movement data. They proposed a novel model called Bimodal Deep AutoEncoder (BDAE) which is, however, actually formed by RBMs. The BDAE received both EEG and eye movement features and shared the information in a fusion layer which connected with an SVM classifier. The results showed that the fearful emotion is more diverse among women compared with men, and men behave more diversely on the sad emotion compared with women. Moreover, individual differences in fear are more pronounced than the other three emotions for females.

To overcome the mismatched distribution among the samples collected from different subjects or different experimental sessions, Chai et al. [34] proposed an unsupervised domain adaptation technology which is called subspace alignment autoencoder (SAAE). SAAE combined an AE and a subspace alignment solution, which could take advantage of both nonlinear transformation and a consistency constraint. The proposed approach obtained a mean accuracy of 77.88% in person independent scenario.

(iii) *Hybrid models*. One common-used hybrid model is a combination of RNN and MLP. For example, Alhagry et al. [8] employed an LSTM architecture for feature extraction from emotional EEG signals, and the features are forwarded into an MLP for classification, which got 85.65%, 85.45%, and 87.99% on arousal, valence, and liking classes, respectively. Furthermore, Yin et al. [237] proposed a multi-view ensemble classifier to recognize emotions using multimodal physiological signals. The ensemble classifier contains several D-AEs with three hidden layers and a fusion structure. Each D-AE receives one physiological signal (e.g., EEG, EOG, EMG) and then sends the outputs of D-AE to a fusion structure which is composed of another D-AE. At last, an MLP classifier classifies the mixed features. Kawde et al. [90] implemented an affect recognition system by combining a DBN-RBM for effective feature extraction and an MLP for classification.

(4) **Mental Disease EEG**. A large number of researchers exploited EEG signals to diagnose neurological disorders, especially epileptic seizure [240].

(i) *Discriminative models*. The CNN is widely used in the automatic detection of epileptic seizure [3, 173, 211, 218]. For example, Johansen et al. [87] adopted CNN to work on the high-passed (1 Hz) EEG signals of epileptic spike and achieved an AUC of 94.7%. Acharya et al. [4] employed a CNN model with 13 layers (5 convolutional layers, five pooling layers, and three fully-connected layers)

on depression detection. The method was evaluated on a local dataset with 30 subjects (15 normal and 15 depressed) and achieved the accuracies of 93.5% and 96.0% using EEG signals from the left and right hemisphere, respectively. Morabito et al. [137] tried to exploit a CNN structure to extract suitable features of multi-channel EEG signals to classify Alzheimer's Disease from a prodromal version of dementia (Mild Cognitive Impairment, MCI) and age-matched Healthy Controls (HC). The EEG signals are filtered in bandpass (0.1 ~ 30 Hz) and finally achieved an accuracy of around 82% for three-class classification.

In some research, the discriminative model is only employed for feature extraction. For example, Ansari et al. [10] used CNN to extract the latent features which will be fed into a Random Forest classifier for the final seizure detection of neonatal babies. Chu et al. [38] employed CNN for feature extraction which was sent to a random forest for schizophrenia recognition.

REM Behavior Disorder (RBD) may cause many mental disorder diseases like Parkinson's disease (PD). Ruffini et al. [164] described an Echo State Networks (ESNs) model to distinguish RBD from healthy individuals. ESN, as a particular class of RNN, implements nonlinear dynamics with memory and seem ideally poised for the classification of complex time series data. The central concept in ESNs and related types of so-called fireservoir computationfi systems is to have data inputs drive a semi-randomly connected, large, fixed recurrent neural network (the fireservoirfi) where each node/neuron in the reservoir is activated in a nonlinear way.

(ii) *Representative models.* For the disease detection, one commonly used method is adopting a representative model (e.g., DBN) followed by a softmax layer for classification [209, 229]. Page et al. [149] adopted DBN-AE to extract useful features from seizure EEG signals. The extracted features were fed into a traditional logistic regression classifier for seizure detection. Al et al. [7] proposed a multi-view DBN-RBM structure to analyze EEG signals from depression patients. The proposed approach contains multiple input pathways, composed of two RBMs, while each corresponded to one EEG channel. All the input pathways would merge into a shared structure which is composed of another RBMs. The results showed that the multi-view DBN-RBM achieved competitive results. Yuan et al. [239] parallelly extract EEG context features by using global principal component analysis (GPCA), deep denoising AE, and EEG embeddings, respectively. The multi-features are concatenated into a fixed-length feature vector for seizure classification.

Some papers would like to preprocess the EEG signals through dimensionality reduction methods such as PCA and ICA [78] while others prefer to direct fed the raw signals to the representative model [111]. Lin et al. [111] proposed a sparse D-AE with three hidden layers to extract the representative features from epileptic EEG signals while Hosseini et al. [78] adopted a similar sparse D-AE with two hidden layers.

(iii) *Hybrid models.* A popular hybrid method is a combination of RNN and CNN. Shah et al. [176] investigated the performance of CNN-LSTM on seizure detection after channel selection. They used a reduced number of channels ranging from 8 to 20 achieved sensitivities between 33% and 37% with false alarms in the range of 38% and 50%. Golmohammadi et al. [56] proposed a hybrid architecture for automatic interpretation of EEG that integrates temporal and spatial context for sequential decoding of EEG events. 2D and 1D CNNs capture the spacial features while LSTM networks capture the temporal features. The authors claimed sensitivity of 30.83% and a specificity of 96.86% on the well-known TUH EEG seizure corpus.

In the detection of early-stage Creutzfeldt-Jakob Disease (SJD), Morabito et al. [138] combined D-AE and MLP together. The EEG signals of SJD were first filtered by bandpass (0.5~70 Hz) and then fed into a D-AE with two hidden layers for feature representation. At last, the MLP classifier obtained the accuracy of 81~ 83% in a local dataset. Convolutional autoencoder, replacing the

fully-connected layers in a standard AE by convolutional and de-convolutional layers, is applied to extract the seizure features in an unsupervised manner [223].

(5) **Data augmentation.** The generative models such as GAN could be used for data augmentation in BCI classification [1]. Palazzo et al. [150] first demonstrated that brain activity EEG signals encode visually-related information that enables to discriminate between visual object categories accurately. Then, they extracted a more compact class-dependent representation of EEG data using recurrent neural networks. At last, they used the learned EEG manifold to condition image generation employing GANs, which, during inference, will read EEG signals and convert them into images. Kavasidis et al. [88] aiming at converting EEG signals into images. The EEG signals were collected when the subjects were observing images on a screen. An LSTM layer was employed to extract the latent features from the EEG signals, and the extracted features were regarded as the input of a GAN structure. The generator and the discriminator of the GAN were both composed of convolutional layers. The generator was supposed to generate an image based on the input EEG signals after the pre-training. Abdelfattach et al. [1] adopted a GAN on seizure data augmentation. The generator and discriminator are both composed of fully-connected layers. The authors demonstrated that GAN outperforms AE and VAE. After the augmentation, the classification accuracy increased dramatically from 48% to 82%.

(6) **Others** Some researches have explored a wide range of exciting topics. The first one is how EEG affected by audio/visual stimuli. This differs from the potentials evoked by audio/visual stimulations because the stimuli in this phenomenon always exist instead of flicking in a particular frequency. Stober et al. [190, 191] claimed that EEG signals of rhythm perception might contain enough information to distinguish different rhythm types/genres or even identify the rhythms themselves. The authors conducted an experiment where 13 participants were stimulated by 23 rhythmic stimuli including 12 East African and 12 Western stimuli. For the 24-category classification, the proposed CNN achieved a mean accuracy of 24.4%. After that, the authors exploited convolutional AE for feature learning and CNN for classification and achieved an accuracy of 27% for 12-class classification [192]. Sternin et al. [189] adopted CNN to extract discriminative features from the EEG signals to distinguish whether the subject was listening or imaging music. Similarly, Sarkar et al. [170] designed two deep learning models to recognize the EEG signals aroused by audio or visual stimuli. For this binary classification task, the proposed CNN and DBN-RBM with three RBMs achieved the accuracy of 91.63% and 91.75%, respectively. Furthermore, the spontaneous EEG could be used to distinguish the user's mental state (logical versus emotional) [21].

Moreover, some researchers focus on the impact of cognitive load on EEG [180] or physical workload [58]. Bashivan et al. [23] first extract informative features through wavelet entropy and band-specific power which would be fed into a DBN-RBM for further refining. At last, an MLP is employed for cognitive load level recognition. The authors, in another work [22], also denoted to find representations that are invariant to inter- and intra-subject differences from multi-channel EEG time-series in the context of the mental load classification task. They transformed EEG activities into a sequence of topology-preserving multi-spectral images and then trained a recurrent-convolutional network to preserve the spatial, spectral, and temporal features of the EEG signals. Yin et al. [236] collected the EEG signals from different mental workload levels (e.g., high and low) for binary classification. The EEG signals are filtered by a low-pass filter, transformed to the frequency domain and be calculated the power spectral density (PSD). The extracted PSD features were fed into a denoising D-AE structure for future refining. They finally got an accuracy of 95.48%. Li et al. [108] worked on the recognition of mental fatigue level including alert, slight fatigue, and severe fatigue. They adopted a simple DBN-RBM to extract the related features from single-channel EEG.

In addition, EEG based driver fatigue detection is an attractive area [33, 45, 65, 65, 67]. Huang et al. [82] designed a 3D CNN to predict the reaction time in drowsiness driving. This is meaningful to reduce traffic accident. Hajinoroozi et al. [64] adopted a DBN-RBM to handle the EEG signals which were processed by ICA. They achieved an accuracy of around 85% in binary classification ('drowsy' or 'alert'). The strength of this paper is that they evaluated the DBN-RBM on three levels: time samples, channel epochs, and windowed samples. The experiments showed that the channel epoch level provided the best performance. San et al. [169] combined deep learning models with a traditional classifier to detect driver fatigue. The model contains a DBN-RBM structure followed by an SVM classifier, which achieved the detection accuracy of 73.29%. Almogbel et al. [9] investigated the drivers' mental state under high workload and low workload. A proposed CNN is claimed to detect the driver's cognitive workload directly based on the raw EEG signals.

The research of the detection of eye state has shown exceeding accuracy. Narejo et al. [141] explored the detection of eye state (closed or open) based on EEG signals. They tried a DBN-RBM with three RBMs and a DBN-AE with three AEs and achieved a very high accuracy of 98.9%. Reddy et al. [159] tried a simpler structure, MLP, for eye state detection and got a slightly lower accuracy of 97.5%.

There are still a lot of promising areas that haven't draw much attention now. Baltatzis et al. [18] adopted CNN to detect school bullying through the EEG when watching the specific video. They achieved 93.7% and 88.58% for binary and four-class classification. Khurana et al. [91] proposed deep dictionary learning that outperformed several deep learning methods. Volker et al. [215] evaluated the use of Deep CNN in flanker task, which achieved an averaging accuracy of 84.1% within subject and 81.7 on the unseen subject. Zhang et al. [246] combined CNN and graph network to discover the latent information from the EEG signal.

Miranda-Correa et al. [136] proposed a cascaded framework by combing RNN and CNN to predict individuals' affective level and personal factors (Big-five personality traits, mood, and social context). An experiment conducted by Putten et al. [157] attempted to identify the user's gender based on their EEG signals. They employed a standard CNN algorithm and achieved the binary classification accuracy of 81% over a local dataset. The detection of emergency braking intention could help to reduce the responses time. Hernandez et al. [73] demonstrated that the driver's EEG signals could distinguish braking intention and normal driving state. They combined a CNN algorithm which achieved the accuracy of 71.8% in binary classification. Behncke et al. [24] applied deep learning, a CNN model, in the context of robot assistive devices. They attempted to use CNN to improve the accuracy of decoding robot errors from EEG while the subject watching the robot both during an object grasping and a pouring task.

Teo et al. [203, 204] tried to combine the BCI and recommender system, which predicted the user's preference by EEG signals. A cohort of 16 users was shown 60 bracelet-like objects as rotating visual stimuli (a 3D object) on a computer display while their preferences and EEGs were recorded. Then, an MLP algorithm was adopted to classify the user like or dislike the object. This exploration got the prediction accuracy of 63.99%. Some researchers have tried to explore a common framework which can be used for various BCI paradigms. Lawhern et al. [99] introduced a compact CNN for EEG-based BCI. The authors described the use of depth-wise and separable convolutions to construct an EEG-specific model which encapsulates well-known EEG feature extraction concepts for BCI. The proposed EEGNet is evaluated on four BCI paradigms: P300 visual-evoked potentials, error-related negativity responses (ERN), movement-related cortical potentials (MRCP), and sensory-motor rhythms (SMR).

5.2.2 Evoked Potential. (1) **ERP** In most situations, the ERP signals are analyzed through P300 phenomena. Meanwhile, almost all the studies on P300 are based on the scenario of ERP. Therefore,

in this section, a majority of the P300 related publications are introduced in the subsection of VEP/AEP according to the scenario.

(i) *VEP* VEP is one of the most popular subcategories of ERP [63, 187, 235]. Ma et al. [135] worked on motion-onset VEP (mVEP) by extracting representative features through deep learning. They used the improved multi-level compressed sensing combined with the genetic algorithm as the first stage to compress the original mVEP EEG. The compressed signals were sent to a DBN-RBM algorithm to capture the more abstract high-level features. Maddula et al. [123] filtered the P300 signals with visual stimuli by a bandpass filter (2 ~ 35 Hz) and then fed into a proposed hybrid deep learning model for further analysis. The model includes a 2D CNN structure to capture the spatial features followed by an LSTM layer for temporal feature extraction. Liu et al. [116] combined a DBN-RBM representative model with an SVM classifier for concealed information test and achieved a high accuracy of 97.3% over a local dataset. Gao et al. [52] employed an AE model for feature extraction followed by an SVM classifier. In the experiment, each segment contains 150 points which were divided into five time-steps, and each step had 30 points. This model achieved an accuracy of 88.1% over a local dataset. A wide range of P300 related studies is based on P300 speller [179] which allows the user to write characters as introduced in Section 3.3.2. Cecotti et al. [29] tried to increase the P300 detection accuracy for more precise word-spelling. A new model was presented based on CNN, which including five low-level CNN classifiers with the different feature set and the final high-level results are voted by the low-level classifiers. The highest accuracy reached 95.5% over the dataset II from the third BCI competition. Liu et al. [115] proposed a Batch Normalized Neural Network (BN³) which is a variant of CNN in P300 speller. The proposed method consists of six layers, and the batch normalization was operated in each batch. Kawasaki et al. [89] employed an MLP model to detect P300 segments from non-P300 segments and achieved the accuracy of 90.8%.

(ii) *AEP* A few works focused on the recognition of AEP. For example, Carabez et al. [28] proposed and tested 18 CNN structures to identify and classify single-trial AEP signals. In the experiment, the auditory stimuli following the oddball paradigm were presented via earphones from six different virtual directions. The authors found that the models that consider data from both the time and space domains and those that overlap in the pooling process usually offer better results regardless of the number of CNN layers. The AEP signals are filtered by 0.1 ~ 8 Hz and downsampled from 256 Hz to 25 Hz. The experimental results showed that the downsampled data works better.

(iii) *RSVP* Among various VEP diagrams, RSVP has attracted much attention [59]. In the analysis of RSVP, a number of discriminative deep learning models (e.g., CNN [29, 112, 185] and MLP [131]) has achieved a big success. A common preprocessing method used in RSVP signals is frequency filtering. The pass bands are generally ranged from 0.1 ~ 50 Hz [126, 178]. Cecotti et al. [30] worked on the classification of ERP signals in RSVP scenario. This paper proposed a CNN algorithm with a layer dedicated to spatial filtering for the detection of the specific target in RSVP. In the experiment, the images of faces and cars were regarded as target or non-target, respectively. Each image was presented for 500 ms and immediately replaced by the subsequent image. In each session, the target probability was 10%. The proposed model offered an AUC of 86.1%. Yoon et al. [238] provided a way to analyze the spatial and temporal features of ERP. The authors trained a CNN with two convolutional layers whose feature maps represented spatial and temporal features of the event-related potential. The results demonstrated that nonilliterate subjects' ERP shows a high correlation between the occipital lobe and parietal lobe, whereas illiterate subjects only show the correlation between neural activities from the frontal lobe and central lobe. Most importantly, they found that the P700 may be used to distinguish illiterate and nonilliterate subjects when the P300

peak is not shown in some subjects' ERP signals. Hajinoroozi et al. [66] adopted a CNN model for cross-subject and cross-task detection of RSVP. CNN was designed to capture both temporal and spatial features. The experimental results showed that CNN worked good in cross-task but failed to get satisfying performance in the cross-subject scenario. Mao et al. [130] compared three different deep learning models in the prediction of whether the subject had seen the target or not. The MLP, CNN, and DBN models obtained the AUC of 81.7%, 79.6%, and 81.6%, respectively. The author also applied a CNN model to analyze the RSVP signals for person identification [132].

The representative deep learning models are also applied in RSVP. Vareka et al. [212] verified if deep learning performs well for single trial P300 classification. They conducted an RSVP experiment while the subjects were asked to recognize the target from non-target and distracters. The A DBN-AE was implemented and compared with some non-deep learning algorithms. The DBN-AE was composed of five AEs while the hidden layer of the last AE only has two nodes which can be used for classification through softmax function. Finally, the proposed model achieved the accuracy of 69.2%. Manor et al. [127] applied two deep learning models to deal with the RSVP signals after lowpass filtering (0 ~ 51 Hz). The discriminative CNN achieved the accuracy of 85.06%. Meanwhile, the representative convolutional D-AE achieved the accuracy of 80.68%.

(3) **SSEP**. Most of deep learning based studies in SSEP area focus on SSVEP like [6, 98]. SSVEP are neural oscillations from the parietal and occipital regions of the brain evoked from flickering visual stimuli. Attia et al. [14] aimed at finding an appropriate intermediate representation of SSVEP. A hybrid method combined CNN and RNN was proposed to capture the meaningful features from the time domain directly, which achieved the accuracy of 93.59%. Waytowich et al. [221] applied a compact CNN model to directly work on the raw SSVEP signals without any hand-crafted features. The reported cross subject mean accuracy was approximately 80%. Thomas et al. [205] first filter the raw SSVEP signals through a bandpass filter (5 ~ 48 Hz) and then operated discrete FFT on consecutive 512 points. The processed data were classified by a CNN (69.03%) and an LSTM (66.89%) independently.

Perez et al. [153] adopted a representative model, a sparse AE, to extract the distinct features from the SSVEP from multi-frequency visual stimuli. The proposed model employed a softmax layer for the final classification and achieved the accuracy of 97.78%. Kulasingham et al. [96] classified SSVEP signals in the context of guilty knowledge test. The authors applied DBN-RBM and DBN-AE independently and achieved the accuracy of 86.9% and 86.01%, respectively. Hachem et al. [62] investigated the influence of fatigue on SSVEP through an MLP model during wheelchair navigation. The goal of this study was to seek the key parameters to switch between manual, semi-autonomous, and autonomous wheelchair command. Aznan et al. [16] explored the SSVEP classification where the signals were collected through dry electrodes. The dry signals were more challenging for the lower SNR than standard EEG signals. This study applied a CNN discriminative model and achieved the highest accuracy of 96% over a local dataset.

5.2.3 ERD/ERS. ERD/ERS is not widely used in BCI due to the drawbacks like unstable accuracy cross subjects [81]. In most situations, the ERD/ERS is regarded as a specific feature of EEG powers for further analysis [41, 198]. In particular, the ERD/ERS were calculated as relative changes in power concerning baseline [37]:

$$ERD/ERS = \frac{P_e - P_b}{P_b}$$

, where P_e denotes the average power over one-second window during the event and P_b denotes the average power in a one-second window during baseline which is before the event. Generally, the baseline refers to the rest state. For example, Sakhavi et al. [167] calculated the ERD/ERS map

and analyzed the different patterns among different tasks. The analysis demonstrated that the dynamic of energy should be considered because static energy is not sufficient for some tasks.

5.3 fNIRS

Up to now, only a few of researchers paid attention on deep learning based fNIRS. Naseer et al. [143] analyzed the difference between two mental tasks (mental arithmetic and rest) based on fNIRS signals. The authors manually extracted six features from the prefrontal cortex fNIRS and compared six different classifiers. The results demonstrated that the MLP with the accuracy of 96.3% outperformed all the traditional classifiers including SVM, KNN, naive Bayes, etc. Huve et al. [83] classified the fNIRS signals which were collected from the subjects during three mental states including abstractions, word generation, and rest. The employed MLP model achieved the accuracy of 66.48% based on the hand-crafted features (e.g., the concentration of OxyHb/DeoxyHb). After that, the authors study the mobile robot control through fNIRS signals and got the binary classification accuracy of 82% (offline) and 66% (online) [84]. Chiarelli et al. [37] exploited the combination of fNIRS and EEG for left/right MI EEG classification. Sixteen features extracted from fNIRS signals (eight from OxyHb and eight from DeoxyHb) were fed into an MLP classifier with four hidden layers.

On the other hand, Hiroyasu et al. [75] attempted to detect the gender of the subject through their fNIRS signals. The authors employed a denoising D-AE with three hidden layers to extract distinctive features to be fed into an MLP classifier for gender detection. The model was evaluated over a local dataset and achieved the average accuracy of 81%. This paper also pointed out that, compared with PET and fMRI, fNIRS is cheaper and can measure cerebral blood flow changes in high time resolution.

5.4 fMRI

Recently, several deep learning methods have been applied to fMRI analysis, especially on the diagnosis of cognitive impairment [213, 222].

(1) Discriminative models

Among the discriminative models, CNN is a promising model to analysis fMRI [182]. For example, Havaei et al. [71] presented brain tumor segmentation approaches based on fMRI. A novel CNN algorithm was proposed, which can capture both the local features and the global features simultaneously. The convolutional filters have different size. Thus, the small-size and large-size filter could exploit the local and global features, independently. Tu et al. [208] used simultaneous EEG-fMRI dataset to demonstrate that the temporal and spatial hierarchical correspondences between the multi-stage processing in CNN and the activity observed in the EEG and fMRI. Sarraf et al. [171, 172] applied deep CNN to recognize Alzheimer's Disease based on fMRI data for three-class recognition (normal, edema, or active tumor). Morenolopez et al. [139] employed a CNN model to deal with fMRI of brain tumor patients. The model was evaluated over BRATS dataset and obtained the F1 score of 88%. Hosseini et al. [79] employed CNN for feature extraction. The extracted features were classified by SVM for the detection of an epileptic seizure.

Furthermore, Li et al. [109] proposed a data completion method based on CNN. In particular, utilizing the information from fMRI data to complete positron emission tomography (PET), then train the classifier based on both fMRI and PET. In the model, the input data of the proposed CNN is the fMRI patch with shape [15, 15, 15] and the output is a PET patch with shape [3, 3, 3]. There are two convolutional layers with ten filters each to mapping the input to output. The experiments illustrated that the classifier trained by the combination of fMRI and PET (92.87%) outperformed the one trained by solo fMRI (91.92%)

Moreover, Koyamada et al. [95] used a nonlinear MLP to extract common features from different subjects. The model is evaluated over a dataset from the Human Connectome Project (HCP).

(2) *Representative models* A wide range of publications demonstrated the effectiveness of representative models in recognition of fMRI data [26, 194]. Hu et al. [80] used demonstrated the advantages of deep learning in diagnosing brain disease and providing clinical decision support in Alzheimer's disease detection. Firstly, the fMRI images were converted to a matrix to represent the activity of 90 brain regions. Secondly, a correlation matrix is obtained by calculating the correlation between each pair of brain regions to represent the functional connectivity between different brain regions. Furthermore, a targeted AE is built to classify the correlation matrix, which is sensitive to AD. The proposed approach achieved an accuracy of 87.5%. Plis et al. [156] employed a DBN-RBM with three RBM components to extract the distinctive features from ICA processed fMRI and finally achieved an average F1 measure of above 90% over four public datasets. Suk et al. [195] compared the effectiveness of DBN-RBM and DBN-AE on Alzheimer's disease detection. The experimental results showed that the former obtained the accuracy of 95.4% which is slightly lower than the latter (97.9%). Suk et al. [196] applied a D-AE model to extract latent features from the resting-state fMRI data on the diagnosis of Mild Cognitive Impairment (MCI). The latent features are classified by SVM and achieved the accuracy of 72.58%. Ortiz et al. [147] proposed a multi-view DBN-RBM to receives the information of MRI and PET simultaneously. The learned representations were sent to several simple SVM classifiers which were ensembled to form a high-level stronger classifier by voting.

(3) *Generative models*

The reconstruction of natural image based on fMRI data has been attracted lots of attention [68, 175, 181, 244]. Seeliger et al. [175] proposed a deep convolutional GAN for reconstructing visual stimuli from fMRI. The objective was to create an image similar to the presented stimulus image through the well-trained generator. The generator is composed of four convolutional layers to convert the input fMRI to a natural image. Han et al. [68] focused on the generation of synthetic multi-sequence fMRI using GAN. The generated image can be used for data augmentation for better diagnostic accuracy or physician training to help better understand various diseases. The authors applied the existing Deep Convolutional GAN (DCGAN) [158] and Wasserstein GAN (WGAN) [13] and found that the former works better. Shen et al. [181] presented a novel image reconstruction method, in which the pixel values of a generated image are optimized to make its features, which is decoded by MLP, similar to those decoded from the real fMRI.

5.5 EOG

In most situations, the EOG signals were regarded as artifacts which should be removed from the collected EEG. However, it also could be used as the informative signals to deployment EOG based BCI. Although there were a few researchers paid attention to EOG analysis, only limited papers utilized deep learning. For example, Xia et al. [224] attempted to detect the subjects' sleep stage only using EOG signals. They employed a DBN-RBM for feature representation and a HMM for classification. Moreover, EOG has been widely used as supplementation of other signals (e.g., EEG) in several research topics such as emotion detection [90, 118, 218], sleep stage recognition [49, 197], and driving fatigue detection [45].

5.6 MEG

Garg et al. [54] worked on the refining of MEG signals by removing the artifacts like eye-blinks and cardiac activity. The MEG singles were decomposed by ICA first and then classified by a 1-D CNN model. At last, the proposed approach achieved the sensitivity of 85% and specificity of 97%

over a local dataset. Hasasneh et al. [70] also focused on artifacts detection (cardiac and ocular artifacts). The proposed approach uses CNN to capture temporal features and MLP to extract spatial information. Shu et al. [183] employed a sparse AE to learn the latent dependencies of MEG signals in the task of single word decoding. The results demonstrated that the proposed approach is advantageous for some subjects although it didn't produce an overall increase in decoding accuracy. Cichy et al. [40] applied a CNN model to recognize visual object based on MEG and fMRI signals.

5.7 Discussion

In this section, we first analyze what is the most suitable deep learning models for BCI signals. Then, we will summarize the popular deep learning models in BCI research. We hope this survey could help our readers to select the most effective and efficient methods when dealing with BCI signals. In Table 5 and Table 5, we summarize the BCI signals and the corresponding deep learning models of the state-of-the-art papers. In hybrid models are divided into three parts: the combination of RNN and CNN, the combination of representative and discriminative models, and others. Figure 20 illustrated of the publications proportion for crucial BCI signals and deep learning models.

5.7.1 BCI Signal based Discussion. Our investigations above reveal that studies on non-invasive signals dominate the BCI research. Among the summarized 238 publications, there are only seven focused on invasive BCI and most of them worked on ECoG instead of intracortical signals. One important reason result in this phenomena is that the invasive BCI has a higher requirement on the hardware and experiment environments. For example, the collection of ECoG signals needs a volunteer patient and a surgeon who can operate craniotomy which makes most researchers unqualified. Moreover, there are few public datasets of invasive brain signals. Therefore, most people can not access the invasive data. In terms of the classification of invasive signals, CNN-related algorithms often have higher ability to recognize the pulse within cortex neurons.

Besides, among the non-invasive signals, the studies on EEG is far more than the sum of all the other BCI paradigms (fNIRS, fMRI, EOG, and MEG). Furthermore, there are about 70% of the EEG papers pay attention to the spontaneous EEG (133 publications). For better understanding, we split the spontaneous EEG into several aspects: the sleeping, the motor imagery, the emotional, the mental disease, the data augmentation, and others. First, the classification of the sleeping EEG mainly depends on the discriminative and the hybrid models. Among the nineteen studies about sleeping stage classification, there are six employed CNN and the modified CNN models independently while two papers adopted RNN models. There are three hybrid models were built based on the combination of CNN and RNN. Second, in terms of the research on MI EEG (30 publications), the independent CNN and CNN based hybrid models are widely used. As for the representative models, DBN-RBM is often applied to capture the latent features from the MI EEG signals. Third, there are twenty-five publications related to spontaneous emotional EEG. More than half of them employed representative models (such as D-AE, D-RBM, especially DBN-RBM) for unsupervised feature learning. Most affective state recognition works recognize the user's emotion as positive, neutral, or negative. Some researchers take a further step to classify the valence, and the arouse rate, which is more complex and challenging. Fourth, the research on mental disease diagnosis is promising and attracting. The majority of the related research focuses on the detection of epileptic seizure and Alzheimer's Disease. Since the detection is a binary classification problem, many studies can achieve a high accuracy like above 90%. In this area, the standard CNN model and the D-AE are prevalent. One possible reason is that CNN and AE are the most well-known and effective deep learning models for classification and dimensionality reduction. Fifth, several publications pay attention to the GAN based data augmentation. At last, about thirty studies are investigating other spontaneous EEG such as driving fatigue, audio/visual stimuli impact,

Table 5. The summary of BCI studies based on deep learning models. Repr + Discr represents the hybrid models which combined representative and distinctive models.

BCI Signals				Deep Learning Models													
				Discriminative Models			Representative Models				Generative Models		Hybrid Models				
				MLP	RNN	CNN	AE (D-AE)	RBM (D-RBM)	DBN		VAE	GAN	LSTM+CNN	Repr + Discr	Others		
						DBN-AE	DBN-RBM										
Invasive				[93]		[12, 77]							[225]	[11, 77] [226]			
Non-invasive Signals	EEG	Spontaneous EEG	Sleeping EEG	[27, 177]	[27, 207]	[214],[35], [186, 206], [27, 49] [100], [210], [145],[242],		[201, 241]					[197] [27]	[50]	[128], [44, 129]		
			MI EEG	[37],[193]	[249], [245, 247]	[86],[99], [69, 232] [202]	[104, 160] [252]		[103]	[97, 162], [121]	[41]		[200, 250]	[198],[46]	[146, 248], [167, 219] [253]		
			Emotional EEG	[51]	[244]	[105],[117], [216], [106, 218] [211],[4], [3],[137],	[34],[230], [118]	[255, 256] [85]		[227]	[85],[227], [110],[228], [107, 258]			[136]	[53, 90] [237]	[8]	
			Mental Disease EEG	[240]	[199],[164]	[173],[79], [10, 87] [77]	[239],[111], [138, 229], [223]			[149]	[209, 254]				[176]	[77, 78], [7, 56]	
			Data Augmentation													[1, 41], [150] [88]	
			Others	[159, 203] [234]	[180]	[24], [82], [18],[190], [180],[215],[73], [9, 157] [65, 65] [38, 189]	[236],[45]			[141]	[64],[141], [108, 169]		[65, 65]	[192],[23, 33]	[246]		

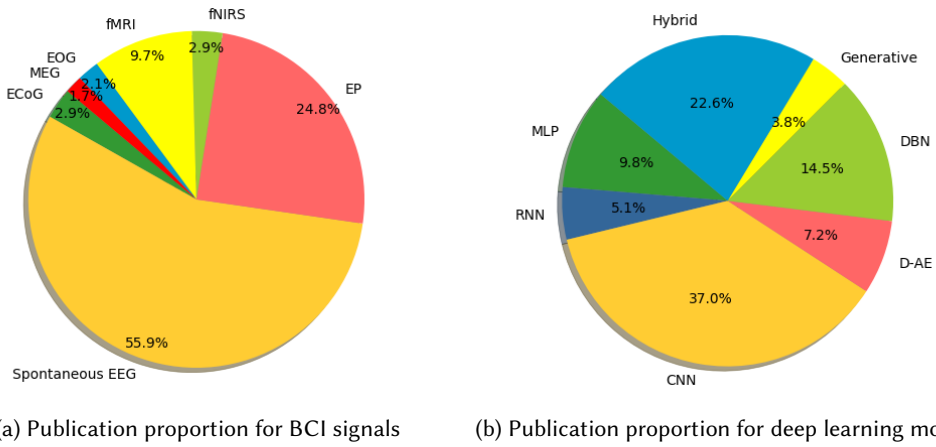


Fig. 20. Illustration of the publications proportion for crucial BCI signals and deep learning models.

cognitive/mental load, and eye state detection. These studies extensively apply standard CNN models and variants.

Moreover, apart from spontaneous EEG, evoked potentials also attracted much attention. On the one hand, in ERP, VEP and the subcategory RSVP has drawn lots of investigations because visual stimuli, compared to other stimuli, is easier to be conducted and more applicable in the real world (e.g., P300 speller can be used for brain typing). For VEP (21 publications), there are 11 studies applied discriminative models and six works adopted hybrid models. In terms of RSVP, the sole CNN dominates the algorithms. Apart from them, five papers focused on the analysis of AEP signals. On the other hand, among the steady-state related researches, only SSVEP has been studied by deep learning models. Most of them only applied discriminative models on the recognition of the target image. At last, few papers attempted to investigate the ERD/ERS singles. Several publications utilized ERD/ERS to analyze the signals and calculated the ERD/ERS value as a distinct feature.

Furthermore, beyond the diverse EEG diagrams, a wide range of papers paid attention to fNIRS and fMRI. The fNIRS images are rarely studied by deep learning and the major studies just employed the simple MLP models. We believe more attention should be paid to the research on fNIRS for the high portability and low cost. As for the fMRI, twenty-three papers proposed deep learning models to the classification. The CNN model is widely used for its outstanding performance in feature learning from images. There are also several papers interested in image reconstruction based on fMRI signals. One reason why fMRI is so hot is that several public datasets are available on the internet although the fMRI equipment is expensive. Nowadays, the EOG was mainly regarded as noise instead of useful signals. However, it enables individuals to communicate with the outer world by reflecting of the user’s eye movement. The MEG signals are mainly used in the medical area, which is insensitive to the deep learning algorithm. Thus, we only found very few studies on MEG. The sparse AE and CNN algorithms have a positive influence on the feature refining and classification of MEG.

5.7.2 Deep Learning Model-based Discussion. In this section, we will discuss the deep learning models which are applied in BCI systems. First of all, in a high-level view, the discriminative models, especially CNN, are most widely adopted in the summarized 238 publications. This is reasonable

because almost all the BCI issues can be regarded as a classification problem. The CNN algorithms take more than 70% proportion of the discriminative models. We provide several possible reasons. First, the design of CNN is powerful enough to extract the latent discriminative features and spatial dependencies from the EEG signals for classification. As a result, CNN structures are adopted for classification in some studies while adopted for feature engineering in some other studies. Second, CNN has been achieved great success in some research areas (e.g., computer vision) which makes it extremely famous and feasible (through the available public code). Thus, the BCI researchers have more chance to understand and apply CNN on their works. Third, some BCI diagrams (e.g., fMRI, MEG) naturally form two-dimension images conducive to processing by CNN. Meanwhile, other 1-D signals (e.g., EEG) could be converted into 2-D images for further analysis by CNN. Here, we provide several methods converting 1-D EEG signals (with multiple channels) to the 2-D matrix: 1) convert each time-point²¹ to a 2-D image; 2) convert a segment into a 2-D matrix. For the first situation, suppose we have 32 channels, and we can collect 32 elements (each element corresponding to a channel) at each time-point. As described in [105], the collected 32 elements could be converted into a 2-D image based on the spatial position as shown in Figure 6. For the second situation, suppose we have 32 channels, and the segment contains 100 time-points. The collected data can be arranged as a matrix with the shape of [32, 100] where each row and column refers to a specific channel and time-point, respectively. Fourth, there are a lot of variants of CNN which are suitable for a wide range of BCI scenarios. For example, the single-channel EEG signals can be processed by 1-D CNN. In terms of RNN, only about 20% of discriminative model based papers adopted RNN, which is much less than we expected since RNN has demonstrated powerful in temporal feature learning. One possible reason for this phenomena is that processing a long sequence by RNN is time-consuming and the EEG signals generally form a long sequence. For example, the sleeping signals are usually sliced into segments with 30 seconds, which has 3000 time-points under 100 Hz sampling rate. For a sequence with 3000 elements, through our preliminary experiments, RNN takes more than 20 folds training time than CNN. Moreover, MLP is not popular due to its inferior effectiveness (e.g., non-linear ability) to the other algorithms its simple deep learning architecture.

Additionally, for the representative models, DBN, especially DBN-RBM, is the most popular model for feature extraction. DBN is widely used in BCI for two advantages: 1) it's an efficient procedure to learn the top-down generative parameters that determine how the variables in one layer depend on the variables in the layer above; 2) the values of the latent variables in every layer can be inferred by a single, bottom-up pass that starts with an observed data vector in the bottom layer and uses the generative weights in the reverse direction. However, most work that employs the DBN-RBM model were published before 2016, indicating DBN is not popular. It can be inferred that the researchers prefer to use DBN for feature learning followed by a non-deep learning classifier before 2016; but recently, an increasing number of studies would like to adopt CNN or hybrid models for both feature learning and classification.

Moreover, generative models are rarely employed independently. The GAN and VAE based data augmentation and image reconstruction are mainly focused on fMRI and EEG signals. It's demonstrated that the trained classifier will achieve more competitive performance after data augmentation. Therefore, this is a promising research prospect in the future.

Last but not least, there are fifty-three publications proposed hybrid models for BCI studies. Among them, the combinations of RNN and CNN take about one-fifth proportion. Since RNN and CNN are illustrated having excellent temporal and spatial feature extraction ability, it's natural to combine them for both temporal and spatial feature learning. Another type of hybrid models is

²¹Time-point represents one sampling point. For example, we can have 100 time-points if the sampling rate is 100 Hz.

the combination of representative and discriminative models. This is easy to understand because the former is employed for feature refining and the latter is employed for classification. There are twenty-eight publications which almost covered all the BCI signals proposed this type of hybrid deep learning models. The adopted representative models are mostly AE or DBN-RBM; at the meanwhile, the adopted discriminative models are mostly CNN. Apart from that, there are twelve papers proposed other hybrid models such as two discriminative models. For example, several studies proposed the combination of CNN and MLP where the CNN structure is used to extract spatial features which are fed into an MLP for classification.

6 BCI APPLICATIONS

Deep learning models have contributed to various of BCI applications including health care, smart environment, security, affective computing, etc. In Table 7, we summarized the deep learning based BCI scenarios. The papers focused on signal classification without application background are not listed in this table. Therefore, the publication amounts in this table are less than in Table 5.

6.1 Health Care

In the health care area, the deep learning based BCI systems mainly works on the detection and diagnosis of mental diseases such as sleeping disorders, Alzheimer's Disease, epileptic seizure, and other disorders. In the first place, for the sleeping disorder detection, most studies are focused on the sleeping stage detection based on sleeping spontaneous EEG. In this situation, the researchers do not need to recruit patients with the sleeping disorder because the sleeping EEG signals can be easily collected from healthy individuals. In terms of the algorithm, it can be observed from Table 7 that the DBN-RBM and CNN are widely adopted for feature engineering and classification. Ruffini et al. [164] walk one step further by detecting the REM Behavior Disorder (RBD) which may cause neurodegenerative diseases such as Parkinson's disease. They achieved an average accuracy of 85% in recognition of the RBD from healthy controls.

Moreover, fMRI is widely used in the diagnosis of Alzheimer's Disease. By taking advantage of the high spatial resolution of fMRI, the diagnosis achieved the accuracy of above 90% in several studies. Another reason that contributes to competitive performance is the binary classification scenario. Apart from that, several publications diagnose the AD based on spontaneous EEG [137, 254].

Besides, the diagnosis of epileptic seizure attracted much attention. The seizure detection mainly based on mental disease spontaneous EEG and a few ECoG signals. The popular deep learning models in this scenario contain the independent CNN and RNN, along with hybrid models combined RNN and CNN. Some models integrated the deep learning models for feature extraction and traditional classifier for detection [149, 209]. For example, Yuan et al. [239] applied a D-AE in feature engineering followed by SVM for seizure diagnosis. Ullah et al. [211] adopted the voting for post-processing, which proposed several different CNN classifiers and predicted the final result by voting.

Furthermore, there are a lot of other heal care issues can be solved by BCI systems. The cardiac artifacts in MEG signals can be automatically detected by deep learning models[54, 70]. Several modified CNN structures are proposed to detect brain tumor based on fMRI from the public BRATS dataset [71, 139, 182]. Literature demonstrated the effectiveness of deep learning models in the detection of a number of mental diseases such as depression [4], Interictal Epileptic Discharge (IED) [12], schizophrenia [156], Creutzfeldt-Jakob Disease (CJD) [138], and Mild Cognitive Impairment (MCI) [196].

Table 7. Summary of deep learning based BCI applications. The ‘local’ dataset refers to private or not available dataset and the public datasets (with links) will be introduced in Section 6.9. In the signals, S-EEG, MD EEG, and E-EEG separately denote sleeping EEG, mental disease EEG, and emotional EEG. The single ‘EEG’ refers to the other subcategory of spontaneous EEG. In the models, RF and LR denote to random forest and logistic regression algorithms, respectively. In the performance column, ‘N/A’, ‘sen’, ‘spe’, ‘aro’, ‘val’, ‘dom’, and ‘like’ denote not-found, sensitivity, specificity, arousal, valence, dominance, and liking, respectively.

BCI Applications	Reference	Signals	Deep Learning Models	Dataset	Performance	
Health Care	Sleeping Quality Evaluation	Vilamala et al. [214]	S-EEG	CNN	Sleep-EDF	0.86
		Chambon et al. [35]	S-EEG	Multi-view CNN	MASS session 3	N/A
		Zhang et al. [241]	S-EEG	DBN + voting	UCD	0.9131
		Tsinalis et al. [206]	S-EEG	CNN	Sleep-EDF	0.82
		Sors et al. [186]	S-EEG	CNN	SHHS	0.87
		Manzano et al. [128]	S-EEG	CNN + MLP	Sleep-EDF University	0.732
		Shahin et al. [177]	S-EEG	MLP	Hospital in Berlin	0.9
		Manzano et al. [129]	S-EEG	CNN, MLP	Sleep-EDF	0.686/0.689
		Supratak et al. [197]	EEG, EOG	CNN + LSTM	MASS/ Sleep-EDF	0.862/0.82
		Xia et al. [224]	EOG	DBN-RBM + HMM	Sleep-EDF	0.833
	Ruffini et al. [164]	S-EEG	RNN	Local	0.85	
	Fraiwan et al. [50]	S-EEG	DBN-AE + MLP	Local	0.804	
	Tan et al. [201]	S-EEG	DBN-RBM	Local	0.9278 (F1)	
	Fernandez et al. [49]	EEG, EOG	CNN	SHHS	0.9 (F1)	
	Biswai et al. [27]	S-EEG	RNN	Local	0.8576	
	AD Detection	Hu et al. [80]	fMRI	D-AE + MLP	ADNI	0.875
		Morabito et al. [137]	MD EEG	CNN	Local	0.82
		Suk et al. [195]	fMRI	DBN-AE; DBN-RBM	ADNI	0.979; 0.954
		Zhao et al. [254]	MD EEG	DBN-RBM	Local	0.92
		Sarraf et al. [171]	fMRI	CNN	ADNI	0.9685
Sarraf et al. [172]		fMRI	CNN	ADNI	0.999	
Bhatkoti et al. [26]		fMRI, PET	AE + MLP	ADNI	0.7922	
Ortiz et al. [147]		fMRI, PET	DBN-RBM + SVM	ADNI	0.9	
Li et al. [109]	fMRI	CNN + LR	ADNI	0.9192		
Seizure Detection	Tsiouris et al. [207]	MD EEG	LSTM	CHB-MIT	0.99	
	Yuan et al. [240]	MD EEG	Attention-MLP	CHB-MIT	0.9661	
	Yuan et al. [239]	MD EEG	D-AE + SVM	CHB-MIT	0.95	
	Ullah et al. [211]	MD EEG	CNN + voting	UBD	0.954	
	Lin et al. [111]	MD EEG	D-AE	UBD	0.96	
	Hosseini et al. [78]	MD EEG	D-AE + MLP	Local	0.94	
	Page et al. [149]	MD EEG	DBN-AE + LR	N/A	0.8 ~ 0.9	
	Golmohammadi et al. [56]	MD EEG	RNN+CNN	TUH	Sen: 0.3083; Spe: 0.9686	
	Wen et al. [223]	MD EEG	AE	Local	0.92	
	Acharya et al. [3]	MD EEG	CNN	UBD	0.8867	
	Schirmeister et al. [173]	MD EEG	CNN	TUH	0.854	
	Hosseini et al. [79]	MD EEG	CNN	Local	N/A	
	Talathi et al. [199]	MD EEG	GRU	BUD	0.996	
	Kiral et al. [93]	EcoG	MLP	Local	Sen: 0.69	
Johansen et al. [87]	MD EEG	CNN	Local	0.947 (AUC)		
Ansari et al. [10]	MD EEG	CNN + RF	Local	0.77		

Table 7. Summary of deep learning based BCI applications (Continued).

BCI Applications	Reference	Signals	Deep Learning Models	Dataset	Performance	
Health Care	Seizure Detection	Hosseini et al. [77]	EEG, EcoG	CNN	Local	0.96
		Shah et al. [176]	MD EEG	CNN+ LSTM	TUH	Sen: 0.39; Spe: 0.9037
		Turner et al. [209]	MD EEG	DBN-RBM + LR	Local	N/A
	Others:					
	Cardiac Detection	Garg [54]	MEG	CNN	Local	Sen: 0.85, Spe: 0.97
		Hasasneh et al. [70]	MEG	CNN + MLP	Local	0.944
	Depression	Acharya et al. [4]	MD EEG	CNN	Local	0.935 ~ 0.9596
		Al et al. [7]	MD EEG	DBN-RBM + MLP	Local	0.695
	Brain Tumor	Morenolopez et al. [139]	fMRI	CNN	BRATS	0.88 (F1)
		Havaei et al. [71]	fMRI	Multi-scale CNN	BRATS	0.88 (F1)
		Shreyas et al. [182]	fMRI	CNNC	BRATS	0.83
	Interictal Epileptic Discharge (IED)	Antoniades et al. [12]	EcoG	CNN	Local	0.8751
		Antoniades et al. [11]	EEG, EcoG	AE + CNN	Local	0.68
	Schizophrenia	Pilis et al. [156]	fMRI	DBN-RBM	Combined	ζ0.9 (F1)
		Chu et al. [38]		CNN + RF + Voting	Local	0.816, 0.967, 0.992
Creutzfeldt-Jakob Disease (CJD)	Morabito et al. [138]	MD EEG	D-AE	Local	0.81 ~ 0.83	
	Suk et al. [196]	fMRI	AE + SVM	ADNI2	0.7258	
Smart Environment	Robot Control	Behncke et al. [24]	EEG	CNN	Local	0.75
		Huve et al. [84]	fNIRS	MLP	Local	0.82
	Exoskeleton Control	Kwak et al. [98]	SSVEP	CNN	Local	0.9403
		Zhang et al. [247]	MI EEG	RNN	EEGMMI	0.9553
Brain Communication	Smart Home	Kawasaki et al. [89]	VEP	MLP	Local	0.908
		Cecotti et al. [31]	VEP	CNN + Voting	The third BCI competition, Dataset II	0.955
	Zhang et al. [250]	MI EEG	LSTM+CNN +AE	Local	0.9452	
	Cecotti et al. [31]	VEP	CNN	The third BCI competition, Dataset II	0.945	
	Maddula et al. [123]	VEP	RCNN	Local	0.65~0.76	
	Liu et al. [115]	VEP	CNN	The third BCI competition, Dataset II	0.92 ~ 0.96	
Security	Identification	Zhang et al. [249]	MI-EEG	Attention-based RNN	EEGMMI + local	0.9882
		Koike et al. [94]	VEP	MLP	Local	0.976
	Authentication	Mao et al. [132]	RSVP	CNN	Local	0.97
		Zhang et al. [245]	MI EEG	Hybrid	EEGMMI + local	0.984
Affective Computing		Mioranda et al. [136]	E-EEG	RNN + CNN	AMIGOS	ζ0.7
		Jia et al. [85]	E-EEG	DBN-RBM	DEAP	0.8 ~ 0.85 (AUC)
		Li et al. [105]	E-EEG	Hierarchical CNN	SEED	0.882
		Xu et al. [227]	E-EEG	DBN-AE, DBN-RBM	DEAP	ζ0.86 (F1)
		Liu et al. [117]	E-EEG	CNN	Local	0.82
		Frydenlund et al. [51]	E-EEG	MLP	DEAP	N/A
		Yin et al. [237]	E-EEG	Multi-view D-AE + MLP	DEAP	Aro: 0.7719; Val: 0.7617
		Chai et al. [34]	E-EEG	AE	SEED	0.818
		Kawde et al. [90]	EEG, EOG	DBN-RBM	DEAP	Aro: 0.7033; Val: 0.7828; Dom: 0.7016
		Li et al. [110]	E-EEG	DBN-RBM	DEAP	Aro:0.642, Val:0.584, Dom:0.658

Table 7. Summary of deep learning based BCI applications (Continued).

BCI Applications	Reference	Signals	Deep Learning Models	Dataset	Performance
Affective Computing	Xu et al. [228]	E-EEG	DBN-RBM	DEAP	Aro:0.6984, Val:0.6688, Lik: 0.7539
	Zheng et al. [258]	E-EEG	DBN-RBM + HMM	Local	0.8762
	Alhagry et al. [8]	E-EEG	LSTM + MLP	DEAP	Aro:0.8565, Val:0.8545, Lik: 0.8799
	Li et al. [75]	E-EEG	CNN	SEED	0.882
	Zhang et al. [255, 256]	E-EEG	DBN-RBM + MLP	SEED	0.8608
	Liu et al. [118]	EEG, EOG	AE	SEED, DEAP	0.9101, 0.8325
	Gao et al. [53]	E-EEG	DBN-RBM + MLP	Local	0.684
	Zhang et al. [244]	E-EEG	RNN	SEED	0.895
Drive Fatigue Detection	Hung et al. [82, 82]	EEG	CNN	Local	0.572 (RMSE)
	Hajinorozi et al. [64]	EEG	DBN-RBM	Local	0.85
	Hung et al. [82]	EEG	CNN	Local	
	Du et al. [45]	EEG, EOG	D-AE + SVM	Local	0.094 (RMSE)
	San et al. [169]	EEG	DBN-RBM + SVM	Local	0.7392
	Almogbel et al. [9]	EEG	CNN	Local	0.9531
	Hachem et al. [62]	SSVEP	MLP	Local	0.75
	Chai et al. [33]	EEG	DBN + MLP	Local	0.931
	Hajinorozi et al. [65, 65]	EEG	CNN	Local	0.8294
Mental Load Measurement	Naseer et al. [143]	fNIRS	MLP	Local	0.963
	Yin et al. [236]	EEG	D-AE	Local	0.9584
	Hennrich et al. [72]	fNIRS	MLP	Local	0.641
	Bashivan et al. [?]	EEG	R-CNN	Local	0.9111
	Bashivan et al. [21]	EEG	DBN + MLP	Local	N/A
	Bashivan et al. [23]	EEG	DBN-RBM	Local	0.92
	Li et al. [108]	EEG	DBN-RBM	Local	0.9886
School Bullying	Baltatzis et al. [18]	EEG	CNN	Local	0.937
	Stober et al. [190]	EEG	CNN	Local	0.776
Music Detection	Stober et al. [192]	EEG	AE + CNN	Open MIIR	0.27 for 12-class
	Stober et al. [191]	EEG	CNN	Local	0.244
Number Choosing	Sternin et al. [189]	EEG, EOG	CNN	Local	0.75
	Waytowich et al. [221]	SSVEP	CNN	Local	0.8
Other Applications	Cichy et al. [40]	fMRI, MEG	CNN	N/A	N/A
	Manor et al. [126]	RSVP	CNN	Local	0.75
	Cecotti et al. [29]	RSVP	CNN	Local	0.897 (AUC)
	Hajinorozi et al. [66]	RSVP	CNN	Local	0.7242 (AUC)
	Perez et al. [153]	SSVEP	AE	Local	0.9778
	Shamwell et al. [178]	RSVP	CNN	Local	0.7252 (AUC)
	Xie et al. [225, 226]	EcoG	RNN+CNN	BCI Competition IV	N/A
	Kulasingham et al. [96]	SSVEP	DBN-RBM; DBN-AE	Local	0.869; 0.8601
	Liu et al. [116]	EEG	DBN-RBM	Local	0.973
	Volker et al. [215]	EEG	CNN	Local	0.841
Finger Trajectory	Narejo et al. [141]	EEG	DBN-RBM	UCI	0.989
	Reddy et al. [159]	EEG	MLP	Local	0.975
Guilty Knowledge Test	Teo et al. [203]	EEG	MLP	Local	0.6399
	Hernandez et al. [73]	EEG	CNN	Local	0.718
Concealed Information Test	Hiroyasu et al. [75]	fNIRS	D-AE + MLP	Local	0.81
	Putten et al. [157]	EEG	CNN	Local	0.81

6.2 Smart Environment

The smart environment is a promising application scenario for BCI in the future. With the development of Internet of Things (IoT), an increasing number smart environment can be connected to BCI. For example, the assisting robot can be used in smart home [247, 253], in which the robot can be controlled by brain signals of the individuals. Moreover, Behncke et al. [24] and Huve et al. [84] investigated the robot control problem based on the visual stimulated spontaneous EEG and fNIRS signals. The BCI controlled exoskeleton could help the disabilities who damaged the motor system in sub-limb in walking and daily activities [98]. In the future, the research on brain-controlled appliances may be beneficial to the elders or disabilities in smart home and smart hospital.

6.3 Brain Communication

The biggest advantage of BCI, compared to other human-machine interface techniques, is that BCI enables the patient who lost most motor abilities like speaking to communicate with the outer world. The deep learning technology improved the efficiency of brain signal based communications. One typical diagram which enables individual typing without any motor system is P300 speller which can convert the user's intent into text [89]. The powerful deep learning models empower the BCI systems to recognize the P300 segment from the non-P300 segment while the former contains the communication information of the user [31]. In a higher level, the representative deep learning models can help to detect what character (as shown in Figure 12b) the user is focusing on and print it on the screen to chat with others [31, 115, 123].

Additionally, Zhang et al. [250] proposed a hybrid model combined RNN, CNN, and AE to extract the informative features from MI EEG to recognize what letter the user wants to speak. The proposed interface including 27 characters (26 English alphabets and the space bar) and all of them are separated typing system totally includes $27 = 3 \times 9$ characters (26 English alphabets and the space bar) and all of them are separated by 3 character blocks (each block contains 9 characters) in the initial interface. Overall, there are three alternative selections, and each selection will lead to a specific sub-interface which includes 9 characters. Again, the $9 = 3 \times 3$ characters are divided into three character blocks, and each of them contains nine characters. Again, the $9 = 3 \times 3$ characters are divided into three character blocks, and each of them is connected to a bottom interface. In the base interface, each block represents only one character. However, compared to P300 speller, the MI-based protocols have lower information transform rate because it requires three operations to find the specific letter at the bottom level.

6.4 Security

Security field has been an interest of BCI researchers. The security problem can be divided into identification (also called recognition) and authentication (also called verification) aspects. The former generally is a multi-class classification problem, and its target is to recognize the identity of the test-person [249]. The latter usually is a binary classification problem, which only cares whether the test-person is authorized or unauthorized [245].

The existing biometric identification/authentication systems are mainly based on individuals' unique intrinsic physiological features (e.g., face, iris, retina, voice, and fingerprint). However, the state-of-the-art person identification systems are vulnerable, e.g., anti-surveillance prosthetic masks can thwart face recognition, contact lenses can trick iris recognition, vocoder can compromise voice identification, and fingerprint films can deceive fingerprint sensors. In this perspective, the EEG (Electroencephalography) based biometric person identification systems are emerging as promising alternatives due to their high attack-resilience. An individual's EEG signals are virtually impossible to mimic for an imposter, thus making this approach highly resilient to spoofing attacks

encountered by other identification techniques. Koike et al. [94] have adopted deep neural networks to identify the user's ID based on the VEP signals while Mao et al. [132] applied CNN for person identification based on RSVP signals. Zhang et al. [249] proposed an attention-based LSTM model and evaluated it over both public and local datasets. The authors [245] then combined EEG signals with gait information to introduce a dual-authentication system with a hybrid deep learning model.

6.5 Affective Computing

Affective states of a user provide critical information for many applications such as personalized information (e.g., multimedia content) retrieval or intelligent human-computer interface design [227]. Recent research illustrated that deep learning models can enhance the performance in affective computing. The emotion can be defined according to several dimensions. Dimensional models of emotion attempt to conceptualize human emotions by defining where they lie in two or three dimensions. The most widely used circumplex model believe the emotions are distributed in two dimensions: arousal and valence. The arousal refers to the intensity of the emotional stimuli or how strong is the emotion. The valence refers to the relationship within the person who experiences the emotion. In some other models, the dominance and liking dimensions are deployed.

Some papers only attempt to classify the user's emotional state into a binary (positive/negative) or three categories (positive, neutral, and negative) problem and recognize them by deep learning algorithms [51]. A range of publications adopted CNN and the variants to classify the emotional EEG signals [105, 117, 216]. The DBN-RBM is the most representative deep learning model to discover the concealed features from emotional spontaneous EEG [227, 256]. Xu et al. [227] applied a DBN-RBM as specific feature extractors for the affective states classification problem using EEG signals.

Furthermore, at a more fundamental level, the researchers aiming at the recognition of a positive/negative state of each specific emotional dimension. For example, Yin et al. [237] proposed a multiple-fusion-layer based ensemble classifier of AE for recognizing emotions. Each AE consists of three hidden layers to filter the unwanted noise in the physiological features and derives the stable feature representations. The proposed model was evaluated over the benchmark DEAP and achieved the arousal of 77.19% and valence of 76.17%. Mioranda et al. [136] presented a multi-task cascaded deep neural network which jointly predicts people's affective levels (valence and arousal) and personal factors using EEG signals recorded in response to the presentation of the affective multimedia content.

6.6 Driver Fatigue Detection

Vehicle driver's ability to maintain optimal performance and attention is essential to ensure the safety of the traffic. EEG signals have been proven to be useful in evaluating the human's cognitive state under specific tasks [9]. Generally, the driver is regarded as in alert state if the reaction time is below or equal to 0.7 seconds and in fatigue state if the reaction time is higher or equal to 2.1 seconds. Hajinoroozi et al. [64] considered the prediction of driver's fatigue from EEG signals by extracting the distinct features. They explored an approach based on DBN for dimension reduction.

The detection of driver fatigue is crucial because the drowsiness of the driver may lead to disaster. On the other hand, driver fatigue detection is feasible in the real world. In the hardware aspect, the collection equipment of EEG singles is off-the-shelf and portable enough to be used in a car. Moreover, the price of an EEG headset is affordable for most people. In the algorithm aspect, deep learning models have enhanced the performance of fatigue detection. As we summarized, the EEG based driving drowsiness can be recognized with high accuracy (82% ~ 95%).

Future scope of drive fatigue detection is in the self-driving scenario. As we know, in the most situation of self-driving (e.g., Automation level 3²²), the human driver is expected to respond appropriately to a request to intervene, which indicates that the driver should keep alert state. Therefore, we believe the application of BCI based drive fatigue detection will benefit the development of the self-driving car.

6.7 Mental Load Measurement

Evaluation of operator Mental Workload levels via ongoing electroencephalogram (EEG) is quite promising in Human-Machine collaborative task environment to alarm the temporal operator performance degradation [236]. The human operator works as a vital component in automation systems for decision making and strategy development. However, different from machines or computers, the human functional states could not always fit requirements of tasks for the limited working memory and time-dependent psychophysiological experience. Therefore, In such a case, operator performance degradation caused by abnormal cognitive states, e.g., high working stress or distraction, is considered to be a crucial factor for catastrophic accidents [152].

A number of researchers have been paid attention to this topic. The mental workload can be measured from fNIRS signals or spontaneous EEG. Naseer et al. [143] analyzed and compared the classification accuracies of six different classifiers, including five traditional classifiers and a MLP classifier for a two-class mental task (mental arithmetic and rest) using fNIRS signals. The experiment results showed that the MLP outperformed the traditional classifiers like SVM, kNN and achieved the highest accuracy of 96.3%. Bashivan et al. [23] presented a statistical approach, a DBN model, to predict cognitive load from single trial EEG. Before the DBN, the authors manually extracted the wavelet entropy and band-specific power from theta, alpha and beta bands. At last, the experiments demonstrated the recognition of cognitive load across four different levels with an overall accuracy of 92% during execution of a memory task.

6.8 Other Applications

Apart from the aforementioned key applications, there are still some interesting scenarios, such as recommender system [203] and emergency braking [73] to which deep learning based BCI can apply. One possible topic is the recognition of a visual object, which may be used in guilty knowledge test [96] and concealed information test [116]. The neurons of the participant will produce a pulse when he/she suddenly watch a similar object. Based on the theory, the visual target recognition is mainly used RSVP signals. Cecotti et al. [29] attempted to investigate the performance of CNNs

²²https://en.wikipedia.org/wiki/Self-driving_car

²³<http://www.bbci.de/competition/iv/>

²⁴<http://www.bbci.de/competition/iii/>

²⁵<https://physionet.org/physiobank/database/sleep-edfx/>

²⁶<https://massdb.herokuapp.com/en/>

²⁷<https://physionet.org/pn3/shhpsgdb/>

²⁸<https://physionet.org/pn6/chbmit/>

²⁹https://www.isip.piconepress.com/projects/tuh_eeg/html/downloads.shtml

³⁰<https://physionet.org/pn4/eegmidb/>

³¹<http://www.bbci.de/competition/ii/>

³²<http://www.eecs.qmul.ac.uk/mmv/datasets/amigos/readme.html>

³³<http://bcmi.sjtu.edu.cn/seed/download.html>

³⁴<https://www.eecs.qmul.ac.uk/mmv/datasets/deap/>

³⁵https://owenlab.uwo.ca/research/the_openmiir_dataset.html

³⁶<http://adni.loni.usc.edu/data-samples/access-data/>

³⁷<https://www.med.upenn.edu/sbia/brats2018/data.html>

Table 10. The summary of public dataset for BCI systems. ‘# Sub’, ‘# Cla’, and S-Rate denote the number of subject, the number of class, and the sampling rate, respectively. FM denote finger movement while BCI-C denote the BCI competition. The datasets may contain more biometric signals (e.g., ECG) but we only list the channels related to BCI.

BCI Signals		Name Link	# Sub	# Cla	S-Rate	# Channel
Inv- -asive	FM EcoG	BCI-C IV ²³ , Dataset IV	3	5	1000	48 ~ 64
	MI EcoG	BCI-C III ²⁴ , Dataset I	1	2	1000	64
EEG	Sleeping EEG	Sleep-EDF ²⁵ : Telemetry	22	6	100	2 EEG, 1 EOG, 1 EMG
		Sleep-EDF: Cassette	78	6	100, 1	2 EEG (100Hz), 1 EOG (100Hz), 1 EMG (1Hz)
		MASS-1 ²⁶	53	5	256	17/19 EEG, 2 EOG, 5 EMG
		MASS-2	19	6	256	19 EEG, 4 EOG, 1EMG
		MASS-3	62	5	256	20 EEG, 2 EOG, 3 EMG
		MASS-4	40	6	256	4 EEG, 4 EOG, 1 EMG
		MASS-5	26	6	256	20 EEG, 2 EOG, 3 EMG
		SHHS ²⁷	5804	N/A	125, 50	2 EEG (125Hz), 1EOG (50Hz), 1 EMG (125Hz)
	Seizure EEG	CHB-MIT ²⁸	22	2	256	18
		TUH ²⁹	315	2	200	19
	MI EEG	EEGMMI ³⁰	109	4	160	64
		BCI-C II ³¹ , Dataset III	1	2	128	3
		BCI-C III, Dataset III a	3	4	250	60
		BCI-C III, Dataset III b	3	2	125	2
		BCI-C III, Dataset IV a	5	2	1000	118
		BCI-C III, Dataset IV b	1	2	1001	119
		BCI-C III, Dataset IV c	1	2	1002	120
		BCI-C IV, Dataset I	7	2	1000	64
		BCI-C IV, Dataset II a	9	4	250	22 EEG, 3 EOG
		BCI-C IV, Dataset II b	9	2	250	3 EEG, 3 EOG
Emotional EEG	AMIGOS ³²	40	4	128	14	
	SEED ³³	15	3	200	62	
	DEAP ³⁴	32	4	512	32	
Others EEG	Open MIIR ³⁵	10	12	512	64	
VEP	BCI-C II, Dataset II b	1	36	240	64	
	BCI-C III, Dataset II	2	26	240	64	
fMRI	ADNI ³⁶	202	3	N/A	N/A	
	BRATS ³⁷ 2013	65	4	N/A	N/A	
MEG	BCI-C IV, Dataset III	2	4	400	10	

in the relation of their architecture and concerning how they are evaluated. More particularly, the authors aimed to build a common model for target recognition which can work for various subjects instead of a specific subject. In detail, they addressed the change of performance that can be observed between specifying a neural network to a subject, or by considering a neural network for a group of subjects, taking advantage of a larger number of trials from different subjects.

Besides, researchers have investigated to distinguish the subject’s gender by the fNIRS [75] and spontaneous EEG [157]. Hiriyasu et al. [75] adopted deep learning to recognize the gender of the subject based on the cerebral blood flow. The experiment results suggested that there exists a relation between cerebral blood flow changes and biological information. Putten et al. [157]

tried to discover the sex-specific information from the brain rhythms and adopted a CNN model to recognize the participant's gender. This paper illustrated that fast beta activity (20 ~25 Hz), and its spatial distribution is one of the main distinctive attributes.

6.9 Benchmark Datasets

In this section, we extensively explore the benchmark datasets which can be used in deep learning based BCI. As listed in Table 10, we provide 31 reusable public datasets with download links, which covered most BCI signals. The BCI competition IV (BCI-C IV) contains five datasets. We give the access link at the first dataset. For better understanding, we present the number of subjects, the number of class (how many categories), sampling rate and the number of channels of each dataset. In the '# Channel' column, the default channel is EEG signals.

7 FUTURE DIRECTIONS

Although deep learning has lifted the performance of BCI systems, technical and usability challenges remains. The technical challenges concern the classification ability in complex BCI scenarios; and the usability challenges refer to limitations in large scale real-world deployment. In this section, we introduce these challenges and point out the possible solutions.

7.1 General Framework

Until now, we have introduce several types of BCI signals (e.g., spontaneous EEG, ERP, fMRI) and deep learning models that have been applied for each type. One promising research direction for deep learning based BCI is to develop a general framework that can handle various BCI signals regardless of the number of channels used for signal collection, the sample dimensions (e.g., 1-D or 2-D sample), and stimulation types (e.g., visual or audio stimuli), etc. The general framework would requires two key capabilities: the attention mechanism and the ability to capture latent feature. The former guarantees the framework can focus on the most valuable parts of input signals and the latter enables the framework to capture the distinctive and informative features.

The attention mechanism can be implemented based on attention scores or by various machine learning algorithms such as reinforcement learning. The attention scores can be inferred from the input data and work as a weight to help the framework to pay attention to the parts with high attention scores. Reinforcement learning has shwon to be able to find the most valuable part through a policy search [248]. CNN is the most suitable structure for capturing features in various levels and ranges. In the future, CNN could be used as a fundamental feature learning tool and be integrated with suitable attention mechanisms to form a general classification framework.

7.2 Person-independent Classification

Until now, most BCI classification tasks focus on person-dependent scenarios, where the training and the testing sets come from the same person. The future direction is to realize person-independent classification so that the testing data will never appear in the training set. High-performance person-independent classification is compulsory for the wide application of BCI Systems in the real-world.

One possible solution to achieving this goal is to build a personalized model with transfer learning. A personalized affective model can adopt a transductive parameter transfer approach to construct individual classifiers and to learn a regression function that maps the relationship between data distribution and classifier parameters [257]. Another potential solution is mining the subject-independent component from the input data. The input data can be decomposed into two parts: a subject-dependent component, which depends on the subject and a subject-independent

component, which is common for all subjects. A hybrid multi-task model can work on two tasks simultaneously, one focusing on person identification and the other on class recognition. A well-trained and converged model is supposed to extract the subject-independent features in the class recognition task.

7.3 Semi-supervised and Unsupervised Classification

The performance of deep learning models highly depends on the size of training data, which, however, requires expensive and time-consuming manual labeling to collect abundant class labels for a wide range of scenarios such as sleeping EEG. While supervised learning requires both observations and labels for the training, unsupervised learning requires no labels and semi-supervised learning only requires partial labels [85]. They are, therefore, more suitable for problems with little ground truth.

Zhang et al. proposed an Adversarial Variational Embedding (AVAE) framework that combines a VAE++ model (as a high-quality generative model) and semi-supervised GAN (as a posterior distribution learner) [251] for robust and effective semi-supervised learning. Jia et al. [85] proposed a semi-supervised framework by leveraging label information in feature extraction and integrating unlabeled information to regularize the supervised training.

Two methods may enhance the unsupervised learning: one is to employ crowd-sourcing to label the unlabeled observations; the other is to leverage unsupervised domain adaptation learning to align the distribution of source BCI signals and the distribution of target signals with a linear transformation.

7.4 Hardware Portability

Poor portability of hardware has been preventing BCI systems from wide application in the real world. In most scenarios, users would like to use small, comfortable, or even wearable BCI hardware to collect brain signals and to control appliances and assistant robots.

Currently, there are three types of EEG collection equipment: the unportable, the portable headset, and ear-EEG sensors. The unportable equipment (e.g., BCI 2000) has high sampling frequency, channel numbers, and signal quality but is expensive. It is suitable for physical examination in hospital. The portable headsets (e.g., Neurosky, Emotiv EPOC) have 1 ~ 14 channels and 128~256 sampling rate but may discomfort people after a long-time use. The ear-EEG sensors, which are attached to the outer ear, have gained increasing attention recently but remain mostly at the laboratory stage [148]. The ear-EEG platform comprises a set of electrodes placed inside each ear canal, together with additional electrodes in the concha of each ear [134]. The EEGGrids, to the best of our knowledge, is the only commercial ear-EEG. It has multi-channel sensor arrays placed around the ear using an adhesive³⁸ and is even more expensive. A promising future direction is to improve the usability by developing a cheaper (e.g., lower than 200\$) and more comfortable (e.g., can last longer than 3 hours without feeling uncomfortable) wireless ear-EEG equipment.

8 CONCLUSION

In this paper, we systematically survey the recent advances in deep learning models for Brain-Computer Interface. Compared with traditional methods, deep learning not only enables to learn high-level features automatically from BCI signals but also depends less on manual-crafted features and domain knowledge. We summarize BCI signals and dominant deep learning models, followed by discussing state-of-the-art deep learning techniques for BCI and identifying the suitable deep

³⁸<http://ceegrid.com/home/concept/>

learning algorithms for each BCI signal type. Finally, we overview deep learning based BCI applications and point out the open challenges and future directions.

REFERENCES

- [1] Sherif M Abdelfattah, Ghodai M Abdelrahman, and Min Wang. 2018. Augmenting The Size of EEG datasets Using Generative Adversarial Networks. In *2018 International Joint Conference on Neural Networks (IJCNN)*. IEEE, 1–6.
- [2] Sarah N Abdulkader, Ayman Atia, and Mostafa-Sami M Mostafa. 2015. Brain computer interfacing: Applications and challenges. *Egyptian Informatics Journal* 16, 2 (2015), 213–230.
- [3] U Rajendra Acharya, Shu Lih Oh, Yuki Hagiwara, Jen Hong Tan, and Hojjat Adeli. 2018. Deep convolutional neural network for the automated detection and diagnosis of seizure using EEG signals. *Computers in biology and medicine* 100 (2018), 270–278.
- [4] U Rajendra Acharya, Shu Lih Oh, Yuki Hagiwara, Jen Hong Tan, Hojjat Adeli, and D Puthankattil Subha. 2018. Automated EEG-based screening of depression using deep convolutional neural network. *Computer methods and programs in biomedicine* 161 (2018), 103–113.
- [5] Minkyu Ahn and Sung Chan Jun. 2015. Performance variation in motor imagery brain-computer interface: a brief review. *Journal of neuroscience methods* 243 (2015), 103–110.
- [6] Min-Hee Ahn and Byoung-Kyong Min. 2018. Applying deep-learning to a top-down SSVEP BMI. In *Brain-Computer Interface (BCI), 2018 6th International Conference on*. IEEE, 1–3.
- [7] Alaa M Al-kaysi, Ahmed Al-Ani, and Tjeerd W Boonstra. 2015. A multichannel deep belief network for the classification of EEG data. In *International Conference on Neural Information Processing*. Springer, 38–45.
- [8] Salma Alhagry, Aly Aly Fahmy, and Reda A El-Khoribi. 2017. Emotion Recognition based on EEG using LSTM Recurrent Neural Network. *Emotion* 8, 10 (2017).
- [9] Mohammad A Almogbel, Anh H Dang, and Wataru Kameyama. 2018. EEG-signals based cognitive workload detection of vehicle driver using deep learning. In *Advanced Communication Technology (ICACT), 2018 20th International Conference on*. IEEE, 256–259.
- [10] Amir H Ansari, Perumpillichira J Cherian, Alexander Caicedo, Gunnar Nauelaers, Maarten De Vos, and Sabine Van Huffel. 2018. Neonatal seizure detection using deep convolutional neural networks. *International journal of neural systems* (2018), 1850011.
- [11] Andreas Antoniadis, Loukianos Spyrou, David Martin-Lopez, Antonio Valentin, Gonzalo Alarcon, Saeid Sanei, and Clive Cheong Took. 2018. Deep neural architectures for mapping scalp to intracranial EEG. *International journal of neural systems* (2018), 1850009.
- [12] Andreas Antoniadis, Loukianos Spyrou, Clive Cheong Took, and Saeid Sanei. 2016. Deep learning for epileptic intracranial EEG data. In *Machine Learning for Signal Processing (MLSP), 2016 IEEE 26th International Workshop on*. IEEE, 1–6.
- [13] Martin Arjovsky, Soumith Chintala, and Léon Bottou. 2017. Wasserstein generative adversarial networks. In *International Conference on Machine Learning (ICML)*. 214–223.
- [14] Mohamed Attia, Imali Hettiarachchi, Mohammed Hossny, and Saeid Nahavandi. 2018. A time domain classification of steady-state visual evoked potentials using deep recurrent-convolutional neural networks. In *Biomedical Imaging (ISBI 2018), 2018 IEEE 15th International Symposium on*. IEEE, 766–769.
- [15] Siriwadee Aungsakun, Angkoon Phinyomark, Pornchai Phukpattaranont, and Chusak Limsakul. 2011. Robust eye movement recognition using EOG signal for human-computer interface. In *International Conference on Software Engineering and Computer Systems*. Springer, 714–723.
- [16] Nik Khadijah Nik Aznan, Stephen Bonner, Jason D Connolly, Noura Al Moubayed, and Toby P Breckon. 2018. On the Classification of SSVEP-Based Dry-EEG Signals via Convolutional Neural Networks. *arXiv preprint arXiv:1805.04157* (2018).
- [17] Tonio Ball, Markus Kern, Isabella Mutschler, Ad Aertsen, and Andreas Schulze-Bonhage. 2009. Signal quality of simultaneously recorded invasive and non-invasive EEG. *Neuroimage* 46, 3 (2009), 708–716.
- [18] Vasileios Baltatzis, Kyriaki-Margarita Bintsis, Georgios K Apostolidis, and Leontios J Hadjileontiadis. 2017. Bullying incidences identification within an immersive environment using HD EEG-based analysis: A Swarm Decomposition and Deep Learning approach. *Scientific reports* 7, 1 (2017), 17292.
- [19] S Kathleen Bandt, Jarod L Roland, Mrinal Pahwa, Carl D Hacker, David T Bundy, Jonathan D Breshears, Mohit Sharma, Joshua S Shimony, and Eric C Leuthardt. 2017. The impact of high grade glial neoplasms on human cortical electrophysiology. *PloS one* 12, 3 (2017), e0173448.
- [20] Ali Bashashati, Mehrdad Fatourehchi, Rabab K Ward, and Gary E Birch. 2007. A survey of signal processing algorithms in brain-computer interfaces based on electrical brain signals. *Journal of Neural engineering* 4, 2 (2007), R32.

- [21] Pouya Bashivan, Irina Rish, and Steve Heisig. 2016. Mental state recognition via Wearable EEG. *arXiv preprint arXiv:1602.00985* (2016).
- [22] Pouya Bashivan, Irina Rish, Mohammed Yeasin, and Noel Codella. 2016. Learning representations from EEG with deep recurrent-convolutional neural networks. *ICLR* (2016).
- [23] Pouya Bashivan, Mohammed Yeasin, and Gavin M Bidelman. 2015. Single trial prediction of normal and excessive cognitive load through EEG feature fusion. In *Signal Processing in Medicine and Biology Symposium (SPMB), 2015 IEEE. IEEE*, 1–5.
- [24] Joos Behncke, Robin T Schirmer, Wolfram Burgard, and Tonio Ball. 2018. The signature of robot action success in EEG signals of a human observer: Decoding and visualization using deep convolutional neural networks. In *Brain-Computer Interface (BCI), 2018 6th International Conference on. IEEE*, 1–6.
- [25] Andrei Belitski, Jason Farquhar, and Peter Desain. 2011. P300 audio-visual speller. *Journal of Neural Engineering* 8, 2 (2011), 025022.
- [26] Pushkar Bhatkoti and Manoranjan Paul. 2016. Early diagnosis of Alzheimer’s disease: A multi-class deep learning framework with modified k-sparse autoencoder classification. In *Image and Vision Computing New Zealand (IVCNZ), 2016 International Conference on. IEEE*, 1–5.
- [27] Siddharth Biswal, Joshua Kulas, Haoqi Sun, Balaji Goparaju, M Brandon Westover, Matt T Bianchi, and Jimeng Sun. 2017. SLEEPNET: automated sleep staging system via deep learning. *arXiv preprint arXiv:1707.08262* (2017).
- [28] Eduardo Carabez, Miho Sugi, Isao Nambu, and Yasuhiro Wada. 2017. Identifying Single Trial Event-Related Potentials in an Earphone-Based Auditory Brain-Computer Interface. *Applied Sciences* 7, 11 (2017), 1197.
- [29] H Cecotti. 2017. Convolutional neural networks for event-related potential detection: impact of the architecture. In *Engineering in Medicine and Biology Society (EMBC), 2017 39th Annual International Conference of the IEEE. IEEE*, 2031–2034.
- [30] Hubert Cecotti, Miguel P Eckstein, and Barry Giesbrecht. 2014. Single-trial classification of event-related potentials in rapid serial visual presentation tasks using supervised spatial filtering. *IEEE transactions on neural networks and learning systems* 25, 11 (2014), 2030–2042.
- [31] Hubert Cecotti and Axel Graser. 2011. Convolutional neural networks for P300 detection with application to brain-computer interfaces. *IEEE transactions on pattern analysis and machine intelligence* 33, 3 (2011), 433–445.
- [32] Hubert Cecotti and Anthony J Ries. 2017. Best practice for single-trial detection of event-related potentials: Application to brain-computer interfaces. *International Journal of Psychophysiology* 111 (2017), 156–169.
- [33] Rifai Chai, Sai Ho Ling, Phyo Phyo San, Ganesh R Naik, Tuan N Nguyen, Yvonne Tran, Ashley Craig, and Hung T Nguyen. 2017. Improving eeg-based driver fatigue classification using sparse-deep belief networks. *Frontiers in neuroscience* 11 (2017), 103.
- [34] Xin Chai, Qisong Wang, Yongping Zhao, Xin Liu, Ou Bai, and Yongqiang Li. 2016. Unsupervised domain adaptation techniques based on auto-encoder for non-stationary EEG-based emotion recognition. *Computers in biology and medicine* 79 (2016), 205–214.
- [35] Stanislas Chambon, Mathieu N Galtier, Pierrick J Arnal, Gilles Wainrib, and Alexandre Gramfort. 2018. A deep learning architecture for temporal sleep stage classification using multivariate and multimodal time series. *IEEE Transactions on Neural Systems and Rehabilitation Engineering* (2018).
- [36] Keith H Chiappa. 1997. *Evoked potentials in clinical medicine*. Lippincott Williams & Wilkins.
- [37] Antonio Maria Chiarelli, Pierpaolo Croce, Arcangelo Merla, and Filippo Zappasodi. 2018. Deep learning for hybrid EEG-fNIRS brain-computer interface: application to motor imagery classification. *Journal of neural engineering* 15, 3 (2018), 036028.
- [38] Lei Chu, Robert Qiu, Haichun Liu, Zenan Ling, Tianhong Zhang, and Jijun Wang. 2017. Individual recognition in schizophrenia using deep learning methods with random forest and voting classifiers: Insights from resting state EEG streams. *arXiv preprint arXiv:1707.03467* (2017).
- [39] Radoslaw Martin Cichy, Aditya Khosla, Dimitrios Pantazis, and Aude Oliva. 2017. Dynamics of scene representations in the human brain revealed by magnetoencephalography and deep neural networks. *Neuroimage* 153 (2017), 346–358.
- [40] Radoslaw Martin Cichy, Aditya Khosla, Dimitrios Pantazis, Antonio Torralba, and Aude Oliva. 2016. Comparison of deep neural networks to spatio-temporal cortical dynamics of human visual object recognition reveals hierarchical correspondence. *Scientific reports* 6 (2016), 27755.
- [41] Mengxi Dai, Dezhi Zheng, Rui Na, Shuai Wang, and Shuailei Zhang. 2019. EEG Classification of Motor Imagery Using a Novel Deep Learning Framework. *Sensors* 19, 3 (2019), 551.
- [42] Li Deng. 2014. A tutorial survey of architectures, algorithms, and applications for deep learning. *APSIPA Transactions on Signal and Information Processing* 3 (2014).
- [43] Li Deng, Dong Yu, and others. 2014. Deep learning: methods and applications. *Foundations and Trends® in Signal Processing* 7, 3–4 (2014), 197–387.

- [44] Hao Dong, Akara Supratak, Wei Pan, Chao Wu, Paul M Matthews, and Yike Guo. 2018. Mixed neural network approach for temporal sleep stage classification. *IEEE Transactions on Neural Systems and Rehabilitation Engineering* 26, 2 (2018), 324–333.
- [45] Li-Huan Du, Wei Liu, Wei-Long Zheng, and Bao-Liang Lu. 2017. Detecting driving fatigue with multimodal deep learning. In *Neural Engineering (NER), 2017 8th International IEEE/EMBS Conference on*. IEEE, 74–77.
- [46] Lijuan Duan, Menghu Bao, Jun Miao, Yanhui Xu, and Juncheng Chen. 2016. Classification Based on Multilayer Extreme Learning Machine for Motor Imagery Task from EEG signals. *Procedia Computer Science* 88 (2016), 176–184.
- [47] Lawrence Ashley Farwell and Emanuel Donchin. 1988. Talking off the top of your head: toward a mental prosthesis utilizing event-related brain potentials. *Electroencephalography and clinical Neurophysiology* 70, 6 (1988), 510–523.
- [48] Mehrdad Fatourehchi, Ali Bashashati, Rabab K Ward, and Gary E Birch. 2007. EMG and EOG artifacts in brain computer interface systems: A survey. *Clinical neurophysiology* 118, 3 (2007), 480–494.
- [49] Isaac Fernández-Varela, Dimitrios Athanasakis, Samuel Parsons, Elena Hernández-Pereira, and Vicente Moret-Bonillo. Sleep staging with deep learning: a convolutional model. In *Proceedings of the European Symposium on Artificial Neural Networks, Computational Intelligence and Machine Learning (ESANN 2018)*.
- [50] Luay Fraiwan and Khaldon Lweesy. 2017. Neonatal sleep state identification using deep learning autoencoders. In *Signal Processing & its Applications (CSPA), 2017 IEEE 13th International Colloquium on*. IEEE, 228–231.
- [51] Arvid Frydenlund and Frank Rudzicz. 2015. Emotional affect estimation using video and EEG data in deep neural networks. In *Canadian Conference on Artificial Intelligence*. Springer, 273–280.
- [52] Wei Gao, Jin-an Guan, Junfeng Gao, and Dao Zhou. 2015. Multi-ganglion ANN based feature learning with application to P300-BCI signal classification. *Biomedical Signal Processing and Control* 18 (2015), 127–137.
- [53] Yongbin Gao, Hyo Jong Lee, and Raja Majid Mehmood. 2015. Deep learning of EEG signals for emotion recognition. In *Multimedia & Expo Workshops (ICMEW), 2015 IEEE International Conference on*. IEEE, 1–5.
- [54] Prabhath Garg, Elizabeth Davenport, Gowtham Murugesan, Ben Wagner, Christopher Whitlow, Joseph Maldjian, and Albert Montillo. 2017. Automatic 1D convolutional neural network-based detection of artifacts in MEG acquired without electrooculography or electrocardiography. In *Pattern Recognition in Neuroimaging (PRNI), 2017 International Workshop on*. IEEE, 1–4.
- [55] Patrick O Glauner. 2015. Comparison of training methods for deep neural networks. *arXiv preprint arXiv:1504.06825* (2015).
- [56] Meysam Golmohammadi, Saeedeh Ziyabari, Vinit Shah, Silvia Lopez de Diego, Iyad Obeid, and Joseph Picone. 2017. Deep Architectures for Automated Seizure Detection in Scalp EEGs. *arXiv preprint arXiv:1712.09776* (2017).
- [57] Ian Goodfellow, Jean Pouget-Abadie, Mehdi Mirza, Bing Xu, David Warde-Farley, Sherjil Ozair, Aaron Courville, and Yoshua Bengio. 2014. Generative adversarial nets. In *Advances in neural information processing systems*. 2672–2680.
- [58] Yuri Gordienko, Sergii Stirenko, Yuriy Kochura, Oleg Alienin, Michail Novotarskiy, and Nikita Gordienko. 2017. Deep learning for fatigue estimation on the basis of multimodal human-machine interactions. *arXiv preprint arXiv:1801.06048* (2017).
- [59] Stephen M Gordon, Matthew Jaswa, Amelia J Solon, and Vernon J Lawhern. 2017. Real world BCI: cross-domain learning and practical applications. In *Proceedings of the 2017 ACM Workshop on An Application-oriented Approach to BCI out of the laboratory*. ACM, 25–28.
- [60] Christoph Guger, Shahab Daban, Eric Sellers, Clemens Holzner, Gunther Krausz, Roberta Carabona, Furio Gramatica, and Guenter Edlinger. 2009. How many people are able to control a P300-based brain–computer interface (BCI)? *Neuroscience letters* 462, 1 (2009), 94–98.
- [61] Qiong Gui, Maria Ruiz-blondet, Sarah Laszlo, and Zhanpeng Jin. 2019. A Survey on Brain Biometrics. *Comput. Surveys* 51, 112 (2019).
- [62] A HACHEM, Mohamed Moncef Ben Khelifa, Adel M Alimi, Philippe Gorce, SP VALAN ARASU, S BAULKANI, SUKANT KISHORO BISOY, PRASANT KUMAR PATTNAIK, SELVI RAVINDRAN, NARAYANASAMY PALANISAMY, and others. 2014. Effect of fatigue on ssvpe during virtual wheelchair navigation. *Journal of Theoretical and Applied Information Technology* 65, 1 (2014).
- [63] Ali Haider and Reza Fazel-Rezai. 2017. Application of P300 Event-Related Potential in Brain-Computer Interface. In *Event-Related Potentials and Evoked Potentials*. InTech.
- [64] Mehdi Hajinoroozi, Zzyy-Ping Jung, Chin-Teng Lin, and Yufei Huang. 2015. Feature extraction with deep belief networks for driver’s cognitive states prediction from EEG data. In *Signal and Information Processing (ChinaSIP), 2015 IEEE China Summit and International Conference on*. IEEE, 812–815.
- [65] Mehdi Hajinoroozi, Zijing Mao, and Yufei Huang. 2015. Prediction of driver’s drowsy and alert states from EEG signals with deep learning. In *Computational Advances in Multi-Sensor Adaptive Processing (CAMSAP), 2015 IEEE 6th International Workshop on*. IEEE, 493–496.
- [66] Mehdi Hajinoroozi, Zijing Mao, Yuan-Pin Lin, and Yufei Huang. 2017. Deep Transfer Learning for Cross-subject and Cross-experiment Prediction of Image Rapid Serial Visual Presentation Events from EEG Data. In *International*

- Conference on Augmented Cognition*. Springer, 45–55.
- [67] Mehdi Hajinoroozi, Jianqiu Zhang, and Yufei Huang. 2017. Prediction of fatigue-related driver performance from EEG data by deep Riemannian model. In *Engineering in Medicine and Biology Society (EMBC), 2017 39th Annual International Conference of the IEEE*. IEEE, 4167–4170.
- [68] Changhee Han, Hideaki Hayashi, Leonardo Rundo, Ryosuke Araki, Wataru Shimoda, Shinichi Muramatsu, Yujiro Furukawa, Giancarlo Mauri, and Hideki Nakayama. 2018. GAN-based synthetic brain MR image generation. In *2018 IEEE 15th International Symposium on Biomedical Imaging (ISBI 2018)*. IEEE, 734–738.
- [69] Kay Gregor Hartmann, Robin Tibor Schirrmeyer, and Tonio Ball. 2018. Hierarchical internal representation of spectral features in deep convolutional networks trained for EEG decoding. In *Brain-Computer Interface (BCI), 2018 6th International Conference on*. IEEE, 1–6.
- [70] Ahmad Hasasneh, Nikolas Kampel, Praveen Sripad, N Jon Shah, and Jürgen Dammers. 2018. Deep Learning Approach for Automatic Classification of Ocular and Cardiac Artifacts in MEG Data. *Journal of Engineering* 2018 (2018).
- [71] Mohammad Havaei, Axel Davy, David Warde-Farley, Antoine Biard, Aaron Courville, Yoshua Bengio, Chris Pal, Pierre-Marc Jodoin, and Hugo Larochelle. 2017. Brain tumor segmentation with deep neural networks. *Medical image analysis* 35 (2017), 18–31.
- [72] Johannes Hennrich, Christian Herff, Dominic Heger, and Tanja Schultz. 2015. Investigating deep learning for fNIRS based BCI. In *EMBC*. 2844–2847.
- [73] Luis G Hernández, Oscar Martínez Mozos, José M Ferrández, and Javier M Antelis. 2018. EEG-Based Detection of Braking Intention Under Different Car Driving Conditions. *Frontiers in neuroinformatics* 12 (2018).
- [74] Geoffrey E Hinton and Ruslan R Salakhutdinov. 2006. Reducing the dimensionality of data with neural networks. *science* 313, 5786 (2006), 504–507.
- [75] Tomoyuki Hiroyasu, Kenya Hanawa, and Utako Yamamoto. 2014. Gender classification of subjects from cerebral blood flow changes using Deep Learning. In *Computational Intelligence and Data Mining (CIDM), 2014 IEEE Symposium on*. IEEE, 229–233.
- [76] Mark L Homer, Arto V Nurmikko, John P Donoghue, and Leigh R Hochberg. 2013. Sensors and decoding for intracortical brain computer interfaces. *Annual review of biomedical engineering* 15 (2013), 383–405.
- [77] Mohammad-Parsa Hosseini, Dario Pompili, Kost Elisevich, and Hamid Soltanian-Zadeh. 2017. Optimized deep learning for EEG big data and seizure prediction BCI via internet of things. *IEEE Transactions on Big Data* 3, 4 (2017), 392–404.
- [78] Mohammad-Parsa Hosseini, Hamid Soltanian-Zadeh, Kost Elisevich, and Dario Pompili. 2017. Cloud-based deep learning of big eeg data for epileptic seizure prediction. *arXiv preprint arXiv:1702.05192* (2017).
- [79] Mohammad-Parsa Hosseini, Tuyen X Tran, Dario Pompili, Kost Elisevich, and Hamid Soltanian-Zadeh. 2017. Deep learning with edge computing for localization of epileptogenicity using multimodal rs-fMRI and EEG big data. In *Autonomic Computing (ICAC), 2017 IEEE International Conference on*. IEEE, 83–92.
- [80] Chenhui Hu, Ronghui Ju, Yusong Shen, Pan Zhou, and Quanzheng Li. 2016. Clinical decision support for Alzheimer’s disease based on deep learning and brain network. In *Communications (ICC), 2016 IEEE International Conference on*. IEEE, 1–6.
- [81] Dandan Huang, Kai Qian, Ding-Yu Fei, Wenchuan Jia, Xuedong Chen, and Ou Bai. 2012. Electroencephalography (EEG)-based brain-computer interface (BCI): A 2-D virtual wheelchair control based on event-related desynchronization/synchronization and state control. *IEEE Transactions on Neural Systems and Rehabilitation Engineering* 20, 3 (2012), 379–388.
- [82] Yu-Chia Hung, Yu-Kai Wang, Mukesh Prasad, and Chin-Teng Lin. 2017. Brain dynamic states analysis based on 3D convolutional neural network. In *Systems, Man, and Cybernetics (SMC), 2017 IEEE International Conference on*. IEEE, 222–227.
- [83] Gauvain Huve, Kazuhiko Takahashi, and Masafumi Hashimoto. 2017. Brain activity recognition with a wearable fNIRS using neural networks. In *Mechatronics and Automation (ICMA), 2017 IEEE International Conference on*. IEEE, 1573–1578.
- [84] Gauvain Huve, Kazuhiko Takahashi, and Masafumi Hashimoto. 2018. Brain-computer interface using deep neural network and its application to mobile robot control. In *Advanced Motion Control (AMC), 2018 IEEE 15th International Workshop on*. IEEE, 169–174.
- [85] Xiaowei Jia, Kang Li, Xiaoyi Li, and Aidong Zhang. 2014. A novel semi-supervised deep learning framework for affective state recognition on eeg signals. In *Bioinformatics and Bioengineering (BIBE), 2014 IEEE International Conference on*. IEEE, 30–37.
- [86] Liu Jingwei, Cheng Yin, and Zhang Weidong. 2015. Deep learning EEG response representation for brain computer interface. In *Control Conference (CCC), 2015 34th Chinese*. IEEE, 3518–3523.
- [87] Alexander Rosenberg Johansen, Jing Jin, Tomasz Mszczczyk, Justin Dauwels, Sydney S Cash, and M Brandon Westover. 2016. Epileptiform spike detection via convolutional neural networks. In *Acoustics, Speech and Signal Processing (ICASSP), 2016 IEEE International Conference on*. IEEE, 754–758.

- [88] Palazzo S, Spampinato C, Giordano D, Shah M, Kavassidis, I. 2017. Brain2image: Converting brain signals into images. In *Proceedings of the 25th ACM international conference on Multimedia*. 1809–1817.
- [89] Koki Kawasaki, Tomohiro Yoshikawa, and Takeshi Furuhashi. 2015. Visualizing extracted feature by deep learning in P300 discrimination task. In *Soft Computing and Pattern Recognition (SoCPaR), 2015 7th International Conference of IEEE*, 149–154.
- [90] Piyush Kawde and Gyanendra K Verma. 2017. Deep belief network based affect recognition from physiological signals. In *Electrical, Computer and Electronics (UPCON), 2017 4th IEEE Uttar Pradesh Section International Conference on*. IEEE, 587–592.
- [91] Prerna Khurana, Angshul Majumdar, and Rabab Ward. 2016. Class-wise deep dictionaries for EEG classification. In *Neural Networks (IJCNN), 2016 International Joint Conference on*. IEEE, 3556–3563.
- [92] Diederik P Kingma and Max Welling. 2013. Auto-encoding variational bayes. *arXiv preprint arXiv:1312.6114* (2013).
- [93] Isabell Kiral-Kornek, Subhrajit Roy, Ewan Nurse, Benjamin Mashford, Philippa Karoly, Thomas Carroll, Daniel Payne, Susmita Saha, Steven Baldassano, Terence O'Brien, and others. 2018. Epileptic seizure prediction using big data and deep learning: toward a mobile system. *EBioMedicine* 27 (2018), 103–111.
- [94] Toshiaki Koike-Akino, Ruhi Mahajan, Tim K Marks, Ye Wang, Shinji Watanabe, Oncel Tuzel, and Philip Orlik. 2016. High-accuracy user identification using EEG biometrics. In *2016 38th Annual International Conference of the IEEE Engineering in Medicine and Biology Society (EMBC)*. IEEE, 854–858.
- [95] Sotetsu Koyamada, Yumi Shikauchi, Ken Nakae, Masanori Koyama, and Shin Ishii. 2015. Deep learning of fMRI big data: a novel approach to subject-transfer decoding. *arXiv preprint arXiv:1502.00093* (2015).
- [96] JP Kulasingham, V Vibujithan, and AC De Silva. 2016. Deep belief networks and stacked autoencoders for the P300 Guilty Knowledge Test. In *Biomedical Engineering and Sciences (IECBES), 2016 IEEE EMBS Conference on*. IEEE, 127–132.
- [97] Shiu Kumar, Alok Sharma, Kabir Mamun, and Tatsuhiko Tsunoda. 2016. A deep learning approach for motor imagery EEG signal classification. In *Computer Science and Engineering (APWC on CSE), 2016 3rd Asia-Pacific World Congress on*. IEEE, 34–39.
- [98] No-Sang Kwak, Klaus-Robert Müller, and Seong-Whan Lee. 2017. A convolutional neural network for steady state visual evoked potential classification under ambulatory environment. *PloS one* 12, 2 (2017), e0172578.
- [99] Vernon Lawhern, Amelia Solon, Nicholas Waytowich, Stephen M Gordon, Chou Hung, and Brent J Lance. 2018. EEGNet: a compact convolutional neural network for EEG-based brain-computer interfaces. *Journal of neural engineering* (2018).
- [100] Hyeon Kyu Lee and Young-Seok Choi. 2018. A convolution neural networks scheme for classification of motor imagery EEG based on wavelet time-frequency image. In *Information Networking (ICOIN), 2018 International Conference on*. IEEE, 906–909.
- [101] Stephanie Lees, Natalie Dayan, Hubert Cecotti, Paul Mccullagh, Liam Maguire, Fabien Lotte, and Damien Coyle. 2018. A review of rapid serial visual presentation-based brain-computer interfaces. *Journal of neural engineering* 15, 2 (2018), 021001.
- [102] Eric C Leuthardt, Gerwin Schalk, Jarod Roland, Adam Rouse, and Daniel W Moran. 2009. Evolution of brain-computer interfaces: going beyond classic motor physiology. *Neurosurgical focus* 27, 1 (2009), E4.
- [103] Junhua Li and Andrzej Cichocki. 2014. Deep learning of multifractal attributes from motor imagery induced EEG. In *International Conference on Neural Information Processing*. Springer, 503–510.
- [104] Junhua Li, Zbigniew Struzik, Liqing Zhang, and Andrzej Cichocki. 2015. Feature learning from incomplete EEG with denoising autoencoder. *Neurocomputing* 165 (2015), 23–31.
- [105] Jimpeng Li, Zhaoxiang Zhang, and Huiguang He. 2016. Implementation of eeg emotion recognition system based on hierarchical convolutional neural networks. In *International Conference on Brain Inspired Cognitive Systems*. Springer, 22–33.
- [106] Jimpeng Li, Zhaoxiang Zhang, and Huiguang He. 2017. Hierarchical convolutional neural networks for EEG-based emotion recognition. *Cognitive Computation* (2017), 1–13.
- [107] Kang Li, Xiaoyi Li, Yuan Zhang, and Aidong Zhang. 2013. Affective state recognition from EEG with deep belief networks. In *2013 IEEE International Conference on Bioinformatics and Biomedicine*. IEEE, 305–310.
- [108] Pinyi Li, Wenhui Jiang, and Fei Su. 2016. Single-channel EEG-based mental fatigue detection based on deep belief network. In *Engineering in Medicine and Biology Society (EMBC), 2016 IEEE 38th Annual International Conference of the*. IEEE, 367–370.
- [109] Rongjian Li, Wenlu Zhang, Heung-Il Suk, Li Wang, Jiang Li, Dinggang Shen, and Shuiwang Ji. 2014. Deep learning based imaging data completion for improved brain disease diagnosis. In *International Conference on Medical Image Computing and Computer-Assisted Intervention*. Springer, 305–312.
- [110] Xiang Li, Peng Zhang, Dawei Song, Guangliang Yu, Yuexian Hou, and Bin Hu. 2015. EEG based emotion identification using unsupervised deep feature learning. (2015).

- [111] Qin Lin, Shu-qun Ye, Xiu-mei Huang, Si-you Li, Mei-zhen Zhang, Yun Xue, and Wen-Sheng Chen. 2016. Classification of epileptic EEG signals with stacked sparse autoencoder based on deep learning. In *International Conference on Intelligent Computing*. Springer, 802–810.
- [112] Zhimin Lin, Ying Zeng, Li Tong, Hangming Zhang, Chi Zhang, and Bin Yan. 2017. Method for enhancing single-trial P300 detection by introducing the complexity degree of image information in rapid serial visual presentation tasks. *PloS one* 12, 12 (2017), e0184713.
- [113] Geert Litjens, Thijs Kooi, Babak Ehteshami Bejnordi, Arnaud Arindra Adiyoso Setio, Francesco Ciompi, Mohsen Ghafoorian, Jeroen Awm Van Der Laak, Bram Van Ginneken, and Clara I Sánchez. 2017. A survey on deep learning in medical image analysis. *Medical image analysis* 42 (2017), 60–88.
- [114] Jin Liu, Yi Pan, Min Li, Ziyue Chen, Lu Tang, Chengqian Lu, and Jianxin Wang. 2018. Applications of deep learning to mri images: a survey. *Big Data Mining and Analytics* 1, 1 (2018), 1–18.
- [115] Mingfei Liu, Wei Wu, Zhenghui Gu, Zhuliang Yu, Feifei Qi, and Yuanqing Li. 2018. Deep learning based on Batch Normalization for P300 signal detection. *Neurocomputing* 275 (2018), 288–297.
- [116] Qi Liu, Xiao-Guang Zhao, Zeng-Guang Hou, and Hong-Guang Liu. 2017. Deep Belief Networks for EEG-Based Concealed Information Test. In *International Symposium on Neural Networks*. Springer, 498–506.
- [117] Wenqiang Liu, Huiping Jiang, and Yao Lu. 2017. Analyze EEG Signals with Convolutional Neural Network Based on Power Spectrum Feature Selection. *Proceedings of Science* (2017).
- [118] Wei Liu, Wei-Long Zheng, and Bao-Liang Lu. 2016. Emotion recognition using multimodal deep learning. In *International Conference on Neural Information Processing*. Springer, 521–529.
- [119] Fabien Lotte, Laurent Bougrain, Andrzej Cichocki, Maureen Clerc, Marco Congedo, Alain Rakotomamonjy, and Florian Yger. 2018. A review of classification algorithms for EEG-based brain–computer interfaces: a 10 year update. *Journal of neural engineering* 15, 3 (2018), 031005.
- [120] Fabien Lotte, Marco Congedo, Anatole Lécuyer, Fabrice Lamarche, and Bruno Arnaldi. 2007. A review of classification algorithms for EEG-based brain–computer interfaces. *Journal of neural engineering* 4, 2 (2007), R1.
- [121] Na Lu, Tengfei Li, Xiaodong Ren, and Hongyu Miao. 2017. A deep learning scheme for motor imagery classification based on restricted boltzmann machines. *IEEE transactions on neural systems and rehabilitation engineering* 25, 6 (2017), 566–576.
- [122] Teng Ma, Hui Li, Hao Yang, Xulin Lv, Peiyang Li, Tiejun Liu, Dezhong Yao, and Peng Xu. 2017. The extraction of motion-onset VEP BCI features based on deep learning and compressed sensing. *Journal of neuroscience methods* 275 (2017), 80–92.
- [123] RK Maddula, J Stivers, M Mousavi, S Ravindran, and VR de Sa. 2017. Deep recurrent convolutional neural networks for classifying P300 BCI signals. In *Proceedings of the 7th Graz Brain-Computer Interface Conference, Graz, Austria*. 18–22.
- [124] Mufti Mahmud, Mohammed Shamim Kaiser, Amir Hussain, and Stefano Vassanelli. 2018. Applications of deep learning and reinforcement learning to biological data. *IEEE transactions on neural networks and learning systems* 29, 6 (2018), 2063–2079.
- [125] Jaakko Malmivuo, Robert Plonsey, and others. 1995. *Bioelectromagnetism: principles and applications of bioelectric and biomagnetic fields*. Oxford University Press, USA.
- [126] Ran Manor and Amir B Geva. 2015. Convolutional neural network for multi-category rapid serial visual presentation bci. *Frontiers in computational neuroscience* 9 (2015), 146.
- [127] Ran Manor, Liran Mishali, and Amir B Geva. 2016. Multimodal neural network for rapid serial visual presentation brain computer interface. *Frontiers in computational neuroscience* 10 (2016), 130.
- [128] Marti Manzano, Alberto Guillén, Ignacio Rojas, and Luis Javier Herrera. 2017. Combination of EEG Data Time and Frequency Representations in Deep Networks for Sleep Stage Classification. In *International Conference on Intelligent Computing*. Springer, 219–229.
- [129] Marti Manzano, Alberto Guillén, Ignacio Rojas, and Luis Javier Herrera. 2017. Deep learning using EEG data in time and frequency domains for sleep stage classification. In *International Work-Conference on Artificial Neural Networks*. Springer, 132–141.
- [130] Zijing Mao. 2016. *Deep learning for rapid serial visual presentation event from electroencephalography signal*. Ph.D. Dissertation. The University of Texas at San Antonio.
- [131] Zijing Mao, Vernon Lawhern, Lenis Mauricio Merino, Kenneth Ball, Li Deng, Brent J Lance, Kay Robbins, and Yufei Huang. 2014. Classification of non-time-locked rapid serial visual presentation events for brain-computer interaction using deep learning. In *Signal and Information Processing (ChinaSIP), 2014 IEEE China Summit & International Conference on*. IEEE, 520–524.
- [132] Zijing Mao, Wan Xiang Yao, and Yufei Huang. 2017. EEG-based biometric identification with deep learning. In *Neural Engineering (NER), 2017 8th International IEEE/EMBS Conference on*. IEEE, 609–612.

- [133] SG Mason, A Bashashati, M Fatourechi, KF Navarro, and GE Birch. 2007. A comprehensive survey of brain interface technology designs. *Annals of biomedical engineering* 35, 2 (2007), 137–169.
- [134] Kaare B Mikkelsen, Simon L Kappel, Danilo P Mandic, and Preben Kidmose. 2015. EEG recorded from the ear: Characterizing the ear-EEG method. *Frontiers in neuroscience* 9 (2015), 438.
- [135] Seonwoo Min, Byunghan Lee, and Sungroh Yoon. 2017. Deep learning in bioinformatics. *Briefings in bioinformatics* 18, 5 (2017), 851–869.
- [136] Juan Abdon Mioranda-Correa and Ioannis Patras. 2018. A Multi-Task Cascaded Network for Prediction of Affect, Personality, Mood and Social Context Using EEG Signals. In *Automatic Face & Gesture Recognition (FG 2018), 2018 13th IEEE International Conference on*. IEEE, 373–380.
- [137] Francesco Carlo Morabito, Maurizio Campolo, Cosimo Ieracitano, Javad Mohammad Ebadi, Lilla Bonanno, Alessia Bramanti, Simona Desalvo, Nadia Mammone, and Placido Bramanti. 2016. Deep convolutional neural networks for classification of mild cognitive impaired and Alzheimer’s disease patients from scalp EEG recordings. In *Research and Technologies for Society and Industry Leveraging a better tomorrow (RTSI), 2016 IEEE 2nd International Forum on*. IEEE, 1–6.
- [138] Francesco Carlo Morabito, Maurizio Campolo, Nadia Mammone, Mario Versaci, Silvana Franceschetti, Fabrizio Tagliavini, Vito Sofia, Daniela Fatuzzo, Antonio Gambardella, Angelo Labate, and others. 2017. Deep learning representation from electroencephalography of Early-Stage Creutzfeldt-Jakob disease and features for differentiation from rapidly progressive dementia. *International journal of neural systems* 27, 02 (2017), 1650039.
- [139] M Moreno Lopez. 2017. Deep learning for brain tumor segmentation. (2017).
- [140] Faezeh Movahedi, James L Coyle, and Ervin Sejdić. 2018. Deep belief networks for electroencephalography: A review of recent contributions and future outlooks. *IEEE journal of biomedical and health informatics* 22, 3 (2018), 642–652.
- [141] Sanam Narejo, Eros Pasero, and Farzana Kulsoom. 2016. EEG based eye state classification using deep belief network and stacked AutoEncoder. *International Journal of Electrical and Computer Engineering (IJECE)* 6, 6 (2016), 3131–3141.
- [142] Noman Naseer and Keum-Shik Hong. 2015. fNIRS-based brain-computer interfaces: a review. *Frontiers in human neuroscience* 9 (2015), 3.
- [143] Noman Naseer, Nauman Khalid Qureshi, Farzan Majeed Noori, and Keum-Shik Hong. 2016. Analysis of different classification techniques for two-class functional near-infrared spectroscopy-based brain-computer interface. *Computational intelligence and neuroscience* 2016 (2016).
- [144] Anthony M Norcia, L Gregory Appelbaum, Justin M Ales, Benoit R Cottreau, and Bruno Rossion. 2015. The steady-state visual evoked potential in vision research: a review. *Journal of vision* 15, 6 (2015), 4–4.
- [145] Ewan Nurse, Benjamin S Mashford, Antonio Jimeno Yepes, Isabell Kiral-Kornek, Stefan Harrer, and Dean R Freestone. 2016. Decoding EEG and LFP signals using deep learning: heading TrueNorth. In *Proceedings of the ACM International Conference on Computing Frontiers*. ACM, 259–266.
- [146] Ewan S Nurse, Philippa J Karoly, David B Grayden, and Dean R Freestone. 2015. A generalizable brain-computer interface (bci) using machine learning for feature discovery. *PloS one* 10, 6 (2015), e0131328.
- [147] Andres Ortiz, Jorge Munilla, Juan M Gorriz, and Javier Ramirez. 2016. Ensembles of deep learning architectures for the early diagnosis of the Alzheimer’s disease. *International journal of neural systems* 26, 07 (2016), 1650025.
- [148] Marlene Pacharra, Stefan Debener, and Edmund Wascher. 2017. Concealed around-the-ear EEG captures cognitive processing in a visual simon task. *Frontiers in human neuroscience* 11 (2017), 290.
- [149] Adam Page, JT Turner, Tinoosh Mohsenin, and Tim Oates. 2014. Comparing Raw Data and Feature Extraction for Seizure Detection with Deep Learning Methods.. In *FLAIRS Conference*.
- [150] Simone Palazzo, Concetto Spampinato, Isaak Kavasidis, Daniela Giordano, and Mubarak Shah. 2017. Generative adversarial networks conditioned by brain signals. In *Proceedings of the IEEE International Conference on Computer Vision*. 3410–3418.
- [151] Chethan Pandarinath, Paul Nuyujukian, Christine H Blabe, Brittany L Sorice, Jad Saab, Francis R Willett, Leigh R Hochberg, Krishna V Shenoy, and Jaimie M Henderson. 2017. High performance communication by people with paralysis using an intracortical brain-computer interface. *Elife* 6 (2017), e18554.
- [152] Raja Parasuraman and Yang Jiang. 2012. Individual differences in cognition, affect, and performance: Behavioral, neuroimaging, and molecular genetic approaches. *Neuroimage* 59, 1 (2012), 70–82.
- [153] JL Pérez-Benitez, JA Pérez-Benitez, and JH Espina-Hernández. 2018. Development of a brain computer interface interface using multi-frequency visual stimulation and deep neural networks. In *Electronics, Communications and Computers (CONIELECOMP), 2018 International Conference on*. IEEE, 18–24.
- [154] Gert Pfurtscheller and FH Lopes Da Silva. 1999. Event-related EEG/MEG synchronization and desynchronization: basic principles. *Clinical neurophysiology* 110, 11 (1999), 1842–1857.
- [155] Gert Pfurtscheller and Christa Neuper. 2001. Motor imagery and direct brain-computer communication. *Proc. IEEE* 89, 7 (2001), 1123–1134.

- [156] Sergey M Plis, Devon R Hjelm, Ruslan Salakhutdinov, Elena A Allen, Henry J Bockholt, Jeffrey D Long, Hans J Johnson, Jane S Paulsen, Jessica A Turner, and Vince D Calhoun. 2014. Deep learning for neuroimaging: a validation study. *Frontiers in neuroscience* 8 (2014), 229.
- [157] Michel JAM Putten, Sebastian Olbrich, and Martijn Arns. 2018. Predicting sex from brain rhythms with deep learning. *Scientific reports* 8, 1 (2018), 3069.
- [158] Alec Radford, Luke Metz, and Soumith Chintala. 2016. Unsupervised representation learning with deep convolutional generative adversarial networks. *International Conference on Learning Representations (ICLR)* (2016).
- [159] Tharun Kumar Reddy and Laxmidhar Behera. 2016. Online Eye state recognition from EEG data using Deep architectures. In *Systems, Man, and Cybernetics (SMC), 2016 IEEE International Conference on*. IEEE, 000712–000717.
- [160] Sangram Redkar. 2015. Using Deep Learning for Human Computer Interface via Electroencephalography. *IAES International Journal of Robotics and Automation* 4, 4 (2015).
- [161] David Regan. 1977. Steady-state evoked potentials. *JOSA* 67, 11 (1977), 1475–1489.
- [162] Yuanfang Ren and Yan Wu. 2014. Convolutional deep belief networks for feature extraction of EEG signal. In *Neural Networks (IJCNN), 2014 International Joint Conference on*. IEEE, 2850–2853.
- [163] Roozbeh Rezaie, Panagiotis G Simos, Jack M Fletcher, Jenifer Juranek, Paul T Cirino, Zhimin Li, Antony D Passaro, and Andrew C Papanicolaou. 2011. The timing and strength of regional brain activation associated with word recognition in children with reading difficulties. *Frontiers in human neuroscience* 5 (2011), 45.
- [164] Giulio Ruffini, David Ibañez, Marta Castellano, Stephen Dunne, and Aureli Soria-Frisch. 2016. EEG-driven RNN classification for prognosis of neurodegeneration in at-risk patients. In *International Conference on Artificial Neural Networks*. Springer, 306–313.
- [165] Sergio Ruiz, Korhan Buyukturkoglu, Mohit Rana, Niels Birbaumer, and Ranganatha Sitaram. 2014. Real-time fMRI brain computer interfaces: self-regulation of single brain regions to networks. *Biological psychology* 95 (2014), 4–20.
- [166] Muhammad Rusydi, Takeo Okamoto, Satoshi Ito, and Minoru Sasaki. 2014. Rotation matrix to operate a robot manipulator for 2D analog tracking objects using electrooculography. *Robotics* 3, 3 (2014), 289–309.
- [167] Siavash Sakhavi, Cuntai Guan, and Shuicheng Yan. 2015. Parallel convolutional-linear neural network for motor imagery classification. In *Signal Processing Conference (EUSIPCO), 2015 23rd European*. IEEE, 2736–2740.
- [168] Wojciech Samek, Klaus-Robert Müller, Motoaki Kawanabe, and Carmen Vidaurre. 2012. Brain-computer interfacing in discriminative and stationary subspaces. In *Engineering in Medicine and Biology Society (EMBC), 2012 Annual International Conference of the IEEE*. IEEE, 2873–2876.
- [169] Phyto Phyto San, Sai Ho Ling, Rifai Chai, Yvonne Tran, Ashley Craig, and Hung Nguyen. 2016. EEG-based driver fatigue detection using hybrid deep generic model. In *Engineering in Medicine and Biology Society (EMBC), 2016 IEEE 38th Annual International Conference of the IEEE*, 800–803.
- [170] Soumalya Sarkar, Kishore Reddy, Alex Dorgan, Cali Fidopiastis, and Michael Giering. 2016. Wearable EEG-based activity recognition in PHM-related service environment via deep learning. *Int. J. Progn. Health Manag* 7 (2016), 1–10.
- [171] Saman Sarraf and Ghassem Tofighi. 2016. Deep learning-based pipeline to recognize Alzheimer's disease using fMRI data. In *Future Technologies Conference (FTC)*. IEEE, 816–820.
- [172] Saman Sarraf, Ghassem Tofighi, and others. 2016. DeepAD: Alzheimer's Disease Classification via Deep Convolutional Neural Networks using MRI and fMRI. *bioRxiv* (2016), 070441.
- [173] R Schirrmeyer, Lukas Gemein, Katharina Eggenberger, Frank Hutter, and Tonio Ball. 2017. Deep learning with convolutional neural networks for decoding and visualization of EEG pathology. In *Signal Processing in Medicine and Biology Symposium (SPMB), 2017 IEEE*. IEEE, 1–7.
- [174] Jürgen Schmidhuber. 2015. Deep learning in neural networks: An overview. *Neural networks* 61 (2015), 85–117.
- [175] K Seeliger, U Güçlü, L Ambrogioni, Y Güçlütürk, and MAJ Van Gerven. 2018. Generative adversarial networks for reconstructing natural images from brain activity. *NeuroImage* 181 (2018), 775–785.
- [176] Vinit Shah, Meysam Golmohammadi, Saeedeh Ziyabari, Eva Von Weltin, Iyad Obeid, and Joseph Picone. 2017. Optimizing channel selection for seizure detection. In *Signal Processing in Medicine and Biology Symposium (SPMB), 2017 IEEE*. IEEE, 1–5.
- [177] Mostafa Shahin, Beena Ahmed, Sana Tmar-Ben Hamida, Fathima Lamana Mulaffer, Martin Glos, and Thomas Penzel. 2017. Deep Learning and Insomnia: Assisting Clinicians With Their Diagnosis. *IEEE journal of biomedical and health informatics* 21, 6 (2017), 1546–1553.
- [178] Jared Shamwell, Hyungtae Lee, Heesung Kwon, Amar R Marathe, Vernon Lawhern, and William Nothwang. 2016. Single-trial EEG RSVP classification using convolutional neural networks. In *Micro-and Nanotechnology Sensors, Systems, and Applications VIII*, Vol. 9836. International Society for Optics and Photonics, 983622.
- [179] Ajay Shanbhag, Aman Prabhu Kholkar, Saish Sawant, Allister Vicente, Sparsh Martires, and Supriya Patil. 2017. P300 analysis using deep neural network. In *2017 International Conference on Energy, Communication, Data Analytics and Soft Computing (ICECDS)*. IEEE, 3142–3147.

- [180] Jian Shang, Wei Zhang, Jiang Xiong, and Qingshan Liu. 2017. Cognitive load recognition using multi-channel complex network method. In *International Symposium on Neural Networks*. Springer, 466–474.
- [181] Guohua Shen, Tomoyasu Horikawa, Kei Majima, and Yukiyasu Kamitani. 2019. Deep image reconstruction from human brain activity. *PLoS computational biology* 15, 1 (2019), e1006633.
- [182] V Shreyas and Vinod Pankajakshan. 2017. A deep learning architecture for brain tumor segmentation in MRI images. In *Multimedia Signal Processing (MMSp), 2017 IEEE 19th International Workshop on*. IEEE, 1–6.
- [183] Michelle Shu and Alona Fyshe. 2013. Sparse autoencoders for word decoding from magnetoencephalography. In *Proceedings of the third NIPS Workshop on Machine Learning and Interpretation in NeuroImaging (MLINI)*.
- [184] Surjo R Soekadar, Niels Birbaumer, Marc W Slutzky, and Leonardo G Cohen. 2015. Brain-machine interfaces in neurorehabilitation of stroke. *Neurobiology of disease* 83 (2015), 172–179.
- [185] Amelia J Solon, Stephen M Gordon, BJ Lance, and VJ Lawhern. 2017. Deep Learning Approaches for P300 Classification in Image Triage: Applications to the NAILS Task. In *Proceedings of the 13th NTCIR Conference on Evaluation of Information Access Technologies, NTCIR-13, Tokyo, Japan*. 5–8.
- [186] Arnaud Sors, Stéphane Bonnet, Sébastien Mirek, Laurent Vercueil, and Jean-François Payen. 2018. A convolutional neural network for sleep stage scoring from raw single-channel eeg. *Biomedical Signal Processing and Control* 42 (2018), 107–114.
- [187] Concetto Spampinato, Simone Palazzo, Isaak Kavasidis, Daniela Giordano, Nasim Souly, and Mubarak Shah. 2017. Deep learning human mind for automated visual classification. In *Proceedings of the IEEE Conference on Computer Vision and Pattern Recognition*. 6809–6817.
- [188] Ghislain St-Yves and Thomas Naselaris. 2018. Generative Adversarial Networks Conditioned on Brain Activity Reconstruct Seen Images. In *2018 IEEE International Conference on Systems, Man, and Cybernetics (SMC)*. IEEE, 1054–1061.
- [189] Avital Sternin, Sebastian Stober, JA Grahn, and AM Owen. 2015. Tempo estimation from the eeg signal during perception and imagination of music. In *1st International Workshop on Brain-Computer Music Interfacing/11th International Symposium on Computer Music Multidisciplinary Research (BCMI/CMMRf15)(Plymouth)*.
- [190] Sebastian Stober, Daniel J Cameron, and Jessica A Grahn. 2014. Classifying EEG Recordings of Rhythm Perception.. In *ISMIR*. 649–654.
- [191] Sebastian Stober, Daniel J Cameron, and Jessica A Grahn. 2014. Using Convolutional Neural Networks to Recognize Rhythm Stimuli from Electroencephalography Recordings. In *Advances in neural information processing systems*. 1449–1457.
- [192] Sebastian Stober, Avital Sternin, Adrian M Owen, and Jessica A Grahn. 2015. Deep feature learning for EEG recordings. *arXiv preprint arXiv:1511.04306* (2015).
- [193] Irene Sturm, Sebastian Lapuschkin, Wojciech Samek, and Klaus-Robert Müller. 2016. Interpretable deep neural networks for single-trial EEG classification. *Journal of neuroscience methods* 274 (2016), 141–145.
- [194] Nur Farahana Mohd Suhaimi, Zaw Zaw Htike, and Nahrul Khair Alang Md Rashid. 2015. Studies on classification of fMRI data using deep learning approach. (2015).
- [195] Heung-Il Suk, Dinggang Shen, Alzheimer’s Disease Neuroimaging Initiative, and others. 2015. Deep learning in diagnosis of brain disorders. In *Recent Progress in Brain and Cognitive Engineering*. Springer, 203–213.
- [196] Heung-Il Suk, Chong-Yaw Wee, Seong-Whan Lee, and Dinggang Shen. 2016. State-space model with deep learning for functional dynamics estimation in resting-state fMRI. *NeuroImage* 129 (2016), 292–307.
- [197] Akara Supratak, Hao Dong, Chao Wu, and Yike Guo. 2017. DeepSleepNet: a model for automatic sleep stage scoring based on raw single-channel EEG. *IEEE Transactions on Neural Systems and Rehabilitation Engineering* 25, 11 (2017), 1998–2008.
- [198] Yousef Rezaei Tabar and Ugur Halici. 2016. A novel deep learning approach for classification of EEG motor imagery signals. *Journal of neural engineering* 14, 1 (2016), 016003.
- [199] Sachin S Talathi. 2017. Deep Recurrent Neural Networks for seizure detection and early seizure detection systems. *arXiv preprint arXiv:1706.03283* (2017).
- [200] Chuanqi Tan, Fuchun Sun, Wenchang Zhang, Jianhua Chen, and Chunfang Liu. 2017. Multimodal Classification with Deep Convolutional-Recurrent Neural Networks for Electroencephalography. In *International Conference on Neural Information Processing*. Springer, 767–776.
- [201] Dakun Tan, Rui Zhao, Jinbo Sun, and Wei Qin. 2015. Sleep spindle detection using deep learning: a validation study based on crowdsourcing. In *Engineering in Medicine and Biology Society (EMBC), 2015 37th Annual International Conference of the IEEE*. IEEE, 2828–2831.
- [202] Zhichuan Tang, Chao Li, and Shouqian Sun. 2017. Single-trial EEG classification of motor imagery using deep convolutional neural networks. *Optik-International Journal for Light and Electron Optics* 130 (2017), 11–18.
- [203] Jason Teo, Chew Lin Hou, and James Mountstephens. 2017. Deep learning for EEG-Based preference classification. In *AIP Conference Proceedings*, Vol. 1891. AIP Publishing, 020141.

- [204] Jason Teo, Chew Lin Hou, and James Mountstephens. 2018. Preference Classification Using Electroencephalography (EEG) and Deep Learning. *Journal of Telecommunication, Electronic and Computer Engineering (JTEC)* 10, 1-11 (2018), 87–91.
- [205] John Thomas, Tomasz Maszczyk, Nishant Sinha, Tilmann Kluge, and Justin Dauwels. 2017. Deep learning-based classification for brain-computer interfaces. In *Systems, Man, and Cybernetics (SMC), 2017 IEEE International Conference on*. IEEE, 234–239.
- [206] Orestis Tsalialis, Paul M Matthews, Yike Guo, and Stefanos Zafeiriou. 2016. Automatic sleep stage scoring with single-channel EEG using convolutional neural networks. *arXiv preprint arXiv:1610.01683* (2016).
- [207] Kostas M Tsiouris, Vasileios C Pezoulas, Michalis Zervakis, Spiros Konitsiotis, Dimitrios D Koutsouris, and Dimitrios I Fotiadis. 2018. A Long Short-Term Memory deep learning network for the prediction of epileptic seizures using EEG signals. *Computers in biology and medicine* 99 (2018), 24–37.
- [208] Tao Tu, Jonathan Koss, and Paul Sajda. 2018. Relating deep neural network representations to EEG-fMRI spatiotemporal dynamics in a perceptual decision-making task. In *Proceedings of the IEEE Conference on Computer Vision and Pattern Recognition Workshops*. 1985–1991.
- [209] JT Turner, Adam Page, Tinoosh Mohsenin, and Tim Oates. 2014. Deep belief networks used on high resolution multichannel electroencephalography data for seizure detection. In *2014 AAAI Spring Symposium Series*.
- [210] Tomas Uktveris and Vacius Jusas. 2017. Application of convolutional neural networks to four-class motor imagery classification problem. *Information Technology And Control* 46, 2 (2017), 260–273.
- [211] Ihsan Ullah, Muhammad Hussain, Hatim Aboalsamh, and others. 2018. An automated system for epilepsy detection using EEG brain signals based on deep learning approach. *Expert Systems with Applications* 107 (2018), 61–71.
- [212] Lukáš Vařeka and Pavel Mautner. 2017. Stacked Autoencoders for the P300 Component Detection. *Frontiers in neuroscience* 11 (2017), 302.
- [213] Sandra Vieira, Walter HL Pinaya, and Andrea Mechelli. 2017. Using deep learning to investigate the neuroimaging correlates of psychiatric and neurological disorders: Methods and applications. *Neuroscience & Biobehavioral Reviews* 74 (2017), 58–75.
- [214] Albert Vilamala, Kristoffer H Madsen, and Lars Kai Hansen. 2017. Neural Networks for Interpretable Analysis of EEG Sleep Stage Scoring. In *INTERNATIONAL WORKSHOP ON MACHINE LEARNING FOR SIGNAL PROCESSING 2017*.
- [215] Martin Völker, Robin T Schirrmester, Lukas DJ Fiederer, Wolfram Burgard, and Tonio Ball. 2018. Deep transfer learning for error decoding from non-invasive EEG. In *Brain-Computer Interface (BCI), 2018 6th International Conference on*. IEEE, 1–6.
- [216] Fang Wang, Sheng-hua Zhong, Jianfeng Peng, Jianmin Jiang, and Yan Liu. 2018. Data Augmentation for EEG-Based Emotion Recognition with Deep Convolutional Neural Networks. In *International Conference on Multimedia Modeling*. Springer, 82–93.
- [217] Jindong Wang, Yiqiang Chen, Shuji Hao, Xiaohui Peng, and Lisha Hu. 2018. Deep learning for sensor-based activity recognition: A survey. *Pattern Recognition Letters* (2018).
- [218] Kai Wang, Youjin Zhao, Qingyu Xiong, Min Fan, Guotan Sun, Longkun Ma, and Tong Liu. 2016. Research on healthy anomaly detection model based on deep learning from multiple time-series physiological signals. *Scientific Programming* 2016 (2016).
- [219] Qian Wang, Yongjun Hu, and He Chen. 2017. Multi-channel EEG Classification Based on Fast Convolutional Feature Extraction. In *International Symposium on Neural Networks*. Springer, 533–540.
- [220] Xiashuang Wang, Guanghong Gong, Ni Li, and Yaofei Ma. 2016. A Survey of the BCI and its Application Prospect. In *Theory, Methodology, Tools and Applications for Modeling and Simulation of Complex Systems*. Springer, 102–111.
- [221] Nicholas R Waytowich, Vernon Lawhern, Javier O Garcia, Jennifer Cummings, Josef Faller, Paul Sajda, and Jean M Vettel. 2018. Compact Convolutional Neural Networks for Classification of Asynchronous Steady-state Visual Evoked Potentials. *arXiv preprint arXiv:1803.04566* (2018).
- [222] Dong Wen, Zhenhao Wei, Yanhong Zhou, Guolin Li, Xu Zhang, and Wei Han. 2018. Deep Learning Methods to Process fMRI Data and Their Application in the Diagnosis of Cognitive Impairment: A Brief Overview and Our Opinion. *Frontiers in neuroinformatics* 12 (2018), 23.
- [223] Tingxi Wen and Zhongnan Zhang. 2018. Deep Convolution Neural Network and Autoencoders-Based Unsupervised Feature Learning of EEG Signals. *IEEE Access* 6 (2018), 25399–25410.
- [224] Bin Xia, Qianyun Li, Jie Jia, Jingyi Wang, Ujwal Chaudhary, Ander Ramos-Murguialday, and Niels Birbaumer. 2015. Electrooculogram based sleep stage classification using deep belief network. In *Neural Networks (IJCNN), 2015 International Joint Conference on*. IEEE, 1–5.
- [225] Ziqian Xie. 2018. Deep Learning Approach for Brain Machine Interface. (2018).
- [226] Ziqian Xie, Odelia Schwartz, and Abhishek Prasad. 2018. Decoding of finger trajectory from ECoG using deep learning. *Journal of neural engineering* 15, 3 (2018), 036009.

- [227] Haiyan Xu and Konstantinos N Plataniotis. 2016. Affective states classification using EEG and semi-supervised deep learning approaches. In *Multimedia Signal Processing (MMSP), 2016 IEEE 18th International Workshop on*. IEEE, 1–6.
- [228] Haiyan Xu and Konstantinos N Plataniotis. 2016. EEG-based affect states classification using deep belief networks. In *Digital Media Industry & Academic Forum (DMIAF)*. IEEE, 148–153.
- [229] Bo Yan, Yong Wang, Yuheng Li, Yejiang Gong, Lu Guan, and Sheng Yu. 2016. An EEG signal classification method based on sparse auto-encoders and support vector machine. In *Communications in China (ICCC), 2016 IEEE/CIC International Conference on*. IEEE, 1–6.
- [230] Xue Yan, Wei-Long Zheng, Wei Liu, and Bao-Liang Lu. 2017. Identifying Gender Differences in Multimodal Emotion Recognition Using Bimodal Deep AutoEncoder. In *International Conference on Neural Information Processing*. Springer, 533–542.
- [231] CC Yang, JS Lieberman, and CZ Hong. 1989. Early smooth horizontal eye movement: a favorable prognostic sign in patients with locked-in syndrome. *Archives of physical medicine and rehabilitation* 70, 3 (1989), 230–232.
- [232] Huijuan Yang, Siavash Sakhavi, Kai Keng Ang, and Cuntai Guan. 2015. On the use of convolutional neural networks and augmented CSP features for multi-class motor imagery of EEG signals classification. In *Engineering in Medicine and Biology Society (EMBC), 2015 37th Annual International Conference of the IEEE*. IEEE, 2620–2623.
- [233] Roy Yannick, Banville Hubert, Albuquerque Isabela, Gramfort Alexandre, Faubert Jocelyn, and others. 2019. Deep learning-based electroencephalography analysis: a systematic review. *arXiv preprint arXiv:1901.05498* (2019).
- [234] Antonio Jimeno Yepes, Jianbin Tang, and Benjamin Scott Mashford. 2017. Improving classification accuracy of feedforward neural networks for spiking neuromorphic chips. *arXiv preprint arXiv:1705.07755* (2017).
- [235] Erwei Yin, Timothy Zeyl, Rami Saab, Tom Chau, Dewen Hu, and Zongtan Zhou. 2015. A hybrid brain–computer interface based on the fusion of P300 and SSVEP scores. *IEEE Transactions on Neural Systems and Rehabilitation Engineering* 23, 4 (2015), 693–701.
- [236] Zhong Yin and Jianhua Zhang. 2017. Cross-session classification of mental workload levels using EEG and an adaptive deep learning model. *Biomedical Signal Processing and Control* 33 (2017), 30–47.
- [237] Zhong Yin, Mengyuan Zhao, Yongxiong Wang, Jingdong Yang, and Jianhua Zhang. 2017. Recognition of emotions using multimodal physiological signals and an ensemble deep learning model. *Computer methods and programs in biomedicine* 140 (2017), 93–110.
- [238] Jaehong Yoon, Jungnyun Lee, and Mincheol Whang. 2018. Spatial and Time Domain Feature of ERP Speller System Extracted via Convolutional Neural Network. *Computational intelligence and neuroscience* 2018 (2018).
- [239] Ye Yuan, Guangxu Xun, Kebin Jia, and Aidong Zhang. 2017. A novel wavelet-based model for eeg epileptic seizure detection using multi-context learning. In *Bioinformatics and Biomedicine (BIBM), 2017 IEEE International Conference on*. IEEE, 694–699.
- [240] Ye Yuan, Guangxu Xun, Fenglong Ma, Qiuling Suo, Hongfei Xue, Kebin Jia, and Aidong Zhang. 2018. A novel channel-aware attention framework for multi-channel EEG seizure detection via multi-view deep learning. In *Biomedical & Health Informatics (BHI), 2018 IEEE EMBS International Conference on*. IEEE, 206–209.
- [241] Junming Zhang, Yan Wu, Jing Bai, and Fuqiang Chen. 2016. Automatic sleep stage classification based on sparse deep belief net and combination of multiple classifiers. *Transactions of the Institute of Measurement and Control* 38, 4 (2016), 435–451.
- [242] Jin Zhang, Chungang Yan, and Xiaoliang Gong. 2017. Deep convolutional neural network for decoding motor imagery based brain computer interface. In *Signal Processing, Communications and Computing (ICSPCC), 2017 IEEE International Conference on*. IEEE, 1–5.
- [243] Pengyue Zhang, Fusheng Wang, Wei Xu, and Yu Li. 2018. Multi-channel generative adversarial network for parallel magnetic resonance image reconstruction in k-space. In *International Conference on Medical Image Computing and Computer-Assisted Intervention*. Springer, 180–188.
- [244] Tong Zhang, Wenming Zheng, Zhen Cui, Yuan Zong, and Yang Li. 2018. Spatial-temporal recurrent neural network for emotion recognition. *IEEE transactions on cybernetics* 99 (2018), 1–9.
- [245] Xiang Zhang, Lina Yao, Kaixuan Chen, Xianzhi Wang, Quanzheng Sheng, and Tao Gu. 2017. DeepKey: An EEG and Gait Based Dual-Authentication System. *arXiv preprint arXiv:1706.01606* (2017).
- [246] Xiang Zhang, Lina Yao, Chaoran Huang, Salil S Kanhere, and Dalin Zhang. 2018. Brain2Object: Printing Your Mind from Brain Signals with Spatial Correlation Embedding. *arXiv preprint arXiv:1810.02223* (2018).
- [247] Xiang Zhang, Lina Yao, Chaoran Huang, Quan Z Sheng, and Xianzhi Wang. 2017. Intent recognition in smart living through deep recurrent neural networks. In *International Conference on Neural Information Processing*. Springer, 748–758.
- [248] Xiang Zhang, Lina Yao, Chaoran Huang, Sen Wang, Mingkui Tan, Guodong Long, and Can Wang. 2018. Multi-modality sensor data classification with selective attention. *International Joint Conferences on Artificial Intelligence (IJCAI)* (2018).

- [249] Xiang Zhang, Lina Yao, Salil S Kanhere, Yunhao Liu, Tao Gu, and Kaixuan Chen. 2018. MindID: Person Identification from Brain Waves through Attention-based Recurrent Neural Network. *Proceedings of the ACM on Interactive, Mobile, Wearable and Ubiquitous Technologies* 2, 3 (2018), 149.
- [250] Xiang Zhang, Lina Yao, Quan Z Sheng, Salil S Kanhere, Tao Gu, and Dalin Zhang. 2018. Converting your thoughts to texts: Enabling brain typing via deep feature learning of EEG signals. In *2018 IEEE International Conference on Pervasive Computing and Communications (PerCom)*. IEEE, 1–10.
- [251] Xiang Zhang, Lina Yao, and Feng Yuan. 2019. Adversarial Variational Embedding for Robust Semi-supervised Learning. In *SIGKDD 2019*.
- [252] Xiang Zhang, Lina Yao, Dalin Zhang, Xianzhi Wang, Quan Z Sheng, and Tao Gu. 2017. Multi-person brain activity recognition via comprehensive eeg signal analysis. In *Proceedings of the 14th EAI International Conference on Mobile and Ubiquitous Systems: Computing, Networking and Services*. ACM, 28–37.
- [253] Xiang Zhang, Lina Yao, Shuai Zhang, Salil Kanhere, Michael Sheng, and Yunhao Liu. 2018. Internet of Things Meets Brain-Computer Interface: A Unified Deep Learning Framework for Enabling Human-Thing Cognitive Interactivity. *IEEE Internet of Things Journal* (2018).
- [254] Yilu Zhao and Lianghua He. 2014. Deep learning in the EEG diagnosis of Alzheimerfis disease. In *Asian Conference on Computer Vision*. Springer, 340–353.
- [255] Wei-Long Zheng, Hao-Tian Guo, and Bao-Liang Lu. 2015. Revealing critical channels and frequency bands for emotion recognition from EEG with deep belief network. In *Neural Engineering (NER), 2015 7th International IEEE/EMBS Conference on*. IEEE, 154–157.
- [256] Wei-Long Zheng and Bao-Liang Lu. 2015. Investigating critical frequency bands and channels for EEG-based emotion recognition with deep neural networks. *IEEE Transactions on Autonomous Mental Development* 7, 3 (2015), 162–175.
- [257] Wei-Long Zheng and Bao-Liang Lu. 2016. Personalizing EEG-based affective models with transfer learning. In *Proceedings of the Twenty-Fifth International Joint Conference on Artificial Intelligence*. AAAI Press, 2732–2738.
- [258] Wei-Long Zheng, Jia-Yi Zhu, Yong Peng, and Bao-Liang Lu. 2014. EEG-based emotion classification using deep belief networks. In *Multimedia and Expo (ICME), 2014 IEEE International Conference on*. IEEE, 1–6.